# PROCEEDINGS

of the

# First International Conference on the Ultrasonic Measurement and Imaging of Tissue Elasticity©

Niagara Falls, Ontario, Canada
October 20-23, 2002

# PROCEEDINGS

of the
First International Conference
on the Ultrasonic Measurement and Imaging
of Tissue Elasticity

Niagara Falls, Ontario, Canada
October 20-23, 2002

## Table of Contents



Original Cover Photo by Zhe Wu

# FOREWORD

Dear Conference Delegate:

Welcome to the First International Conference on the Ultrasonic Measurement and Imaging of Tissue Elasticity.

In recent years there has been a steady growth of this field; there are now numerous laboratories worldwide that are developing new methodologies for extracting and imaging tissue elasticity parameters. We have felt for some time that while papers were being presented at more broadly targeted conferences, there has been a general lack of sharp focus on this topic at any one of them. Hence, it was our desire to organize a new conference that would provide a unified and consistent forum for researchers from the various disciplines that are involved in this emerging field, namely ultrasonics, biomechanics, radiology, imaging and related areas such as MR and optical elastography. It is our hope that this Conference will be a catalyst for accelerating the progress of this field toward better understanding of the mechanical behavior of tissue and improved imaging and diagnosis of disease.

When this Conference was conceived over a year ago, we were estimating that there could be at best some 35-40 papers. The actual response resulted in more than 70 papers from a dozen countries! While we have felt overwhelmed by this response, we took it to be a good sign for this Conference and for the field in general. The strong participation of delegates from the medical community and industry, as well as by many students, bodes well for the future of this field. We have endeavored to provide as much time as possible for discussion inside and outside the lecture hall, and a comfortable and interesting venue for you and your guests.

We would like to thank all the delegates, the reviewers and the session chairs for their support of this Conference. We are indebted to Professor Don Plewes for agreeing to present the keynote lecture at the Conference dinner on Monday evening. Special thanks are in order to our support staff at the Conference Secretariat office, Ms. Pam Clark and Ms. Manette Price, who have spent much time and effort handling most of the Conference organizational duties that included the website, the CME credits, the announcements, correspondence, finances, and the negotiations with the Sheraton Hotel. Special thanks also go to Ms. Karen Ophir who volunteered to design the Conference logo, letterhead and publications.

While the Conference is conducted under the joint auspices of the University of Rochester Center for Biomedical Ultrasound and the Ultrasonics Laboratory at the University of Texas Medical School at Houston, all funding for the Conference is derived from registration fees alone. With your support, we hope to be able to make this Conference an annual event, and we are looking forward to hearing your presentations for many years to come.

Enjoy your Conference, and we look forward to seeing you at next year's Conference in Texas!

J. Ophir, K. Parker and D. Rubens
Conference Organizers
October 20, 2002

# Conference Evaluation and Questionnaire

| SCORING: | Very Poor | | | | Mid | | | | | Excellent |
|---|---|---|---|---|---|---|---|---|---|---|
| | 1 | 2 | 3 | 4 | 5 | 6 | 7 | 8 | 9 | 10 |

## SCIENTIFIC PROGRAM

| | | | | | | | | | | |
|---|---|---|---|---|---|---|---|---|---|---|
| Quality of the presentations | 1 | 2 | 3 | 4 | 5 | 6 | 7 | 8 | 9 | 10 |
| Number of presentations | 1 | 2 | 3 | 4 | 5 | 6 | 7 | 8 | 9 | 10 |
| Relevance of presentations to the Conference's theme | 1 | 2 | 3 | 4 | 5 | 6 | 7 | 8 | 9 | 10 |
| Time allotted for presentations | 1 | 2 | 3 | 4 | 5 | 6 | 7 | 8 | 9 | 10 |
| Time allotted for discussion | 1 | 2 | 3 | 4 | 5 | 6 | 7 | 8 | 9 | 10 |
| Poster session | 1 | 2 | 3 | 4 | 5 | 6 | 7 | 8 | 9 | 10 |
| Keynote lecture – Subject | 1 | 2 | 3 | 4 | 5 | 6 | 7 | 8 | 9 | 10 |
| Keynote lecture – Speaker | 1 | 2 | 3 | 4 | 5 | 6 | 7 | 8 | 9 | 10 |
| Program and sessions | 1 | 2 | 3 | 4 | 5 | 6 | 7 | 8 | 9 | 10 |
| Student participation | 1 | 2 | 3 | 4 | 5 | 6 | 7 | 8 | 9 | 10 |
| Clinical participation and CME | 1 | 2 | 3 | 4 | 5 | 6 | 7 | 8 | 9 | 10 |
| Additional comments: | | | | | | | | | | |
| | | | | | | | | | | |
| | | | | | | | | | | |

## CONFERENCE MATERIALS:

| | | | | | | | | | | |
|---|---|---|---|---|---|---|---|---|---|---|
| Proceedings | 1 | 2 | 3 | 4 | 5 | 6 | 7 | 8 | 9 | 10 |
| Registration materials | 1 | 2 | 3 | 4 | 5 | 6 | 7 | 8 | 9 | 10 |
| | | | | | | | | | | |
| Additional comments: | | | | | | | | | | |
| | | | | | | | | | | |
| | | | | | | | | | | |

## CONFERENCE FACILITIES

| | | | | | | | | | | |
|---|---|---|---|---|---|---|---|---|---|---|
| Room: | 1 | 2 | 3 | 4 | 5 | 6 | 7 | 8 | 9 | 10 |
| Temperature | 1 | 2 | 3 | 4 | 5 | 6 | 7 | 8 | 9 | 10 |
| Size: 10=Too Big; 5=just right; 1=Too Small | 1 | 2 | 3 | 4 | 5 | 6 | 7 | 8 | 9 | 10 |
| Seating | 1 | 2 | 3 | 4 | 5 | 6 | 7 | 8 | 9 | 10 |
| Registration Desk and Conference Office | 1 | 2 | 3 | 4 | 5 | 6 | 7 | 8 | 9 | 10 |
| Meals: | 1 | 2 | 3 | 4 | 5 | 6 | 7 | 8 | 9 | 10 |
| Conference breakfasts and lunches | 1 | 2 | 3 | 4 | 5 | 6 | 7 | 8 | 9 | 10 |
| Conference dinner | 1 | 2 | 3 | 4 | 5 | 6 | 7 | 8 | 9 | 10 |
| Coffee breaks | 1 | 2 | 3 | 4 | 5 | 6 | 7 | 8 | 9 | 10 |
| Audio-visual equipment | 1 | 2 | 3 | 4 | 5 | 6 | 7 | 8 | 9 | 10 |
| | | | | | | | | | | |
| Additional comments: | | | | | | | | | | |
| | | | | | | | | | | |
| | | | | | | | | | | |

## VENUE AND HOTEL

| | | | | | | | | | | |
|---|---|---|---|---|---|---|---|---|---|---|
| Venue - Niagara Falls and Environs | 1 | 2 | 3 | 4 | 5 | 6 | 7 | 8 | 9 | 10 |
| Area attractions | 1 | 2 | 3 | 4 | 5 | 6 | 7 | 8 | 9 | 10 |
| Hotel: | 1 | 2 | 3 | 4 | 5 | 6 | 7 | 8 | 9 | 10 |
| Reservations | 1 | 2 | 3 | 4 | 5 | 6 | 7 | 8 | 9 | 10 |
| Transportation and accessibility | 1 | 2 | 3 | 4 | 5 | 6 | 7 | 8 | 9 | 10 |
| Reception | 1 | 2 | 3 | 4 | 5 | 6 | 7 | 8 | 9 | 10 |
| Accommodations | 1 | 2 | 3 | 4 | 5 | 6 | 7 | 8 | 9 | 10 |
| Facilities | 1 | 2 | 3 | 4 | 5 | 6 | 7 | 8 | 9 | 10 |
| | | | | | | | | | | |
| Additional comments: | | | | | | | | | | |
| | | | | | | | | | | |
| | | | | | | | | | | |

## ADMINISTRATION

| | | | | | | | | | | |
|---|---|---|---|---|---|---|---|---|---|---|
| Website | 1 | 2 | 3 | 4 | 5 | 6 | 7 | 8 | 9 | 10 |
| Registration off-site | 1 | 2 | 3 | 4 | 5 | 6 | 7 | 8 | 9 | 10 |
| Registration on-site | 1 | 2 | 3 | 4 | 5 | 6 | 7 | 8 | 9 | 10 |
| Administrative staff | 1 | 2 | 3 | 4 | 5 | 6 | 7 | 8 | 9 | 10 |
| Correspondence | 1 | 2 | 3 | 4 | 5 | 6 | 7 | 8 | 9 | 10 |
| | | | | | | | | | | |
| Additional comments: | | | | | | | | | | |
| | | | | | | | | | | |
| | | | | | | | | | | |

## GENERAL INFORMATION

| | | | | |
|---|---|---|---|---|
| Should this conference be held annually? | Yes | | No | |
| If Yes: | | | | |
| I would plan to attend the next conference | Yes | Perhaps | No | |
| and present a paper(s) / poster(s) | Yes | Perhaps | No | |
| Other(s) from my lab would attend the next conference | Yes | Perhaps | No | |
| and he/she / they would present a paper(s) / poster(s) | Yes | Perhaps | No | |
| | | | | |
| Should this conference have tutorials? | Yes | | No | |
| Should this conference be held in other locations? | Yes | | No | |
| Time of year for the conference | FALL | Winter | Spring | Summer |
| Duration of the conference | Shorter | OK as is | Longer | |
| Tutorial suggestions: | | | | |
| Location suggestions: | | | | |
| Additional comments: (Improvements or Suggestions) | | | | |
| | | | | |
| | | | | |
| | | | | |
| | | | | |
| | | | | |

# PROGRAM

First International Conference
on the Ultrasonic Measurement and Imaging
of Tissue Elasticity

Niagara Falls, Ontario, Canada
October 20-23, 2002

## CONFERENCE-AT-A-GLANCE

### Sunday, October 20 — 4:00P - 9:00P

| | | |
|---|---|---|
| 4:00P - 9:00P | | Registration |
| 6:00P – 9:00P | | Opening Reception |
| | **Session P:** | Posters |

### Monday, October 21 — 7:00A - 10:00P

| | | |
|---|---|---|
| 7:00A - 8:00A | | *Group Breakfast* |
| 8:00A - 5:00P | | Registration |
| | **Session P:** | Posters |
| 8:00A - 8:08A | | Opening Remarks |
| 8:08A - 10:00A | **Session A:** | Mechanical Measurement Techniques for Tissues |
| 10:00A - 10:30A | | *Coffee Break* |
| 10:30A - 12:00P | **Session B:** | Mechanical Properties of Tissues |
| 12:00P - 1:30P | | *Group Lunch* |
| 1:30P - 3:30P | **Session C-1:** | Methods for Imaging Elastic Tissue Properties I |
| 3:30P - 4:00P | | *Coffee Break* |
| 4:00P - 4:48P | **Session D:** | Biomechanical Tissue Modeling |
| 4:48P - 5:36P | **Session E:** | Instrumentation and Phantoms |
| 6:30P - 10:00P | | Conference Dinner and Keynote Lecture by Donald B. Plewes |

### Tuesday, October 22 — 7:00A – 5:30P

| | | |
|---|---|---|
| 7:00A - 8:00A | | *Group Breakfast* |
| 8:00A - 5:00P | | Registration |
| | **Session P:** | Posters |
| 8:00A - 10:00A | **Session C-2:** | Methods for Imaging Elastic Tissue Properties II |
| 10:00A - 10:30A | | *Coffee Break* |
| 10:30A - 12:00P | **Session F-1:** | Clinical and Animal Applications and Results I |
| 12:00P - 1:30P | | *Group Lunch* |
| 1:30P - 2:38P | **Session G-1:** | Signal and Image Processing, and New Algorithms I |
| 2:38P - 3:30P | **Session H:** | Complementary Elasticity Imaging Techniques |
| 3:30P - 4:00P | | *Coffee Break* |
| 4:00P - 5:30P | **Session F-2:** | Clinical and Animal Applications and Results II |

### Wednesday, October 23 — 7:00A -12:30P

| | | |
|---|---|---|
| 7:00A - 8:00A | | *Group Breakfast* |
| 8:00A - 11:00A | | Registration |
| 8:00A - 9:08A | **Session G-2:** | Signal and Image Processing, and New Algorithms II |
| 9:08A - 9:42A | **Session I:** | Three-Dimensional and Multi-Modality Applications |
| 9:42A - 10:00A | | *Coffee Break* |
| 10:00A – 11:08A | **Session J:** | Forward and Inverse Problems |
| 11:30A - 12:30P | | *Group Lunch* |

## Sunday, October 20 4:00P - 9:00P

**4:00P - 9:00P**
Registration
**6:00P – 9:00P**
Opening Reception
**Session P: Posters**

## Monday, October 21 7:00A - 10:00P

**7:00A - 8:00A**
GROUP BREAKFAST
**8:00A - 5:00P**
Registration
**Session P: Posters**

## Monday 8:00A - 8:08A
## OPENING REMARKS
*J Ophir, KJ Parker, DJ Rubens*

## Monday 8:08A - 10:00A
## Session A: Mechanical Measurement Techniques for Tissues
*Chair: S Levinson, USA*

**8:08A - 8:24A**
01 A STUDY OF MUSCLE ANISOTROPY WITH TRANSIENT ELASTOGRAPHY.
*JL Gennisson, S Catheline, S Chaffaï, M Fink.*
Laboratoire Ondes et Acoustique, E.S.P.C.I., Paris, FRANCE.

**8:24A - 8:40A**
04 MEASURING NON-LINEAR ELASTIC PARAMETERS OF SOFT SOLIDS USING TRANSIENT ELASTOGRAPHY.
*S Catheline, JL Gennisson, S Chaffaï, M Fink.*
Laboratoire Ondes et Acoustique, E.S.P.C.I., Paris, FRANCE.

**8:40A - 8:56A**
15 A QUANTITATIVE COMPARISON OF ULTRASOUND ELASTOGRAPHY- BASED STRAIN IMAGES WITH NANO-INDENTATION BASED MODULUS IMAGES OF TISSUES.
*S Srinivasan[1,2], TA Krouskop[1,3], J Ophir[1,2].*
[1]University of Texas Medical School, Houston, TX, USA; [2]University of Houston, Houston, TX, USA; [3]Baylor College of Medicine, Houston, TX, USA.

**8:56A - 9:12A**
18 REALIZATION OF COMBINED DIAGNOSIS/TREATMENT STYLE BY ULTRASONIC STRAIN MEASUREMENT-BASED MECHANICAL PROPERTIES IMAGING TECHNIQUE - EXAMPLES WITH APPLICATIONS TO INTERSTITIAL RF-ELECTROMAGNETIC WAVE THERMAL THERAPY.
*C Sumi.*
Sophia University, Tokyo, JAPAN.

**9:12A - 9:28A**
20 USING ELASTOGRAPHY TO DETECT BRACHYTHERAPY SEEDS: A FEASIBILITY STUDY.
*G Rossignol, R Souchon, YC Angel, JY Chapelon.*
INSERM, Lyon, FRANCE.
(Session A continues on next page)

**9:28A - 9:44A**

37 DEPTH-DEPENDENT STRAIN FILTER IN RADIAL COMPRESSION ELASTOGRAPHY: EXPERIMENTAL MEASUREMENTS.
*R Souchon[1], J Ophir[2,3], S Srinivasan[2,3], JY Chapelon[1].*
[1]INSERM, Lyon, FRANCE; [2]University of Texas Medical School, Houston, TX, USA; [3]University of Houston, Houston, TX, USA.

**9:44A - 10:00A**

66 EXPERIMENTAL OBSERVATION OF FREQUENCY DEPENDENT CONTRAST DURING SONOELASTIC IMAGING OF BOVINE LIVER.
*LS Taylor, P Wang, DJ Rubens, KJ Parker.*
University of Rochester, Rochester, NY, USA.

**10:00A - 10:30A**

COFFEE BREAK

## Monday 10:30A – 12:00P
## Session B: Mechanical Properties of Tissues

*Chair: M Fink, France*

**10:30A - 10:48A**

12 MODULUS VARIATIONS IN BREAST TISSUES.
*TA Krouskop[1], RE Price[2], T Wheeler[1], PS Younes[1].*
[1]Baylor College of Medicine, Houston, TX, USA; [2]University of Texas M.D. Anderson Cancer Center, Houston, TX, USA.

**10:48A - 11:05A**

69 IN-VITRO BREAST TISSUE ELASTIC MODULUS MEASUREMENT USING UNIAXIAL INDENTATION TECHNIQUE.
*A Samani, DB Plewes.*
Sunnybrook and Women's College Health Sciences Centre, Toronto, Ontario, CANADA.

**11:05A - 11:23A**

22 ULTRASONIC MEASUREMENT OF IN-VITRO TRANSIENT AND DEPTH-DEPENDENT COMPRESSIVE STRAINS OF ARTICULAR CARTILAGE IN COMPRESSION.
*Y Zheng[1], D Luo[2], J Shi[1], AWT Shum[1], L Qin[3], AFT Mak[1].*
[1]Hong Kong Polytechnic University, Kowloon, HONG KONG; [2]Beijing University of Physical Education, Beijing, CHINA; [3]Chinese University of Hong Kong, NT, HONG KONG.

**11:23A - 11:41A**

57 ELASTIC MODULI OF CONNECTIVE TISSUES DETERMINED BY SCANNING ACOUSTIC MICROSCOPY.
*JL Katz[1, 2], P Spencer[1], Y Wang[1], A Wagh[3], S Bumrerraj[4], T Nomura[5], HJ Hein[6].*
[1]University of Missouri-Kansas City Dental School, Kansas City, MO, USA; [2]University of Texas Medical School, Houston, TX, USA; [3]University of Memphis Engineering School, Memphis, TN, USA; [4]Khon Kaen University Medical School, Khon Kaen, THAILAND; [5]Niigata University Dental School, Niigata, JAPAN; [6]Martin-Luther-University Halle-Wittenburg Medical School, Halle/Saale, GERMANY.

**11:41A - 12:00P**

68 QUANTITATIVE ULTRASOUND METHOD FOR MICROSTRUCTURE-ACCOUNTING ANALYSIS ON THIN SLICES OF BREAST TISSUE.
*J Liu, M Ferrari.*
Ohio State University, Columbus, Ohio, USA.

**12:00P - 1:30P**

GROUP LUNCH

## Monday 1:30P - 3:30P
## Session C-1: Methods for Imaging Elastic Tissue Properties I

*Chair: JC Bamber, UK*

**1:30P - 1:47P**

67 NON-INVASIVE ELASTICITY IMAGING IN SMALL VESSELS.
*N Pivert[1], R Maurice[1], M Daronat[1], FS Foster[2], G Cloutier[1].*
[1]University of Montreal, Québec, CANADA; [2]Sunnybrook and Women's College Health Sciences Centre, University of Toronto, Ontario, CANADA.

**1:47P - 2:04P**

02 ULTRAFAST IMAGING OF SHEAR WAVES INDUCED BY ACOUSTIC RADIATION-FORCE IN SOFT TISSUES.
*J Bercoff, M Tanter, S Chaffaï, M Fink.*
Laboratoire Ondes et Acoustique, E.S.P.C.I., Paris, FRANCE.

**2:04P - 2:21P**

11 INFLUENCE OF NON-UNIFORM TRANSDUCER ROTATION ON THE CORRELATION COEFFICIENT IN INTRAVASCULAR ULTRASOUND ELASTOGRAPHY.
*C Perrey, T Neumann, HB Salameh, H Ermert.*
Ruhr University, Bochum, GERMANY.

**2:21P - 2:38P**

21 DEVELOPMENT OF AN ULTRASOUND ELASTOMICROSCOPY (UEM) SYSTEM: PRELIMINARY RESULTS.
*Y Zheng[1], A Saïed[2], B Jaffre[2], T Lu[1], L Bridal[2], P Laugier[2], AFT Mak[1].*
[1]Hong Kong Polytechnic University, Kowloon, HONG KONG; [2]University of Paris VI, Paris, FRANCE.

**2:38P - 2:55P**

26 DEALING WITH CARDIOVASCULAR MOTION FOR STRAIN IMAGING OF THE LIVER.
*AF Kolen, JC Bamber.*
Institute of Cancer Research and Royal Marsden NHS Trust, Sutton, Surrey, UK.

**2:55P - 3:12P**

25 ELASTICITY IMAGING USING TACTILE SENSORS.
*A Sarvazyan.*
ARTANN Laboratories, Inc., Lambertville, NJ, USA.

**3:12P - 3:30P**

27 HUMAN AND COMPUTER-ASSISTED PERCEPTION OF ELASTIC LESIONS IN ULTRASOUND IMAGES.
*NR Miller, JC Bamber.*
Institute of Cancer Research and Royal Marsden NHS Trust, Sutton, Surrey, UK.

**3:30P - 4:00P**

COFFEE BREAK

## Monday 4:00P - 4:48P
## Session D: Biomechanical Tissue Modeling
*Chair: SK Alam, USA*

**4:00P - 4:16P**

50 TIME-DOMAIN MODELS TO EXPLAIN MEASUREMENTS OF COMPLEX-VALUED SHEAR MODULUS AS A FUNCTION OF FREQUENCY IN ISOTROPIC SOFT TISSUES.
*TE Oliphant[1], R Kinnick[2], JF Greenleaf[2], A Dresner[2], R Ehman[2].*
[1]Brigham Young University, Provo, UT, USA; [2]Mayo Foundation, Minneapolis, MN, USA.

**4:16P - 4:32P**

51 A REVIEW OF ELASTICITY IMAGING IN SKELETAL MUSCLE. PART 1 – BIOMECHANICAL MODELS.
*SF Levinson, SM Gracewski.*
University of Rochester, Rochester, NY, USA.

**4:32P - 4:48P**

52 A REVIEW OF ELASTICITY IMAGING IN SKELETAL MUSCLE. PART 2 – DYNAMICS AND PHYSICAL ACOUSTICS.
*SF Levinson, SM Gracewski.*
University of Rochester, Rochester, NY, USA.

## Monday 4:48P - 5:36P
## Session E: Instrumentation and Phantoms
*Chair: T Hall, USA*

**4:48P - 5:04P**

54 PHANTOMS FOR ELASTICITY IMAGING.
*T Hall.*
University of Kansas Medical Center, Kansas City, KS, USA.

**5:04P - 5:20P**

29 STABLE HETEROGENEOUS PHANTOMS FOR TESTING PERFORMANCE OF US AND MR ELASTOGRAPHY SYSTEMS.
*EL Madsen[1], GR Frank[1], TA Krouskop[2], T Varghese[1], F Kallel[3], TA Stiles[1], J Ophir[3].*
[1]University of Wisconsin, Madison, WI, USA; [2]Baylor University, Houston, TX, USA; [3]University of Texas Medical School, Houston, TX, USA.

**5:20P - 5:36P**

62 USING THE ATL HDI-1000 ULTRASOUND SCANNER FOR TISSUE ELASTICITY IMAGING.
*A Anand[1], P Kaczkowski[1], R Daigle[2], L Crum[1].*
[1]University of Washington, Seattle, WA, USA; [2]Intersonics, Redmond, WA, USA.

## Monday 7:00P - 10:00P
## Conference Dinner And Keynote Lecture by Donald B. Plewes

**7:00P - 10:00P**

CONFERENCE DINNER

**8:15P - 9:00P**

00 KEYNOTE LECTURE: AN OVERVIEW OF MRI FOR MOTION IMAGING: APPLICATIONS IN ELASTOGRAPHY, TISSUE CHARACTERIZATION AND ULTRASOUND BIOPHYSICS.
*Donald B. Plewes, Professor and Senior Scientist, Imaging Research.*
Sunnybrook and Women's College Health Sciences Centre, University of Toronto, Toronto, Ontario, CANADA.

## Tuesday, October 22 7:00A – 5:30P

**7:00A - 8:00A**
GROUP BREAKFAST
**8:00A - 5:00P**
Registration
**Session P: Posters**

## Tuesday 8:00A - 10:00A
## Session C-2: Methods for Imaging Elastic Tissue Properties II
*Chair: KM Hiltawsky, Germany*

**8:00A - 8:17A**
28 TEMPERATURE IMAGING BY MEANS OF ULTRASONIC STRAIN ESTIMATION FOR THE GUIDANCE OF FOCUSED ULTRASOUND SURGERY.
*NR Miller[1], JC Bamber[1], GR ter Haar[1], PM Meaney[2].*
[1]Institute of Cancer Research and Royal Marsden NHS Trust, Sutton, Surrey, UK; [2]Dartmouth College, Hanover, NH, USA.

**8:17A - 8:34A**
32 REAL-TIME ROBUST IMAGING OF TISSUE ELASTICITY BASED ON THE EXTENDED COMBINED AUTOCORRELATION METHOD.
*T Shiina[1], M Yamakawa[1], N Nitta[1], E Ueno[1], T Matsumura[2], S Tamano[2], T Mitake[2].*
[1]University of Tsukuba, JAPAN, [2]Research & Development Center, Hitachi Medical Corporation, JAPAN.

**8:34A - 8:51A**
35 ACOUSTIC RADIATION FORCE IMPULSE IMAGING: IMAGING THE VISCO-ELASTIC PROPERTIES OF TISSUES.
*K Nightingale, S McAleavey, D Stutz, M Palmeri, R Nightingale, R Bentley, G Trahey.*
Duke University, Durham, NC, USA.

**8:51A - 9:08A**
36 ACOUSTIC RADIATION FORCE IMPULSE IMAGING OF ARTERIES.
*G Trahey, J Dahl, S McAleavey, C Gallippi, K Nightingale.*
Duke University, Durham, NC, USA.

**9:08A - 9:25A**
40 THE APPLICATION OF RADIATION FORCE FOR DYNAMIC ASSESSMENT OF THROMBOSIS.
*WF Walker, F Viola, MD Kramer, MB Lawrence.*
University of Virginia, Charlottesville, VA, USA.

**9:25A - 9:42A**
41 LOCALIZED HARMONIC MOTION IMAGING: THEORY, SIMULATIONS AND EXPERIMENTS.
*EE Konofagou, K Hynynen.*
Brigham and Women's Hospital - Harvard Medical School, Boston, MA, USA.

**9:42A - 10:00A**
46 REAL-TIME IMAGING OF LOCAL TISSUE MOTION FOR ULTRASONIC VISUALIZED PALPATION.
*S Yagi[1], S Akimoto[2].*
[1]Meisei University, Tokyo, JAPAN; [2]Yokohama General Hospital, Yokohama, JAPAN.

**10:00A - 10:30A**
COFFEE BREAK

## Tuesday 10:30A - 12:00P
## Session F-1: Clinical and Animal Applications and Results I

*Chair: CRB Merritt, USA*

**10:30A - 10:48A**

06 CARDIAC ELASTOGRAPHY: 2D IMAGING OF MYOCARDIAL STRAIN.
*T Varghese , JA Zagzebski, P Rahko, CS Breburda.*
University of Wisconsin-Madison, Madison, WI, USA.

**10:48A - 11:06A**

10 ELASTOGRAPHY IN ANIMAL MODELS: LESION DETECTION AND COMPARISON WITH SONOGRAPHY.
*CRB Merritt[1], C Dascenzo[1], F Forsberg[1], J Ophir[2].*
[1]Thomas Jefferson University, Philadelphia, PA, USA; [2]University of Texas Medical School, Houston, TX, USA.

**11:06A - 11:24A**

13 IN VIVO ELASTOGRAPHY OF THE BREAST: PRELIMINARY FINDINGS.
*CRB Merritt[1], C Dascenzo[1], F Forsberg[1], J Ophir[2].*
[1]Thomas Jefferson University, Philadelphia, PA, USA; [2]University of Texas Medical School, Houston, TX, USA.

**11:24A - 11:42A**

14 REAL-TIME ULTRASOUND ELASTICITY IMAGING IN THE BREAST CLINIC – WORK IN PROGRESS.
*WE Svensson[1], A Connors[1], S Comitis[1], D Chopra[1], D Sinnett[1], P Forouhi[1], G Layer[1], C Lowery[2], P Von Behren[2].*
[1]Charing Cross Hospital (Hammersmith Hospitals Trust), Imperial College School of Medicine, London, UK; [2]Siemens Medical Systems Ultrasound Group, USA.

**11:42A - 12:00P**

30 ULTRASOUND ELASTICITY IMAGING OF DEEP VENOUS THROMBOSIS.
*JM Rubin, S Aglyamov, AR Skovoroda, DD Myers, Jr., SK Wrobleski, TW Wakefield, M O'Donnell, SY Emelianov.*
University of Michigan, Ann Arbor, MI, USA.

**12:00P - 1:30P**

GROUP LUNCH

## Tuesday 1:30P - 2:38P
## Session G-1: Signal and Image Processing, and New Algorithms I

*Chair: T Shiina, Japan*

**1:30P - 1:47P**

07 COMPLETE PROCESSING FOR QUANTITATIVE INTRAVASCULAR ULTRASOUND ELASTOGRAPHY.
*E Brusseau[1], J Fromageau[1], C de Korte[2,3], P Delachartre[1], D Vray[1], AFW van der Steen[2,3].*
[1]CREATIS UMR CNRS 5515, affiliated to INSERM, Lyon, FRANCE; [2]Erasmus University Rotterdam, Rotterdam, The NETHERLANDS; [3]Interuniversity Cardiology Institute of the Netherlands (ICIN), The NETHERLANDS.

**1:47P - 2:04P**

17 RESOLUTION IN ELASTOGRAPHY.
*R Righetti, S Srinivasan, J Ophir.*
University of Texas Medical School, Houston, TX, USA; University of Houston, Houston, TX, USA.

**2:04P - 2:21P**

16 TRADEOFFS BETWEEN THE AXIAL RESOLUTION AND THE SIGNAL-TO-NOISE RATIO IN ELASTOGRAPHY.
*S Srinivasan, R Righetti, J Ophir.*
University of Texas Medical School, Houston, TX, USA; University of Houston, Houston, TX, USA.

(Session G-1 continues on next page)

**2:21P - 2:38P**

19 AXIAL AND CONTRAST RESOLUTION OF ELASTOGRAPHY BASED ON TIME DELAY ESTIMATION.
*KM Hiltawsky, H Ermert.*
Ruhr University, Bochum, GERMANY.

## Tuesday 2:38P - 3:30P
## Session H: Complementary Elasticity Imaging Techniques

*Chair: K Nightingale, USA*

**2:38P - 2:55P**

24 HAPTIZATION OF ELASTIC OBJECT USING MAGNETIC RESONANCE ELASTOGRAPHY.
*M Imura, M Suga, O Oshiro, K Minato, K Chihara.*
Nara Institute of Science and Technology, Nara, JAPAN.

**2:55P - 3:12P**

31 PROCESSING ALGORITHMS FOR TRACKING LASER SPECKLE SHIFTS IN ACOUSTO-OPTICAL ELASTOGRAPHY OF SKIN.
*SJ Kirkpatrick[1], DD Duncan[2].*
[1]Oregon Medical Laser Center, Providence St. Vincent Medical Center, Portland, OR, USA; [2]Johns Hopkins University, Laurel, MD, USA.

**3:12P - 3:30P**

45 STEADY-STATE MAGNETIC RESONANCE HARMONIC ELASTOGRAPHY: CONTRAST DETAILED ANALYSIS AND PRELIMINARY CLINICAL EVALUATION.
*MM Doyley[1,2], JB Weaver[1,2], EEW Houten[2], FE Kennedy[2], KD Paulsen[2,3].*
[1]Dartmouth-Hitchcock Medical Center, Lebanon, NH, USA; [2]Dartmouth College, Hanover, NH, USA; [3]Norris Cotton Cancer Center, Lebanon, NH, USA.

**3:30P - 4:00P**

COFFEE BREAK

## Tuesday 4:00P - 5:30P
## Session F-2: Clinical and Animal Applications and Results II

*Chair: JM Rubin, USA*

**4:00P - 4:18P**

39 A FAST ACQUISITION SYSTEM FOR RADIAL COMPRESSION ELASTOGRAPHY OF THE PROSTATE IN-VIVO.
*R Souchon, V Detti, JY Chapelon.*
INSERM, Lyon, FRANCE.

**4:18P - 4:36P**

42 CARDIAC ELASTOGRAPHY: DETECTING PATHOLOGICAL CHANGES OF THE MYOCARDIUM.
*EE Konofagou[1], T Harrigan[2], S Solomon[1].*
[1]Brigham and Women's Hospital, Harvard Medical School, Boston, MA, USA; [2]Exponent, Inc, Failure Analysis Associates, Houston, TX, USA.

**4:36P - 4:54P**

43 REAL-TIME STRAIN IMAGING FOR PROSTATE CANCER DIAGNOSTICS – NEW CLINICAL RESULTS.
*U Scheipers[1], H Ermert[1], A Lorenz[1,2], A Pesavento[1,2], HJ Sommerfeld[3], M Garcia-Schuermann[3], K Kuehne[3], T Senge[3], S Philippou[4].*
[1]Ruhr-Universitaet, Bochum, GERMANY; [2]Ingenieurbuero Lorenz & Pesavento GmbH, Bochum, GERMANY; [3]Urologische Universitaetsklinik, Marienhospital, Herne, GERMANY; [4]Institut für Pathologie, Augustakrankenanstalten, Bochum, GERMANY; [1,2,3,4]Kompetenzzentrum Medizintechnik Ruhr, Bochum, GERMANY.

(Session F-2 continues on next page)

**4:54P - 5:12P**

53 REAL-TIME FREEHAND ELASTICITY IMAGING.
*T Hall, Y Zhu.*
University of Kansas Medical Center, Kansas City, KS, USA.

**5:12P - 5:30P**

58 ULTRASOUND FREEHAND ELASTOGRAPHY: EVALUATION OF DIAGNOSTIC POTENTIAL IN CLINICAL BREAST IMAGING.
*JC Bamber[1], NL Bush[1], DO Cosgrove[2], MM Doyley[1], FG Fuechsel[2], NR Miller[1], F Tranquart[3].*
[1]Institute of Cancer Research and Royal Marsden NHS Trust, Sutton, Surrey, UK; [2]Hammersmith Hospitals Trust, London, UK; [3]University Hospital, Tours, FRANCE.

## Wednesday, October 23 7:00A -12:30P

**7:00A - 8:00A**

GROUP BREAKFAST

**8:00A - 11:00A**

Registration

## Wednesday 8:00A - 9:08A
## Session G-2: Signal and Image Processing, and New Algorithms II

*Chair: MM Doyley, USA*

**8:00A - 8:17A**

08 THE ESTIMATION OF MOTION GRADIENTS BY MEANS OF TWO-DIMENSIONAL CUBIC B-SPLINES.
*J D'hooge, P Claus, B Bijnens, J Thoen, F Van de Werf, GR Sutherland, P Suetens.*
Katholieke Universiteit Leuven, Leuven, BELGIUM.

**8:17A - 8:34A**

09 A SIMULATION STUDY ON THE PERFORMANCE OF DIFFERENT ESTIMATORS FOR TWO-DIMENSIONAL VELOCITY ESTIMATION.
*S Langeland[1], J D'hooge[1], H Torp[2], B Bijnens[1], P Suetens[1].*
[1]Katholieke Universiteit Leuven, Leuven, BELGIUM; [2]Norwegian University of Science and Technology, Trondheim, NORWAY.

**8:34A - 8:51A**

59 FAST AND ROBUST STRAIN ESTIMATION IN ELASTOGRAPHY.
*SK Alam.*
Riverside Research Institute, New York, NY, USA.

**8:51A - 9:08A**

64 CONVERGENCE AND REGULARIZATION IN TISSUE MOTION ESTIMATION USING THE LAGRANGIAN SPECKLE MODEL.
*G Charron, R Maurice, M Bertrand.*
Institut de génie biomedical, École Polytechnique, Montréal, Québec, CANADA.

## Wednesday 9:08A - 9:42A
## Session I: Three-Dimensional and Multi-Modality Applications
*Chair: A Sarvazyan, USA*

**9:08A - 9:25A**

05 ELASTOGRAPHIC IMAGING OF THERMAL LESION FORMATION IN-VIVO ALONG WITH 3-D VISUALIZATION DURING RF ABLATION.
*T Varghese, JA Zagzebski, Q Chen, U Techavipoo, W Liu, FT Lee, Jr.*
University of Wisconsin-Madison, Madison, WI, USA.

**9:25A - 9:42A**

65 THREE-DIMENSIONAL FUSION OF PROSTATE HISTOLOGY WITH SONOELASTOGRAPHY IMAGES.
*LS Taylor, KJ Parker, BC Porter, CZ Wu, DJ Rubens, GM Nadasdy, PA di'Santagnese, D Pasternack, RB Baggs.*
University of Rochester, Rochester, NY, USA.

**9:42A - 10:00A**

COFFEE BREAK

## Wednesday 10:00A – 11:08A
## Session J: Forward and Inverse Problems
*Chair: M Bertrand, Canada*

**10:00A - 10:17A**

23 UNIQUE ELASTIC MODULUS RECONSTRUCTION WITH LITTLE OR NO BOUNDARY DATA.
*PE Barbone[1], JC Bamber[2].*
[1]Boston University, Boston, MA, USA; [2]Institute of Cancer Research and Royal Marsden Hospital, Sutton, Surrey, UK.

**10:17A - 10:34A**

34 A FAST ITERATIVE SCHEME FOR QUANTITATIVE ELASTICITY IMAGING BASED ON AN ADJOINT FORMULATION.
*AA Oberai[1], N Gokhalei[1], MM Doyley[2,3].*
[1]Boston University, Boston, MA, USA; [2]Dartmouth College, Hanover, NH, USA; [3]Dartmouth-Hitchcock Medical Center, Lebanon, NH, USA.

**10:34A - 10:51A**

48 MAXIMUM-LIKELIHOOD ESTIMATOR FOR QUANTITATIVE VIBRATION ELASTOGRAPHY IN SOTROPIC SOFT-TISSUES.
*TE Oliphant.*
Brigham Young University, Provo, UT, USA.

**10:51A - 11:08A**

56 PARAMETER SENSITIVITY IN RECONSTRUCTIVE ELASTIC PROPERTY IMAGING.
*EEW Houten[1], KD Paulsen[1,3], MM Doyley[1,2], FE Kennedy[1], JB Weaver[1,2].*
[1]Dartmouth College, Hanover, NH, USA; [2]Dartmouth-Hitchcock Medical Center, Lebanon, NH, USA; [3]Norris Cotton Cancer Center, Lebanon, NH, USA.

**11:30A - 12:30P**

GROUP LUNCH

## Sunday, October 20, 6:00P – Tuesday, October 22, 5:00P

### Session P: Posters

*Chair: Y Zheng, Hong Kong*

55 MEASUREMENTS OF TENDON ELASTIC PROPERTIES.
*PC Li, PL Kuo.*
National Taiwan University, Taipai, TAIWAN, ROC.

33 DEVELOPMENT OF FREEHAND ULTRASOUND ELASTICITY IMAGING SYSTEM AND IN-VIVO RESULTS.
*T Matsumura[1], S Tamano[1], T Mitake[1], T Shiina[2], M Yamakawa[2], N Nitta[2], E Ueno[3].*
[1]Research & Development Center, Hitachi Medical Corporation, JAPAN; [2]Institute of Information Sciences & Electronics, University of Tsukuba, JAPAN; [3]Institute of Clinical Medicine, University of Tsukuba, JAPAN.

61 ELASTOGRAPHIC IMAGING OF SMALL ANIMAL ONCOLOGY MODELS.
*M Bilgen[1], S Srinivasan[1,2], LB Lachman[3], J Ophir[1,2].*
[1]University of Texas Medical School, Houston, TX, USA; [2]University of Houston, Houston, TX, USA; [3]University of Texas M.D. Anderson Cancer Center, Houston, TX, USA.

63 STRAIN INDUCED DAMAGE TO BREAST TUMOR TISSUE.
*TA Krouskop, PS Younes, T Wheeler.*
Baylor College of Medicine, Houston, TX, USA.

03 2-D TRANSIENT ELASTOGRAPHY WITH AN ULTRA-FAST ULTRASONIC SCANNER.
*M Fink, L Sandrin, M Tanter, S Catheline, S Chaffai, J Bercoff, JL Gennisson.*
Laboratoire Ondes et Acoustique, E.S.P.C.I., Paris, FRANCE.

44 MONITORING OF MODULUS CHANGES WITH TEMPERATURE USING A FREQUENCY SHIFT METHOD.
*EE Konofagou, K Hynynen.*
Brigham and Women's Hospital – Harvard Medical School, Boston, MA, USA.

49 DIRECTIONAL FILTERING AND SIMPLE FREQUENCY ESTIMATION: A FAST, SIMPLE METHOD FOR QUANTITATIVE VIBRATION ELASTOGRAPHY RECONSTRUCTION.
*DA Thayer, TE Oliphant.*
Brigham Young University, Provo, UT, USA.

38 PROSTATE ELASTOGRAPHY: CAUSES OF DECORRELATION IN-VIVO.
*R Souchon[1], J Ophir[2,3], S Srinivasan[2,3], JY Chapelon[1].*
[1]INSERM, Lyon, FRANCE; [2]University of Texas Medical School, Houston, TX, USA; [3]University of Houston, Houston, TX, USA.

60 MAPPING OF TEMPERATURE ELEVATION USING ULTRASOUND PHASED ARRAYS.
*EE Konofagou[1], S Sokka[1,2], J Thierman[1,2], K. Hynynen[1].*
[1]Brigham and Women's Hospital – Harvard Medical School, Boston, MA, USA; [2]Health Science and Technology Program, Harvard-MIT Division, Cambridge, MA, USA.

70 CONSTRAINED BREAST ELASTOGRAPHY: PHANTOM STUDY AND APPLICATION IN IN-VITRO BREAST TISSUE MEASUREMENT.
*A Samani, DB Plewes.*
Sunnybrook and Women's College Health Sciences Centre, Toronto, Ontario, CANADA.

47 DEVELOPMENT AND APPLICATIONS OF A TISSUE ULTRASOUND PALPATION SENSOR (TUPS).
*Y Zheng, G Pan, J Ho, AFT Mak.*
Hong Kong Polytechnic University, Kowloon, HONG KONG.

71 THE DEPENDENCE OF ULTRASOUND STIMULATED ACOUSTIC EMISSIONS ON STIFFNESS, FREQUENCY, AND DEPTH IN A PHANTOM GEL.
*J Thierman[1,2], EE Konofagou[1], K Hynynen[1].*
[1]Brigham and Women's Hospital – Harvard Medical School, Boston, MA, USA; [2]Health Science and Technology Program, Harvard-MIT Division, Cambridge, MA, USA.

72 IN-VIVO RESULTS USING A ZERO-CROSSING STRAIN ESTIMATOR FOR ELASTOGRAPHY†
*S Srinivasan[1,2], R Souchon[3], J Ophir[1,2].*
[1]University of Texas Medical School, Houston, TX, USA; [2] University of Houston, Houston, TX, USA; [3]INSERM, Lyon, FRANCE.

# ABSTRACTS

First International Conference
on the Ultrasonic Measurement and Imaging
of Tissue Elasticity

Niagara Falls, Ontario, Canada
October 20-23, 2002

## Keynote Lecture

00 **AN OVERVIEW OF MRI FOR MOTION IMAGING: APPLICATIONS IN ELASTOGRAPHY, TISSUE CHARACTERIZATION AND ULTRASOUND BIOPHYSICS.**

*Donald B Plewes, Professor and Senior Scientist.*
Imaging Research, Sunnybrook and Women's College Health Sciences Centre, University of Toronto, Toronto, Ontario, CANADA.

Elastography originated within the ultrasound community with the goal of providing new classes of tissue contrast. Since its introduction, ultrasound (US) Elastography has seen rapid progress on many fronts with a wide range of potential clinical applications. Magnetic Resonance Imaging (MRI) can be used to image subtle tissue motions based on the detection of spin-phase in the presence of motion encoding gradients. Current applications include time-resolved quantitative blood flow imaging in 3D, tissue tracking, perfusion measurements and estimation of proton self-diffusion. A number of groups have extended the capabilities of MRI to explore its application in Elastography, coupling imaging with some form of mechanical stimulus. MRI has the advantage of sensitive motion detection in all directions with equal sensitivity but tends to be a slow imaging system in comparison to US. Imaging of harmonic shear waves or quasi-static strain throughout tissue can be imaged in 3D from which tissue modulus obtained by appropriate inverse techniques. In general, inversion of these techniques data is challenging and a number of approaches have been proposed to simplify the Elastography experiment. These include the use of a-priori information to constrain reconstruction, the use of local stimulus approaches or quasi real-time MR methods for dynamic assessment from restricted tissue volumes. However, in general, these approaches tend to parallel the imaging objectives of US Elastography.

Alternatively, MRI offers the option to image tissue features that may be related to tissue biomechanical properties but not involve an Elastography experiment. For example, through the use of appropriate pulses gradients, the statistical properties of spin diffusion through tissue can be measured. By this means, anisotropy of spin diffusion at the cellular level can be used to report tissue microstructure with complimentary information to that obtained from measures of bulk modulus. MRI offers the potential to image extremely small, high frequency mechanical motions. We have used this capability to image the propagation of ultrasound fields in a non-invasive manner throughout tissue equivalent materials. Based on the use of high frequency pulse gradients, motions in the nano-meters range has been resolved, which permits the direct probing of ultrasound interactions with tissue in a non-invasive manner. Taken together, MRI offers a unique vantage point from which tissue mechanical properties over a wide frequency range and spatial scale can be resolved. In this presentation, we will review these inter-related topics and forward speculative research questions and challenges for the application of imaging to the field of soft tissue biomechanics and Elastography.

01 **A STUDY OF MUSCLE ANISOTROPY WITH TRANSIENT ELASTOGRAPHY.**

*Jean-Luc Gennisson, Stefan Catheline, Sana Chaffaï, Mathias Fink.*
Laboratoire Ondes et Acoustique, E.S.P.C.I., 10 rue Vauquelin 75231 Paris cedex 05, FRANCE.

From low frequency shear waves velocity (150Hz), transient elastography can precisely measure the Young's modulus in isotropic soft tissues. Using polarized shear waves, the character of an anisotropic medium like muscle fiber is clearly visible. The polarization of elastic shear waves is obtained with the use of a rod (3 x 80 $mm^2$). A numeric simulation of anisotropic Green's functions for a hexagonal system, display the influence of the rod on the shear waves velocity measurement. The experiments *in vitro* led on beef muscle prove the pertinent of this simple anisotropic pattern. Moreover results *in vivo* on human biceps show the existence of low and fast shear waves.

04 **MEASURING NON-LINEAR ELASTIC PARAMETERS OF SOFT SOLIDS USING TRANSIENT ELASTOGRAPHY.**

*Stefan Catheline, Jean-Luc Gennisson, Sana Chaffaï, Mathias Fink.*
Laboratoire Ondes et Acoustique, E.S.P.C.I., 10 rue Vauquelin 75231 Paris cedex 05, FRANCE.

Pulsed elastography allows one to accurately achieve the young modulus of soft tissues from the measurement of the shear wave velocity. Because the low-frequency shear wave can easily be polarized by using a rod source, one can extend this technique to measure the elastic parameters of anisotropic media like muscles. Moreover, as it is shown in a first part, the same technique used in an acoustoelasticity-like experiment allows one to measure the non-linear third order elastic Landau coefficients A, B, C in an agar-gelatin based phantom. In a second part, the behavior of a finite amplitude transverse wave is compared to a simulation based on the modified Burger's equation. In both approaches, it appears that contrary to longitudinal wave for which even harmonics are created during the propagation, only odd harmonics are present on the displacement spectra of a finite amplitude transverse wave.

15 **A QUANTITATIVE COMPARISON OF ULTRASOUND-ELASTOGRAPHY BASED STRAIN IMAGES WITH NANO-INDENTATION BASED MODULUS IMAGES OF TISSUES.**

*S. Srinivasan[1,2], T. Krouskop[1,3] , J. Ophir[1,2].*

[1]The University of Texas Medial School, Department of Radiology, Ultrasonics Laboratory, 6431 Fannin St., Houston, TX, 77030, USA; [2]University of Houston, Electrical and Computer Engineering Department, 4800 Calhoun Rd., Houston, TX, 77204, USA; [3]Baylor College of Medicine, Department of Physical Medicine and Rehabilitation, 1333 Moursund St., Houston, TX, 77030, USA.

Conventional elastography involves static mechanical compression (external or internal) of the tissue and ultrasound to obtain RF A-lines before and after compression. Cross-correlation of the pre- and post-compression A-lines results in displacement images whose gradients produce the strain images (the elastograms). Though the strain images show structural similarities with the modulus images, they are not the exact inverse of the Young's moduli of the tissue. Quantification of the similarities between the strain and modulus images can be performed using parameters such as the first order statistics of the distributions, and second order statistics such as the cross-correlation, size, shape and orientation of the structures.

To demonstrate similarities between modulus and strain images, a nano-indenter was used to obtain modulus images of thin slices of samples (tissue and agar-gelatin mixtures) and elastograms were obtained by embedding those slices in gelatin blocks. Preliminary results indicated that a good visual as well as quantitative correspondence between structures in the modulus and strain images could be obtained at a 3-mm scale. Simulations were performed to obtain bounds on the parameters used to quantify the similarity between strain and modulus images. The experimental results corroborated the simulation results and indicated that under certain experimental conditions it is feasible to perform quantitative comparisons between strain images (using elastography) and modulus images.

Supported by National Cancer Institute Program Project Grant P01-CA64597.

18 **REALIZATION OF COMBINED DIAGNOSIS/TREATMENT STYLE BY ULTRASONIC STRAIN MEASUREMENT-BASED MECHANICAL PROPERTIES IMAGING TECHNIQUE - EXAMPLES WITH APPLICATIONS ON THE INTERSTITIAL RF-ELECTROMAGNETIC WAVE THERMAL THERAPY.**

*Chikayoshi Sumi.*
Department of Electrical and Electric Engineering, Faculty of Science and Technology, Sophia University, Tokyo 102-8554, JAPAN.

For various soft tissues (e.g., breast, liver, etc.), we are developing the ultrasonic strain measurement-based mechanical properties (shear modulus, visco-shear modulus, etc.) reconstruction/imaging technique [1]. To clarify the limitation of our technique as the diagnostic tool for differentiating malignancies, together with improving the spatial resolution and the dynamic range, we are collecting clinical mechanical property image data. Furthermore, we are applying this technique as a monitoring technique for the effectiveness of chemical therapy (e.g., anticancer drug, ethanol) and thermal therapy (e.g., RF electromagnetic wave, HIFU, etc.).

In this report, we exhibit the superiority of our technique to conventional B-mode imaging in diagnosis and monitoring for these therapies. As soft tissues are deformed in 3-D space due to externally situated quasi-static and/or low frequency mechanical sources, multidimensional signal processing improves strain measurement accuracy and reduces inhomogeneity-dependent reconstruction artifacts. We have verified this through simulations and agar phantom experiments. Particularly, here we show shear modulus images obtained in quasi-real time (several ten seconds) from *in vivo* human breast tissues and from *in vivo* human liver tissues using the conventional ultrasonic diagnosis equipment (7.5 MHz and 8.0 MHz) and a conventional Work Station (500 MHz). For instance, on *in vivo* human papillotubular carcinoma case, a shear modulus image was obtained with the very large dynamic range of 35.8 dB and with the high spatial resolution of 0.8 mm x 3.8 mm, where the tumor was estimated to have considerably high shear modulus value. The highest value of the lesion was $6.33 \times 10^6$ N/m$^2$.

Furthermore, to obtain insights into tissue electricity and thermal elasticity (e.g., shear modulus vs. electric energy, and temperature) and degeneration of protein and blood, we are conducting shear modulus imaging RF-electromagnetic wave-induced thermal lesions in calf livers *in vitro*. For instance, in RF-electromagnetic wave thermal experiment, the pair of needle electrodes with the diameters of several millimeters is used to apply the electric currents (13.56 MHz). The change of the tissue electric impedance can be automatically matched, and the currents with the high power of less than 1kW can be constantly applied. Spatio-temporal change of shear modulus due to heating and cooling down are obtained. Although the obtained sequences of B-mode images visualize generation of bubbles due to water boiling and fade of the bubbles during cooling down, we cannot specify the affected region. However, sequences of shear modulus images can well visualize the spatio-temporal change of tissue elasticity (soften and harden) and the coagulated region detected in the cutting surface including the ROI. Moreover, sequences of shear modulus images can visualize fragile. That is, when exposed energy is extra, it gets difficult to detect coagulated region. The capillary vessels (diameter being less than 1 mm) and the neighborhood tissues have interesting thermal elasticity. That is, these capillary vessels and the neighborhood tissues are normally soft compared with the surroundings, and their elasticity does not so change though they are coagulated earlier compared with their surrounding. Now, we are examining the relation between these thermal elasticity and the structure dimensions of parenchyma and vessel as well. Low-invasively obtained various insights about tissue thermal elasticity will significantly contribute to improve the efficiencies of thermal therapies. That is, to shorten the exposure time, shear modulus monitoring data can be effectively utilized as the measure for controlling the power and the foci as well.

Suitable combination of various therapy techniques with our imaging technique will open up a new clinical style allowing diagnosis and the subsequently immediate treatment. This must substantially reduce the total medical expenses.

[1] C. Sumi, and R. Kojima, Proc. of the 23rd Annual International Conference of the IEEE Engineering in Medicine and Biology Society, Istanbul, October 2001.

20 **USING ELASTOGRAPHY TO DETECT BRACHYTHERAPY SEEDS: A FEASIBILITY STUDY.**

*G. Rossignol, R. Souchon, Y.C. Angel, J.Y. Chapelon.*
INSERM, Lyon, FRANCE.

Brachytherapy, which is used to treat prostate cancer, consists of inserting radioactive cylinders into the prostate under echographic guidance. In this technique, it is desirable to insert an optimal distribution of cylinders (seeds), which requires precise information about the seed locations. However, at the present time, echography alone cannot yield this information, because ultrasound beams are reflected specularly from the metallic seeds and back-scattered wave motion cannot reach the echographic probe, unless incidence happens to be normal.

In this work, strain concentration around seeds has been investigated. Elastography can be used naturally for this purpose, since an echographic probe is already available in the clinical set-up for brachytherapy. The displacements and strains around seeds are obtained by using the finite element code ANSYS.

Experimental elastograms of cylindrical samples, made of a homogeneous gel, are generated to evaluate the experimental noise. In these experiments, one uses a 5.5MHz endorectal probe covered with a balloon allowing radial compression, which approximates closely the clinical conditions. The radial and azimuthal displacements $U_r$ and $U_\theta$ are obtained from a search of crosscorrelation maxima between the RF pre-compression signal and the RF stretched post-compression signal provided by the echograph.

A quality criterion Q, which is defined as the contrast to noise ratio, makes it possible to quantify the sensitivity of the parameters (displacements and strains) in relation to the detection of the seeds. The contrast corresponds to the difference between the peak concentration integrated over a square of a given resolution R and the average concentration at the same depth. The noise is the standard deviation calculated from the experimental data. The quantities $U_r$ and $U_\theta$ and the partial derivative $\partial U_r / \partial\theta$, $\partial U_r / \partial r$, $\partial U_\theta / \partial\theta$ and $\partial U_\theta / \partial r$ are measured.

The window-size parameter T and the slide parameter G, which define the image resolution, are chosen to be T = 1.5R and G = 0.95T. For a 5MHz probe the finest possible resolution is 0.5mm [1], of the same order of magnitude as the seed diameter (0.6 mm). In order to take into account the resolution effect, several window sizes between 0.2 and 2mm have been investigated. The first step consists of identifying the parameter for which Q reaches a maximum, given a fixed resolution of 0.5 mm. The second step consists of investigating the variations of Q as a function of R.

The feasibility of the method can be inferred from the value of Q, which must be greater than one if strain concentrations are to be detected around the seeds. Preliminary results show that the derivatives $\partial U_r / \partial r$ and $\partial U_r / \partial\theta$ are the most appropriate parameters. However, the values of Q are of order one or are less than one, independently of the value chosen for R.

It is expected that these preliminary results can be improved by using a higher frequency and thus, increasing the resolution.

[1] R. Righetti, J Ophir, P. Ktonas, Axial resolution in elastography, Ultras. Med. and Biol., Vol 28(1), pp 101-113, 2002.

37 **DEPTH-DEPENDENT STRAIN FILTER IN RADIAL COMPRESSION ELASTOGRAPHY: EXPERIMENTAL MEASUREMENTS.**

*Rémi Souchon[1], Jonathan Ophir[2,3], Seshadri Srinivasan[2,3], Jean-Yves Chapelon[1].*
[1]INSERM, Lyon, FRANCE; [2]Ultrasonics Laboratory, Dept. of Radiology, University of Texas Medical School, Houston, TX, 77030, USA; [3]University of Houston, Electrical and Computer Engineering Department, 4800 Calhoun Rd., Houston, TX, 77204, USA.

Systems proposed for prostate or intravascular elastography use a balloon to apply a radial compression. Because of the strain decay with depth, one expects the strain filter to be depth-dependent. Experimental measurements of elastographic signal to noise ratio (SNRe) were made to obtain the strain filter. The influence of depth and strain on SNRe was investigated.

Elastograms were acquired using a 5.5 MHz transducer covered by a balloon, which was inflated to apply a slight compression in a homogeneous gel-based phantom. Strain was estimated from the gradient of the displacements, using the cross-correlation technique. Lateral motion was estimated, and adaptive stretching of the post-compression signal was performed. A 5x5 median filter was applied to the displacements. A 2 mm window length and 0.4 mm window shift were used. Average compressions between 0.23 and 1.57% were applied. To investigate the influence of depth, SNRe was measured from the average and the standard deviations of the strain at constant depth. Four independent measurements were averaged. A global strain filter was estimated from the maximum SNRe on small strain intervals. It shows the best SNRe that can be achieved for a given strain, but does not account for depth. The dynamic range and the sensitivity were estimated using an $N^{th}$ degree polynomial fitted to the experimental strain filter. N was the minimal degree associated with an $R^2$ value of the fit higher than 0.80. Then local strain filters were estimated at various depths using the same technique.

The strain profiles show strain decay with depth. For average strains between 0.2 and 0.6%, SNRe is maximal in the first 15 mm, and then it decreases steadily with depth. SNRe does not change significantly for applied strain between 0.2% and 0.6%. For 0.9% and higher applied strains, SNRe drops drastically below one at low depth, while it does not change significantly at large depth. An abrupt transition can be observed between the low SNRe and high SNRe regions. The depth of the transition increases when the compression level is increased. On the global strain filter, the highest SNRe was 3.3 and was observed between 0 and 15 mm for strains close to 1%. The local strain filters at different depths show that the highest achievable SNRe decreases with depth, and is associated with decreasing optimal strains.

As expected, experimental results show the depth-dependence of the strain filter. The results also suggest that small compression steps (<0.6%) should be used to maximize SNRe, and that SNRe will be maximal near the balloon as long as low strains are used. It was expected from strain filter theory that increasing strain in low strain areas would increase SNRe until the Barankin bound is reached, but experimental data showed no significant change until the expected drop in SNRe was measured. This phenomenon might be related to depth-dependent sonographic SNR due to attenuation.

This work was supported in part by the National Cancer Institute (USA) Program Project Grant 2P01-CA64597 to the University of Texas Medical School.

66 **EXPERIMENTAL OBSERVATION OF FREQUENCY DEPENDENT CONTRAST DURING SONOELASTIC IMAGING OF BOVINE LIVER.**

*L. S. Taylor[1], P. Wang[3], D. J. Rubens[2], K. J. Parker[1].*

[1]Department of Electrical and Computer Engineering, University of Rochester; [2]Department of Radiology, Strong Memorial Hospital, University of Rochester; [3]Department of Biomedical Engineering, University of Rochester, Rochester, NY, USA.

Shear wave dispersion in the MHz ultrasonic range has been observed and reported previously in bovine liver. In this work we report an experimental observation of frequency dependent shear modulus in bovine liver. In the theory of sonoelastography three parameters affect tumor detectability and contrast: (1) lesion size; (2) relative elasticity lesion/background tissue and (3) vibration frequency. When a small lesion is surrounded by normal parenchymal tissue it will exhibit display different responses to vibration depending on its elasticity relative to the normal tissue. If the shear modulus of the lesion is lower than that of the normal parenchymal tissue the lesion will vibrate with greater amplitude than its surroundings. However, if the shear modulus of the lesion is higher than that of the normal parenchymal tissue the lesion will vibrate with lower amplitude. Calf liver was obtained from a butcher, cut into 3 cm cubes and embedded in a 0.9% agar gel within a larger bowl shaped phantom of 2% agar. The agar served as a reference material and was verified by cyclic testing to have a shear modulus that is frequency independent. Two specimens were tested. The agar-liver assembly was placed on top of a low frequency source of shear waves and imaged using sonoelastography. In both specimens when the applied vibration frequency was increased, the peak vibration amplitude of the tissue region changed from higher than agar gel, to lower than agar gel. It was concluded that the observed change in contrast implies that liver has a frequency dependent shear modulus. Further evidence for the frequency-dependent contrast behavior of agar and liver is given from mechanical tests and application of a Kelvin-Voigt fractional derivative viscoelastic model.

12 **MODULUS VARIATIONS IN BREAST TISSUES.**

*Thomas A. Krouskop[1], Roger E. Price[2], Thomas Wheeler[3], Pamela S. Younes[3].*
[1]Dept. of Physical Medicine and Rehabilitation, Baylor College of Medicine, Houston, TX, 77030, USA; [2]Dept. of Veterinary Medicine and Surgery, University of Texas M.D. Anderson Cancer Center, Houston, TX, 77030, USA; [3]Dept. of Pathology, Baylor College of Medicine, Houston, TX, 77030, USA.

During the development of elastographic technology, soft tissues have been modeled as homogeneous, isotropic, linear elastic materials. However, soft tissues, like other composite materials, have a hierarchical structure and the mechanical properties associated with the material depend on the scale used to make the measurements. In this study, different size compressors were used to test a series of tissue samples from the breast and explore at what scales homogeneity of the material can be assumed and if modulus variations in the tissues may contain information that can be used to uniquely identify the type of material being compressed.

Tissue samples were cycled at a rate of 1 hertz over the strain range of 5-10 percent with a 4 mm diameter compressor. This compressor diameter was selected after testing 20 samples of tissue to determine the smallest compressor, which produced data that did not vary more than 5% at different locations within the sample. In this work, a 2 mm diameter compressor has been used to extend the original work. The 2 mm diameter compressor was selected as the smallest compressor that did not punch through the tissue at the maximum strain level. The displacement and load data were recorded using a servo hydraulic Instron Testing System and analyzed to calculate the modulus at 4 mm centers across the surface of the tissue slices. Single line modulus maps of 10 ductal carcinomas *in situ*, 14 infiltrating ductal carcinomas, 28 normal glandular tissue samples, 20 breast fat samples and 5 fibroadenomas have been created. Typical data from these experiments are summarized in the following table.

| Tissue Type | Median Stiffness (kPa) | Stiffness Variation (kPa) |
|---|---|---|
| Normal glandular tissue | 46 | ±15 |
| Breast fat | 18 | ±4 |
| Ductal carcinoma *in situ* | 24 | ±10 |
| Infiltrating ductal carcinoma | 84 | ±25 |
| Fibroadenoma | 120 | ±6 |

The data collected in this study show that malignant breast tumors have measurable stiffness variations when their stiffness is measured with a 2 mm compressor; but so does normal glandular tissue. To test the significance of the variations, Hartley's F test was performed on the data. This test indicates that the differences in the variations exhibited by normal glandular tissue and ductal carcinoma *in situ* are not significant at $p < 0.1$ nor are the variations exhibited by breast fat and fibroadenoma at $p < 0.1$. So using just the magnitude of the stiffness variation within the tissue may not provide sufficient information to differentiate between normal and malignant tissues; but, when coupled with the median stiffness of the tissue, it seems that differentiating between tissue types in the breast may be feasible using the information which can be collected from a strain elastogram.

This work was been supported in part by NIH Grant P01-CA64597.

69 ***IN-VITRO* BREAST TISSUE ELASTIC MODULUS MEASUREMENT USING UNIAXIAL INDENTATION TECHNIQUE.**

*A. Samani, D.B. Plewes.*
Department of Medical Biophysics, Sunnybrook and Women's College Health Sciences Centre, University of Toronto, Toronto, Ontario, CANADA.

Mechanical properties of biological tissues have been a subject of interest in various medical applications. In the medical imaging community, a new imaging technique called elastography has been developed for imaging soft tissue elasticity. This technique can be used effectively provided the elasticity of normal and various abnormal tissues are known. Modeling soft tissue deformation has recently been incorporated in other applications such as image co-registration.

Such models require the biomechanical parameters of the tissues and their reliability is highly dependent on the accuracy of these parameters. Measurement of the biomechanical parameters of soft tissues with conventional techniques is very difficult, as providing *ex-vivo* homogeneous specimens with regular geometry to ensure stress and strain uniformity is almost impossible. Furthermore, excising and separating breast tumors from the surrounding normal tissue is usually not allowed because it would lead to difficulties in determining the tumors' margins. To address these difficulties, we have developed uniaxial indentation techniques to measure the elastic modulus of normal breast tissues and tumors *in-vitro*. One technique applies uniaxial indentation on excised tissues while the other indents the tissue of interest without excising it from the surrounding tissues. Although it can be used for normal tissues, the latter was designed to measure the elastic modulus of tumors because tissue slices coming from surgery would remain intact. The stress and strain distribution throughout the tissue specimen is non-uniform in both techniques. Therefore, inverse models were developed to calculate the elastic modulus using the measured force-displacement data obtained from the indentation experiments. Results obtained from ~70 normal and abnormal breast tissue specimens will be presented. Although the focus of this research is breast tissue elasticity measurement, the concept can be applied to other biological soft tissues.

22 **ULTRASONIC MEASUREMENT OF *IN-VITRO* TRANSIENT AND DEPTH-DEPENDENT COMPRESSIVE STRAINS OF ARTICULAR CARTILAGE IN COMPRESSION.**

*Yongping Zheng[1], Dongmei Luo[2], Jun Shi[1], Anita W.T. Shum[1], Ling Qin[3], Arthur F.T. Mak[1].*
[1]Rehabilitation Engineering Center, The Hong Kong Polytechnic University, Kowloon, HONG KONG; [2]Department of Sports Anatomy, Beijing University of Physical Education, Beijing, 100084, CHINA; [3]Department of Orthopaedics and Traumatology, The Chinese University of Hong Kong, NT, HONG KONG.

Articular cartilage (AC) is a biological weight-bearing tissue covering the ends of articulating bones within synovial joints. Because of the spatial variations of the orientation of the collagen fibrils and the proteoglycan concentration, and the water content, the mechanical properties of the cartilage are different at different depths. Subtle changes in AC structure or composition can lead to degeneration of cartilage such as in osteoarthritis (OA), and ultimately significant compromises in joint functions and thus patient disabilities. The changes in cartilage during OA may first occur in the superficial layer of AC. This change is very important for the detection of early OA, but very difficult to be determined. Ultrasonic characterization of AC has been the subject of many recent investigations due to its nondestructive manner and penetration ability. The purpose of this study was to investigate the depth-dependent material properties of AC in both equilibrium and transient situations using an ultrasound-compression method.

Fresh mature bovine patellae were used in this study. Osteochondral cylinders were cored out from the flat area of the patellae, and a cartilage disk specimen with thin layer of bone was prepared from each cylinder. An ultrasound-compression testing system was developed to compress AC specimens meanwhile to allow the collection of ultrasound signals scattered from AC tissues. The tests were performed in saline solution with the AC disk placed at the center of a specimen platform with the cartilage surface facing the compressor. 50 MHz focused ultrasound beam transmitted into the cartilage through a hole at the center of the specimen platform and through the thin layer of bone attached to the AC tissues. The specimen was first compressed by 0.1mm in approximately 30 sec then followed by a force-relaxation period. The ultrasound signals and the load applied were collected in real time during the compression and force-relaxation. The transient deformations of tissues at different depths of AC were determined from the ultrasound reflection signals using a cross-correlation tracking technique.

It was observed that the strains in the superficial zone were much larger than those in the middle and deep zones in an equilibrium state. For two steps of 0.1mm compression, the average strain at the superficial 0.2 mm thick layer ($0.35 \pm 0.09$) was significantly ($p < 0.05$) larger than that at the subsequent 0.2 mm thick layer ($0.05 \pm 0.07$) and those at deeper layers ($0.01 \pm 0.02$). It was demonstrated that the tissues inside the AC layer would keep moving in the force-relaxation phase after the compression was completed. While this process can be predicted by the biphasic theory, there is lack of experimental findings to support it in the literature. It was also observed that the tissue deformations at different depths of AC were much more evenly distributed before force-relaxation.

A dynamic ultrasound measurement system has been successfully developed for the study of the transient deformations of tissues at different depths of AC specimens in compression. It provided a novel approach to determine not only the depth-dependent but also transient responses of AC tissues. Such a technique would also be attractive for the assessment of early OA due to the nondestructive manner of ultrasound. It could also be used for the assessment of other types of biological tissues, biomaterials and bioengineered tissues.

Acknowledgement: This work is partially supported by the Research Grant Council of Hong Kong (PolyU21/96M, PolyU5199/02E).

57 **ELASTIC MODULI OF CONNECTIVE TISSUES DETERMINED BY SCANNING ACOUSTIC MICROSCOPY.**

*J. Lawrence Katz[1, 2], Paulette Spencer[1], Yong Wang[1], Ajay Wagh[3], Sauwanan Bumrerraj[4], Tsutomu Nomura[5], Hans-Joachim Hein[6].*

[1]University of Missouri-Kansas City Dental School, Kansas City, MO, USA; University of Texas Medical School, Houston, TX, USA; [3]University of Memphis Engineering School, Memphis, TN, USA; [4]Khon Kaen University Medical School, Khon Kaen, THAILAND; [5]Niigata University Dental School, Niigata, JAPAN; [6]Martin-Luther-University Halle-Wittenburg Medical School, Halle/Saale, GERMANY.

Scanning acoustic microscopy (SAM) at frequencies from 400 MHz to 800 MHz has been used to measure the elastic moduli of various connective tissues: human femoral cortical and trabecular bone; demineralized human dentin collagen with and without adhesive infiltration; and human dentin both fully mineralized and partially demineralized. Two different SAMs were used in these studies. An Olympus UH3 SAM (Olympus, Co., Japan) at 400 MHz (nominal lateral resolution 2.5 ϒm) was used in all the above studies. In addition a Kraemer KSI SAM 2000 (Kraemer Scientific Co., Germany) was used in a qualitative study of the anisotropy and aging of both human female and male femoral cortical bone. All the bone specimens in both the Olympus and Kraemer studies were cut with a diamond blade under flowing water and maintained at 4°C until thawed for analysis. The dentin and dentin collagen studies required complementary Raman and SEM analyses in order to confirm the chemical and morphological characteristics of the specimens. Extracted unerupted human third molars stored at 4°C in 0.9% w/v NaCl containing 0.002% sodium azide were used for all of the dentin studies. The occlusal one-third of the crown was sectioned perpendicular to the long axis of the tooth by means of a water-cooled low-speed saw (Beuhler). Parallel cuts, 1to 2 mm deep, were made perpendicular to this surface. Each slab was placed in a vial containing 10 ml of 05M EDTA (pH 7.3). This solution was changed on alternate days and continued for 7 days. A Raman spectrum of each specimen was acquired and the absence of spectral features associated with the mineral (P-O band at 960 cm-1) indicated that the mineralization process was complete. The demineralized dentin collagen was dehydrated through an ascending series of ethanols: 70, 95, 100 %; the total dehydration time was 36 hours. The specimens then were immersed in Single bond adhesive (3M Corp. St. Paul, MN). The demineralized dentin collagen /adhesive specimens was kept in the dark for 72 hours and then polymerized with visible light. These specimens were then mounted on the Olympus UH3 SAM for the micro-mechanical measurements. The study was performed using the 400 MHz Lens; scan widths ranged from 250 ϒm to 2 mm. Calibration curves based on known materials were used to obtain the following Young's moduli: E = 1.76 GPa for demineralized dentin collagen; E = 1.84 GPa for demineralized dentin collagen infused with adhesive; E = 5.84 GPA for partially demineralized dentin; and E = 28 GPa for fully mineralized dentin, a value comparable to those obtained for human bone in the above studies.

Supported in part USPHS DE 12487.

68 **QUANTITATIVE ULTRASOUND METHOD FOR MICROSTRUCTURE-ACCOUNTING ANALYSIS ON THIN SLICES OF BREAST TISSUE.**

*Jun Liu, Mauro Ferrari.*
Biomedical Engineering Center, The Ohio State University, Columbus, Ohio, USA.

Tissue physical properties have been studied for diagnosis purposes because change in these properties signifies disease conditions. In this study we have developed a novel ultrasonic system that is capable of characterizing the mechanical and micro-structural properties of tissue through in combination of a theoretical model that solves the forward wave propagation problem in microstructure-complex biological media. This system includes an experimental setup to detect the different mechanical responses from normal and diseased tissue, and a theoretical model to predict tissue mechanical responses determined by micro-level mechanisms.

Surgical snap-frozen malignant and normal breast tissue from a few subjects were obtained. The tissue was cut to 150-micron as thin slices, and placed between two pieces of glass to create sandwich structures. The sandwich structure was then sealed for waterproof and mounted on a table in a water tank. Two broadband transducers (central frequency 10 MHz) were used to generate and receive ultrasonic signals that interacted with the three-layered sandwich structure. The reflection spectra were obtained through standard FFT. A discrete-based microstructure-accounting mechanical field theory, named doublet mechanics [1], was employed to predict the responses of tissue by solving the elastic plane wave propagation problem in microstructured, multi-layered media. The preliminary studies showed that the spectra from normal and malignant tissue were appreciably and consistently different. The quantitative information on the micro-level mechanical and structural properties was made available through an inverse algorithm that searches in the parameter space to generate the set of values that allows the optical agreement between the model prediction and the experimental data. Several of the reconstructed parameter values showed significant difference comparing normal and malignant tissue. A differential study was also carried out to compare the results from the doublet mechanics model with those from conventional continuum mechanics. We concluded that the ultrasonic system developed in this study was sensitive in detecting the differences in the physical properties of normal and malignant tissue; and microstructural differences in the tissue appear to make significant contribution to the difference in their mechanical responses.

[1] Mauro Ferrari et. al., Advances in Doublet Mechanics, Springer, 1997.

67 **NON-INVASIVE ELASTICITY IMAGING IN SMALL VESSELS.**

*Nicolas Pivert[1], Roch Maurice[1], Michel Daronat[1], F. Stuart Foster[2], Guy Cloutier[1].*
[1]Laboratory of Biorheology and Medical Ultrasonics, Research Center, University of Montreal Hospital; and Department of Radiology, University of Montreal, Québec, CANADA; [2]Department of Medical Biophysics, Sunnybrook and Women's College Health Sciences Centre, University of Toronto, Toronto, Ontario, CANADA.

Background: Pathological conditions often induce changes in biological tissue stiffness. Tissue elasticity imaging was proposed as a method to detect hard tumors in the breast, prostate and other organs. The characterization of plaque based on intravascular elasticity imaging is another growing field of interest. In the present study, non-invasive ultrasound elastography was developed for the purpose of studying small vessels in humans and small animals. An emerging field is the use of this method for vascular phenotyping in mice.

Methods: All experiments were performed *in vitro* on small vessels (1.5 mm lumen diameter and 1.5 mm wall thickness). Polyvinyl alcohol cryogel (PVA) was used to create vessels embedded in an agar matrix. The phantoms were insonified with an ultrasound biomicroscanning system (Visualsonics, Toronto, Canada) providing access to the radio-frequency (RF) raw data. The measurements were performed with a single-element oscillating transducer with a central frequency of 32 MHz, and a bandwidth at –6 dB of 100%. The frame rate of the instrument was around 8 Hz. Radial stress was applied within the lumen of the phantom by applying incremental static pressure with a column of water-glycerol. The decorrelation of the RF signals and elastograms were computed over two consecutive recordings obtained at a given pressure gradient. The elastograms were computed with a Lagrangian tissue motion estimator (Maurice and Bertrand, IEEE Trans. Med. Imag., 1999). Finite-element simulations (ANSYS, Canonsburg, PA, ver. 6.0) were performed to validate the strain images.

Results: The Lagrangian estimator allowed the detection of displacements of the order of 3–10 % in the longitudinal axis of the ultrasound beam. The full 2D correlation patterns and displacements were available for analysis. High correlations were detected all over the 2D plane. The displacements varied as a function of depth for the agar matrix, whereas constant movements were detected within the inner PVA gel. Qualitatively, a good correlation was obtained between the finite-element modeling and elastograms.

Conclusions: The signal-to-noise ratios of the elastograms were satisfying for this *in vitro* study. Currently, the method is limited by the frame rate of the instrument. Improving the frame rate or the access to ECG-gated RF signals should allow obtaining *in vivo* elastograms in humans and small animals.

02 **ULTRAFAST IMAGING OF SHEAR WAVES INDUCED BY ACOUSTIC RADIATION-FORCE IN SOFT TISSUES.**

*Jérémy Bercoff, Michael Tanter, Sana Chaffaï, Mathias Fink.*
Laboratoire Ondes et Acoustique, E.S.P.C.I., 10 rue Vauquelin 75231 Paris cedex 05, FRANCE.

Several techniques based on acoustic radiation force have been proposed to induce shear waves in soft tissues. In our experiments, an ultrafast scanner is used to both generate and detect shear wave propagation. Focusing an amplitude modulated high intensity ultrasonic beam at a chosen location creates the shear wave. Our ultrafast scanner allows applying very high ultrasound frame rates (up to 5000 images/s) in order to follow the shear wave propagation (whose velocity reaches a few meters/s). Displacements induced by this wave are measured using a cross-correlation technique, giving a complete 2D reconstruction of the propagation in the medium. By solving the shear wave propagation inverse problem, we can compute the shear elastic modulus map of the medium. This technique could represent a new step for transient elastography where the shear waves are usually generated by external excitations. The electronics allow us to induce several shear sources at different time and locations in order to compute a real “shear wave beamforming”. Measurements have been performed in several soft tissue mimicking phantoms with different elastic properties and in beef muscles. A finite differences simulation has been used to support our experimental results and to evaluate the heating induced by the acoustic focused beam generating the force.

11 **INFLUENCE OF NON-UNIFORM TRANSDUCER ROTATION ON THE CORRELATION COEFFICIENT IN INTRAVASCULAR ULTRASOUND ELASTOGRAPHY.**

*C. Perrey, T. Neumann, H. Bany Salameh, H. Ermert.*
Institute of High Frequency Engineering, Ruhr University, Bochum, GERMANY.

Coronary artery diseases are among the highest mortality factors in industrialized countries. Due to that the analysis of coronary arteriosclerosis became of great interest in recent years. Intravascular Ultrasound (IVUS) is considered as a gold standard for the morphological assessment of arteriosclerotic lesions. Acute coronary syndromes are often caused by unstable coronary plaques, but these lesions cannot be reliably distinguished with conventional IVUS. It was shown that Intravascular Elastography could be used for plaque characterization by visualizing the mechanical properties of plaque tissue. This method heavily depends on the correlation between consecutively acquired RF image data sets. IVUS catheters with a rotating shaft are known to show artifacts due to non-uniform transducer rotation (NURD), especially when a catheter angularity is present. This effect can degrade the correlation between acquisitions, leading to errors in Elastography images. In this work the impact of non-uniform transducer rotation in conjunction with catheter angularity is investigated. Phantom experiments are performed with different angles of catheter bends, the normalized correlation coefficient of baseband data is evaluated as an indicator for the errors caused by non-uniform rotation.

Methods: A Clearview Ultra IVUS scanner (Boston Scientific Corp., USA) is used for the experiments, operating at 30 MHz. Analog RF data is sampled with an A/D converter (Gage Applied Inc., Canada). Trigger sequence generation and compensation of depth dependent attenuation are realized by custom-made hardware. Vessel-mimicking homogeneous phantoms are created from polyvinyl cryogel. The phantom experiments are performed in a water tank without intraluminal pressure difference between acquisitions. Thus image pairs of the same region of interest without tissue motion are compared. The local distribution of the normalized correlation coefficient of corresponding A-Lines is then calculated using sliding windows with a local axial shift correction. This is a measure of image similarity. Any deviation from the coefficient's maximum is thus caused by non-uniform rotation. Four catheters are used for the evaluation with a variety of shaft bends. To simulate the angles that can occur with *in vivo* experiments the shaft is placed in guiding catheters of different angularity (Cordis Corp., USA).

Results and Conclusions: In our investigation the mean correlation coefficient is > 0.95 with all tested catheter bends. Some images of the correlation coefficient distribution show spoke patterns apparently caused by lateral decorrelation due to non-uniform rotation. These patterns do not depend on a specific catheter angularity. In these spoke areas the correlation coefficient locally drops below 0.85, which decreases SNR in elastograms. Axial shift estimation in these areas shows higher standard deviations, but still yields acceptable results. Thus elastography is practicable for rotating transducer IVUS, SNR might be further increased by lateral correction.

A project of the Ruhr Center of Competence for Medical Engineering (KMR), funded by the German Federal Ministry of Education and Research (bmb+f grant No. 13N8079).

21 **DEVELOPMENT OF AN ULTRASOUND ELASTOMICROSCOPY (UEM) SYSTEM: PRELIMINARY RESULTS.**

*Yongping Zheng[1], Amena Saïed[2], Britta Jaffre[2], Tracy Lu[1], Lori Bridal[2], Pascal Laugier[2], Arthur F.T. Mak[1].*

[1]Rehabilitation Engineering Center, The Hong Kong Polytechnic University, Kowloon, HONG KONG; [2]Laboratoire d'Imagerie Paramétrique, UMR CNRS 7623 – University of Paris VI, Paris France, 15, rue de l'école de médecine, 75006 Paris, FRANCE.

Ultrasound tissue elasticity imaging has attracted much attention during the last decade. Previous elasticity imaging research, typically operating in the 1 to 10 MHz ultrasound frequency range typically used for medical applications. The resolutions of systems in this frequency range are on the order of several millimeters, which are not sufficient for application to skin, articular cartilage, scar tissues, or other fine structures. Ultrasound biomicroscopy in the 20 MHz to 100 MHz frequency range has been widely used for the high-resolution characterization (axial resolution approximately 100 to 20 μm in soft tissues) of both engineering materials and biological tissues. Adding elastographic measurements to ultrasound biomicroscopy could potentially provide complementary high-resolution information linked to material stiffness.

In the current study, we developed an ultrasound elastomicroscopy system consisting of a compression system and a backscatter ultrasound microscope system. A calibrated compression system was developed for application to various types of small tissue specimens (cartilage, skin). We demonstrated that this system could be used in conjunction with mechanically scanned ultrasound biomicroscopy systems. The specimen platform, in-series with a load cell on its bottom, could be moved up and down via a hydraulic mechanism. The specimen was installed on the top of the specimen platform, and covered by a rigidly fixed plate. As the specimen was pressed against the plate, the load applied to the specimen was measured by the load cell. A 1mm-wide slit in the compressing plate allowed the passage of the ultrasound beam from the ultrasound biomicroscopy system. Preliminary tests were performed using specimens of mouse skin and bovine and human patellar cartilage. Using the ultrasound biomicroscope system, a 35-MHz focused ultrasound transducer was placed so that its beam was perpendicular to the specimen and compressor surfaces, centered between the edges of the 1-mm slit and focused within the region of the tissue to be imaged. A computer-controlled stepper-motor system allowed the movement of the transducer in 50 μm steps along the slit length. At each scan site, the backscattered radio frequency signal was digitized at 500 MHz using a digital oscilloscope and transferred to a computer for off-line processing. Local tissue strain maps were constructed by applying a cross-correlation tracking method to signals obtained at the same site at different compression levels.

Scanning was repeatable as demonstrated by high correlation of radio frequency signals obtained from the same site during different scans ($R^2 > 0.97$). Progressive compressions could be applied to the specimen smoothly using the compression system. It was verified that any side-lobe echoes that may have originated from the passage of the sound beam through the slit were negligible in the studied tissue region (SNR > 26 dB). More uniform compressions were obtained using plastic film covering of the skin and the overlying thin bone layer of the cartilage than when these materials were not placed between the specimen and the compressing plate. The strains at different depths can be obtained for both cartilage and skin specimens under step compression. It was noted that the ultrasound scattering signal from cartilage was approximately 20dB smaller than that from skin tissues even without the bone layer.

This work is partially supported by the PROCORE France/Hong Kong Joint Research Scheme (F-HK12/01T) and Research Grant Council of Hong Kong (PolyU5199/02E).

26 **DEALING WITH CARDIOVASCULAR MOTION FOR STRAIN IMAGING OF THE LIVER.**

*Alexander F. Kolen, Jeffrey C. Bamber.*
Joint Department of Physics, Institute of Cancer Research and Royal Marsden NHS Trust, Sutton, Surrey SM2 5PT, UNITED KINGDOM.

Elastography, which uses ultrasound to image tissue strain due to an applied displacement, can display stiff tumours and heat-ablated tissue with high contrast in static situations. However, its application to liver *in vivo* is problematic because the organ is already in motion. In a previous study, we characterised the cardiovascular component of liver motion, with the objective of understanding it well enough to propose strategies for its correction and to simulate it in computer and phantom experiments when testing these strategies. The temporal-spatial relationship of liver motion, its repeatability, and its variation from liver segment-to-segment and individual-to-individual, were studied using proper orthogonal (eigenvector) decomposition. The motion patterns of some liver segments were found to be complex, but they were also cyclic and repeatable, indicating that motion compensation could be possible. This paper presents a study in which we evaluated experimentally the following strategies for dealing with cardiovascular motion for strain imaging in the liver: (1) Extrapolation and subtraction of pre-existing motion if an external stress is applied. (2) Identify a time window in the heart cycle where the motion is negligible compared to the externally applied motion. (3) Identify periodic moments in the heart cycle for combined phase-shifted multistep strain estimation. (4) Utilise the cardiovascular motion to produce internal strain without external stress. The evaluation was carried out in part using a phantom, containing soft gelatine with a stiffer inclusion, that was exposed to simulated cardiac motion while being manually palpated using the ultrasound imaging transducer. For relatively simple sinusoidal motions, the technique of extrapolating the cyclic motion while the tissue is exposed to external palpation performs well. However, because cardiovascular motion is more complex, our extrapolation algorithms need to be improved to predict the motion sufficiently in order to use this technique *in vivo*. Analysing the liver motion in volunteers, we found that not all subjects displayed motion patterns that contained time-windows of sufficient length to palpate and derive the tissue strain. This depended on heart rate and the characteristics of the cardiac cycle. Strain images derived from combined phase-shifted multistep strain estimation suffered from displacement tracking inaccuracies due to a low correlation between frames. This technique was not robust and therefore not considered useful for *in vivo* strain imaging. The displacements in the liver due to cardiovascular activity produced measurable strains but the strain values were very close to the strain sensitivity obtained from an experimentally measured strain filter for the system used, suggesting that changes to improve strain sensitivity would be desirable. As a result of this study, we suggest different strategies dealing with cardiovascular motion for different parts of the liver. However, if a single general approach to deal with cardiac motion is desired, we suggest that for each elastogram pre-existing motion data be acquired prior to compression. Using these data, parameters can be derived for extrapolation to subtract the pre-existing motion during external compression.

25 **ELASTICITY IMAGING USING TACTILE SENSORS.**

*Armen Sarvazyan.*
ARTANN Laboratories, Inc., Lambertville, NJ, USA.

This paper describes several new modalities of Elasticity Imaging (EI), which are based on the use of force sensor arrays measuring surface pressure patterns over the compressed tissue. One of such modalities is Mechanical Imaging (MI) also called Tactile Imaging. The essence of MI is analysis of the changes in stress pattern on the surface of the compressed tissue while moving the force sensor array over the examined tissue. Temporal and spatial changes in the stress pattern provide information on the mechanical structure of the examined tissue and enable 3-D reconstruction of internal structures and mechanical heterogeneities in the tissue.

Several prototypes of prostate MI and breast MI systems were developed and extensively tested in laboratory and clinical studies. The trials demonstrated the effectiveness of the prototypes in visualizing tissue mechanical structure and quantitative assessment of hard lesions. Laboratory studies of the MI devices included development of phantoms that realistically mimic tissue viscoelastic properties covering the range of Young's modulus from 5 to 500 kPa. The search for an adequate material yielded the elastomers Semicosil 921 and Semicosil 932 produced by Wacker Silicones Co, WI. These elastomers are clear, transparent, two-component materials, which are chemically inert in the cured state. They allow production of tissue phantoms with the required degree of hardness by varying the ratio of two components in the mixture. The skin was simulated by a compatible material, SWS-960 Dispersion Coating (Wacker Silicones Corporation, WI) with Young's modulus of the order of 1MPa.

The last version of the breast MI device comprises of a hand held probe connected to a laptop computer. The capacitive force sensor array that is used in the probe is designed and manufactured by PPS Inc., of California. The sensors provide the possibility of measurements in the range of pressures typical for palpation examination, which can be roughly estimated as 0.1 - 10 kPa.

The prostate MI System comprises a hand held transrectal probe with a position sensor and a force sensor array mounted in the tip of the probe connected to a computer via an interface electronic unit. The miniBird motion tracker of Ascension Technologies, MA, tracks the motion of the probe relative to the transmitter mounted on a belt fastened to the patient's back during an examination.

Another EI modality using force sensor array is Acousto-Mechanical Imaging (AMI). AMI includes unique features of both MI and conventional ultrasonic EI: the data on the stress pattern measured by the force sensor array of MI complement the ultrasonic data on strain. The paramount element of an AMI device is a force-sensing array incorporated on the ultrasonic probe surface contacting the tissue. This combined ultrasonic and pressure array probe is, therefore, capable of simultaneous registration of surface stress and internal strain patterns in tissue necessary for subsequent unambiguous and artifact free elasticity imaging.

Acknowledgements: This work was supported in part by the NCI NIH grants R43 CA91392-01, R44 CA69175, R43 CA82620 and R43 CA94444-01.

27 **HUMAN AND COMPUTER-ASSISTED PERCEPTION OF ELASTIC LESIONS IN ULTRASOUND IMAGES.**

*Naomi R. Miller, Jeffrey C. Bamber.*
Joint Department of Physics, Institute of Cancer Research and Royal Marsden NHS Trust, Sutton, Surrey SM2 5PT, UNITED KINGDOM.

As implemented hitherto, elasticity imaging has required substantial modification to standard ultrasound imaging procedures and equipment. However, the mechanical properties of tissues are already assessed in routine ultrasound examinations by subjective interpretation of tissue motion seen in real-time B-mode images (movies) during palpation (applied strain ~10%). This method is referred to as relative motion assessment (RMA). In a previous study, we performed an objective comparison between the quality of the information provided by elastography and that provided by RMA. Perception experiments were conducted using simulated strain images and RMA movies (consisting of 2 frames). Observer ability to detect lesions of different sizes and Young's modulus contrast was investigated using a two-alternative forced choice method. There was no ultrasound echo contrast between the lesion and the background, so for RMA the lesion could only be detected due to the different motion of the speckle within it, compared to the motion of the background speckle. Contrast thresholds for lesion detection by RMA were within the range of contrasts that have been measured *in vitro* for breast tumours. However, contrast thresholds for elastography were substantially lower. For example, for the lesion containing 77 speckle cells, the average threshold value was 35 times lower for elastography than for RMA.

The technique of elastography can therefore be regarded as using a computer to extract dynamic information that is difficult to perceive (tissue strain) and redisplaying it in a form that is easy to perceive (grey scale intensity). Our aim in the present study was to determine whether alternative processing methods might exist that will also enhance the perception of tissue strain but that could be implemented on the envelope-detected data obtained using RMA. This approach would enable the use of standard imaging procedures and equipment and would retain, in the same image, the sonographic features that are already useful for tumour detection and diagnosis. We hypothesised that the task of perceiving relative motion between lesion and background might be facilitated if the background were rendered stationary. We therefore developed a simple algorithm that corrected the post-deformed B-scan for global distortion on the assumption that the elasticity distribution was uniform. In a movie of the pre-distorted and distortion-compensated images, an isolated elastic non-uniformity (i.e., the lesion) is seen as a moving object in a stationary background with the amplitude of the motion determined by the elastic contrast. We refer to this novel processing technique as global distortion compensation (GDC). A further perception study, similar to that described above, demonstrated that GDC enhanced lesion detectability relative to RMA. For example, for the lesion containing 77 speckle cells, the average modulus contrast threshold for GDC was a factor of ~6.5 lower than for RMA. Although the degree of improvement was not as great as that observed for elastography, it was sufficient to suggest that the technique would be worthwhile implementing for clinical evaluation, especially since in practice, perception would be further enhanced by the presence of sonographic information.

Acknowledgements: Medical Research Council and Institute of Cancer Research.

28 **TEMPERATURE IMAGING BY MEANS OF ULTRASONIC STRAIN ESTIMATION FOR THE GUIDANCE OF FOCUSED ULTRASOUND SURGERY.**

*Naomi R. Miller[1], Jeffery C. Bamber[1], Gail R. ter Haar[1], Paul M. Meaney[2].*
[1]Joint Department of Physics, Institute of Cancer Research and Royal Marsden NHS Trust, Sutton, Surrey SM2 5PT, UNITED KINGDOM; [2]Thayer School of Engineering, Dartmouth College, Hanover, NH, USA.

Ultrasonic estimation of heat-induced echo strain has been suggested as a technique for the guidance of focused ultrasound surgery (FUS) by predicting the location of the thermal lesion before it is formed. Since the speed of sound in tissue varies with temperature, and the scanner assumes a constant sound speed, changes in transit time due to tissue heating are interpreted as axial displacements. The gradient of local displacement (strain) is proportional to the local temperature rise. Previous investigations of this technique have produced optimistic results since they were carried out with rubber phantoms and used room temperature, rather than body temperature, as the baseline. The aim of the present study was to determine, through modelling and *in vitro* experimentation, the likely feasibility of using ultrasonic temperature imaging to detect and localise the focal region of the heating beam for a medium with a realistic temperature dependence of sound speed subjected to a realistic temperature rise.

The specific objective of the simulation study was to determine the minimum sonographic signal-to-noise ratio ($SNR_S$) required to visualise the heated region for liver of varying fat content. Due to the small (0.5%) change in sound speed at the focus, the maximum strain to be measured was 0.5%. Therefore the threshold $SNR_S$ for normal liver (low fat content) was found to be at least 20dB. This implies that temperature imaging in this tissue type will only be feasible if the effects of electronic noise can be minimised. For liver of intermediate fat content, the hot spot could not be visualised even when the echo data were noise-free. Tissues with a very high fat content are likely to represent the most favourable conditions for temperature imaging.

Preliminary investigations were then carried out using *in vitro* bovine liver from a healthy animal (i.e., low fat content). For technical reasons, the starting temperature was room temperature rather than body temperature. However, the temperature rise induced by the FUS system (~10°C) was chosen so as to generate a maximum strain of 0.5–1%. A radiofrequency ultrasound image was acquired before and after heating using a 3.5 MHz linear array transducer. The displacements were measured using 1-D cross-correlation and the strains were computed using least squares strain estimation. This was repeated in several tissue samples and in all cases the strain images possessed excellent spatial and contrast resolution. The elastographic signal-to-noise ratio was higher than expected from the simulation study. A characteristic pattern of strain noise due to thermoacoustic refraction was visible in the tissue distal to the heated region. However, the appearance of this artifact was not disturbing in the sense that the position and spatial extent of the hot spot could still be easily identified. We conclude that the proposed technique is feasible in liver of normal fat content, although additional sources of error that will arise *in vivo* (in particular cardiac-induced motion) are likely to require correction.

Acknowledgements: EPSRC and Institute of Cancer Research.

32 **REAL-TIME ROBUST IMAGING OF TISSUE ELASTICITY BASED ON THE EXTENDED COMBINED AUTOCORRELATION METHOD.**

*Tsuyoshi Shiina[1], Makoto Yamakawa[1], Naotaka Nitta[1], Ei Ueno[2], Takeshi Matsumura[3], Satoshi Tamano[3], Tsuyoshi Mitake[3].*

[1]Institute of Information Sciences & Electronics, University of Tsukuba, JAPAN; [2]Institute of Clinical Medicine, University of Tsukuba, JAPAN; [3]Research & Development Center, Hitachi Medical Corporation, JAPAN.

The technique of elasticity imaging is a potential modality for directly measuring material parameters related to tissue elasticity and can subsequently be applied for cancer diagnosis. Therefore, various techniques to estimate strain distribution have been proposed. Recently, some proposals have reached the stage of being developed as practical systems. Practical systems applied in clinical use require real-time processing and ease of measurement. We have therefore developed a method suited to clinical use with real-time processing and robustness for free manipulation of the probe.

The method is based on the Combined Autocorrelation Method (CAM) previously developed for estimating strain distribution. It produces an elasticity image with high-speed processing and accuracy and achieves a wide dynamic range for strain estimation by combining envelope correlation and phase shift while avoiding the aliasing of the Doppler method. However, CAM is based on 1-D processing and thus assumes that the probe compresses the tissue in the beam direction without sideslip. For freehand compression, it is important to avoid errors due to the decorrelation caused by tissue sideslip in clinical use. To overcome this, we extended the CAM to be robust for sideslip and suited to freehand compression while preserving the advantages of the CA method. The new method overcomes the sideslip problem by doing a 2-D or 3-D search in the lateral or elevation directions. Also, the extended CA method is faster than the conventional spatial correlation method because we calculate a correlation coefficient for only the 1/2 wavelength interval in the direction of the axis. The 1/2 wavelength interval enables us to optimize computing efficiency without phase aliasing.

We were able to demonstrate the effectiveness of the proposed method with computer simulations. Specifically, we compressed a cubic tissue model with sides of 60mm in the axis direction, and apply a lateral and elevation displacement of up to 5%. RF signals were generated before and after the deformation with a center frequency of 5.0 MHz. The simulation results verified that the new method could cope with lateral displacement and attain more precise and stable estimates of strain than conventional methods.

To verify the feasibility of the new method, we realized an imaging system by adopting its algorithm and using a scanner operating at 7.5MHz and a PC with dual Pentium 4 processors. The probe presses the body in free-hand operation, and the echo signals that correspond to multi-frame images are captured by the PC. As a result, it takes around 0.2 seconds to generate an elasticity image and a 2D image. High-quality *in vivo* elasticity images for breast and liver were easily obtained from more than 20 volunteer subjects. The details will be reported in another work submitted to this conference.

We will further investigate how to quantify the elasticity parameters, including estimation of the elastic modulus and analyze the correspondence between the elasticity image and pathology.

35 **ACOUSTIC RADIATION FORCE IMPULSE IMAGING: IMAGING THE VISCO-ELASTIC PROPERTIES OF TISSUES.**

*Kathy Nightingale, Steve McAleavey, Deborah Stutz, Mark Palmeri, Roger Nightingale, Rex Bentley, Gregg Trahey.*
Duke University, Durham, NC, USA.

Acoustic Radiation Force Impulse (ARFI) imaging is a new modality that utilizes brief, high energy, focused acoustic pulses to generate radiation force in tissue, and conventional diagnostic ultrasound methods to detect the resulting tissue displacements in order to image the mechanical properties of tissue. Tissue displacement magnitude is inversely related to local tissue stiffness, and the temporal response of the tissue is related to its viscosity. Tissue displacements *in vivo* approach 15 microns and tissue heating is less than 1 degree Celsius. The duration of tissue excitation is 1 msec, and tissue recovery to its original position typically occurs within 1 to 2 msec. ARFI data acquisition is performed in real-time using a modified Siemens Elegra scanner that allows user control of the beam sequences, transmit intensities, and provides access to the raw Radio Frequency data.

Results from ongoing human *in vivo* and *ex vivo* studies evaluating the correlation between ARFI images and tissue pathology will be presented. *In vivo* images of human breast, thyroid, abdomen, and skeletal muscle demonstrate good correlation between structures on matched B-mode and ARFI displacement images. Parametric images of the local tissue response to radiation force that demonstrate differences between tissues include: maximum displacement, the time it takes the tissue to reach its maximum displacement, and the recovery time constant. In general, fatty tissues move farther than fibrous or muscular tissues, and fibrous tissues recover more slowly than fat or muscle. In some cases, malignant breast lesions appear larger in the ARFI images than they do on matched B-mode images. The spatial and temporal patterns of radiation force induced target motion in phantoms and *in vivo* for varying transmit aperture characteristics, transducer frequencies, and target characteristics will be discussed. Images of radiation force induced shear waves both *in vivo* and *ex vivo* will also be presented. Tissue structural boundaries are apparent in the propagating shear wave images. Clinical applications, system optimization, tissue heating, and real time implementation will be discussed.

36 **ACOUSTIC RADIATION FORCE IMPULSE IMAGING OF ARTERIES.**

*Gregg Trahey, Jeremy Dahl, Steve McAleavey, Caterina Gallippi, Kathy Nightingale.*
Duke University, Durham, NC, USA.

Arteries stiffness increases with age and with smoking, diabetes, hypercholesteremia, and other disease states. Atherosclerotic plaques are generally quite stiff, though they may include soft, lipid- rich regions. Currently, global and local arterial stiffnesses are estimated by a wide range of methods, including ultrasonic measurements of arterial distensibility and pulse wave velocity, and by conventional B-mode imaging. We have investigated the spatio-temporal response of *in vivo* arterial tissues to brief, localized applications of radiation force. These acoustic radiation force impulse (ARFI) images were acquired over extended vessel regions throughout the cardiac cycle coincidentally with B-mode images and ECG recordings. The images were filtered to remove physiologic vessel motion. These images reveal good definition of the medial and adventitial vessel layers and reveal similar vessel stiffness, for a given patient, over extended vessel lengths and through the cardiac cycle. We discuss the applications of ARFI imaging in the measurement of diffuse and focal atherosclerosis.

40 **THE APPLICATION OF RADIATION FORCE FOR DYNAMIC ASSESSMENT OF THROMBOSIS.**

*W.F. Walker, F. Viola, M.D. Kramer, M.B. Lawrence.*
University of Virginia, Biomedical Engineering, Room 2123, 415 Lane Road, Charlottesville, VA, 22908, USA.

Inappropriate blood coagulation plays a central role in heart attack, stroke, deep vein thrombosis, and a broad variety of other medical conditions. While the failure to clot, such as that associated with hemophilia, has been well studied and can be relatively easily diagnosed in the clinic, a heightened propensity to clot, which is seen in the above conditions, is much harder to diagnose. A variety of techniques have been proposed to measure the viscoelastic properties of forming thrombi. Unfortunately, none are clinically valuable, perhaps because they tend to disrupt the clot structure as it forms. We have developed a technique that uses acoustic radiation force to measure the viscoelastic properties of forming thrombi without significantly disrupting its forming structure. We apply a series of acoustic pulses to generate radiation force and induce displacement. We then process the echoes received from these pulses to form time-displacement curves at each location within the blood sample. Non-linear parameter estimation is used to determine the viscoelastic parameters of a modified Voigt model, which give the best fit to experimental data. Our modified Voigt model consists of a spring in parallel with a dashpot, all in series with a mass.

We have performed experiments on blood samples from a number of subjects in their 20s. We are able to reliably estimate displacements as low as 0.5 microns while generating displacements on the order of 30 microns. We perform repeated measurements on a given sample over a period of 70 minutes to determine the dynamic changes which occur in blood viscoelastic properties during thrombosis. Data follows expected trends and coagulation continues throughout the experiment, suggesting that our method does not disrupt clot formation.

We were quite surprised to find that the rate of clotting was significantly faster in some of our blood samples. After eliminating possible sources of experimental error we discussed our result with the subjects. One indicated a recent medical history including a clotting disorder. While he is currently taking antithrombogenic medication, it appears that our technique identified a continued propensity to clot in this subject. We are continuing human trials and will seek to identify the causes of variation between clotting rates. Our initial results suggest that radiation force may offer a novel and valuable method for assessing the thrombogenicity of blood samples.

41 **LOCALIZED HARMONIC MOTION IMAGING: THEORY, SIMULATIONS AND EXPERIMENTS.**

*Elisa Konofagou, Kullervo Hynynen.*
Focused Ultrasound Laboratory, Department of Radiology, Brigham and Women's Hospital - Harvard Medical School, Boston, MA, USA.

Several techniques have been developed in an effort to estimate mechanical properties of tissues. These techniques typically estimate static or harmonic motion resulting from an externally or internally applied mechanical stimulus. The method of Ultrasound-Stimulated Acoustic Emission utilizes two overlapping ultrasonic beams with slightly different frequencies in order to generate an oscillatory radiation force. This radiation force perturbs the tissue locally and converts into an acoustic source, whose amplitude is recorded by a hydrophone. In this paper, we will discuss the advantages of utilizing a new technique that performs RF signal tracking in order to estimate the localized oscillatory motion resulting from the harmonic radiation force produced by two focused ultrasound transducer elements with overlapping beams oscillating at distinct frequencies.

Finite-element and Monte-Carlo simulations were performed in order to characterize the range of oscillatory displacements produced by a harmonic radiation force. The frequencies investigated ranged from 200 Hz to 800 Hz. The stiffness of the target ranged between 20 and 80 kPa. In the experimental verification, three transducers were utilized: two single-element transducers operating at 3.75 MHz with a focal depth equal to 9 mm, and a 16-element PZT composite transducer (Imasonics, Inc.) with a frequency equal to 1.1 MHz focused at a depth of 100 mm and operating at pulse/receive mode. The pulse duration was equal to 0.28 ms and a PRF of 3.1 kHz was used. The RF data acquired were of duration equal to10 ms and acquired at a sampling frequency equal to 50 MHz. The Imasonics transducer was placed between the other two transducers so as to be aligned perpendicularly to their overlapping foci. Agar gels (containing glass beads of 71 micron in size for scattering) of four different stiffnesses, i.e., 7.1, 25.9, 55.2 and 94.6 kPa, were utilized in order to determine the effect of stiffness on the motion amplitude. Estimates of the displacement relative to the initial position (i.e., at the onset of the application of the radiation force) using a window size of 1-2 mm were obtained during the application of the radiation force that oscillated at frequencies ranging between 200 Hz and 800 Hz.

In the simulations, the estimated oscillatory displacement spanned from –800 to 600 microns and the frequencies of excitation could easily be estimated from the temporal variation of the displacement. In addition, a frequency upshift (on the order of tens of Hz) was estimated with stiffness increase. Furthermore, an exponential decrease of the displacement amplitude with stiffness was observed at all frequencies investigated. An M-mode version to depict both the spatial and temporal variation of the locally induced displacement was used. In the experiments, the resulting amplitude of the harmonic displacement estimated oscillated at the same frequencies and ranged from -300 to 250 microns for ultrasound intensities that ranged between 380 and 1400 W/cm$^2$ and an exponential decrease of the displacement amplitude with the gel stiffness was also observed.

These preliminary results demonstrate the feasibility of imaging localized harmonic motion as induced by an oscillatory ultrasound radiation force. Due to the highly localized and harmonic nature of the estimated response, this technique may be proven highly suitable for accurate estimation of the elastic modulus variation in tissues due to disease.

46 **REAL-TIME IMAGING OF LOCAL TISSUE MOTION FOR ULTRASONIC VISUALIZED PALPATION.**

*S. Yagi[1], S. Akimoto[2].*
[1]Medical Imaging Laboratory, Meisei University, Tokyo, JAPAN; [2]Department of Surgery, Yokohama General Hospital, Yokohama, JAPAN.

Introduction: Despite of currently developed ultrasonic imaging of static tissue strain or elasticity, it is still hard to undergo a clinical application to abdominal tissue in the physiological state because of dynamical stress change due to the pulsatile circulation through living tissues. Thus we pursued the straightforward but physiological and dynamic image of small tissue motion in this study. This dynamic imaging of local tissue motion was realized by utilizing real-time local cross-correlation processing of successive 2D complex speckle echo signals. The displayed images from phantom experiment and clinical data proved that this real-time imaging was a practically promising approach toward an advanced version of conventional clinical palpation coupled with physician's active diagnosis for tissue characterization.

Method: For real-time imaging of local tissue motion along the beam axis, the 2D RF echo signal from a conventional array transducer is A-D converted (12-bit, 4 times the center frequency of transducer), detected in a complex version and put into successive frame memory. Thus a couple of successive 2 time-phases of 2D complex echo at each corresponding scan lines of the frames are processed to detect the longitudinal axial motion from their local cross-correlation by real-time operation of custom-designed Field Programmable Gate Array circuit. The total performance of this imaging system was visually examined under phantom experiments, in which an internal stress source can be manually simulated by injecting water into a thin rubber tube embedded through the phantom substance. Furthermore as a clinical estimation, continuous physiological changes in velocity and acceleration around a systolic peak are visualized by processing successive real-time echo frames obtained from the hepato-hemangioma.

Results: The remarkable propagation and reflection of shear waves caused by flush-injection of water were observed across the phantom medium with a velocity of 80 cm/s in each opposite direction alternatively. The slowly injected water visualized the continuous change in surrounding velocity on the rubber tube. For clinical data the distribution of small displacement inside the hemangioma was reflecting that the filling motion of blood by surrounding arteries continued up to just-before the systolic peak pressure phase, which was followed by the shrinking motion of hemangioma beyond the peak phase. Furthermore a typical zero-acceleration profile evaluated just before the systolic peak appeared inside the hemangioma and a drastic change to a negative acceleration profile at the systolic peak occurred, which are complying with clinical diagnosis in fine accuracy.

Conclusion: The proposed imaging for local dynamics in abdominal tissue was proved to be a promising step to Ultrasonic Visualized Palpation.

Acknowledgement: This work was partly supported by Toyota Physical and Chemical Research Institute in 2001.

50 **TIME-DOMAIN MODELS TO EXPLAIN MEASUREMENTS OF COMPLEX-VALUED SHEAR MODULUS AS A FUNCTION OF FREQUENCY IN ISOTROPIC SOFT TISSUES.**

*Travis Oliphant[1], Randy Kinnick[2], James F. Greenleaf[2], Alex Dresner[3], Richard Ehman[3].*
[1]Brigham Young University, Provo, UT, 84602, USA; [2]Ultrasound Research Laboratory, Mayo Foundation, Minneapolis, MN, USA; [3]Magnetic Resonance Research Laboratory, Mayo Foundation, Minneapolis, MN, USA.

Quantitative Vibration Elastography allows estimation of mechanical modulus from displacement measurements on materials that have been excited using low-frequency mechanical waves. In isotropic soft-tissues at low frequencies (10-1000 Hz), only shear-modulus has been reliably estimated. Several reconstructions methods are available that can recover a complex-valued shear modulus from the Fourier transform of time-domain measurements of displacement.

Complex-valued shear modulus in the frequency domain arises from potentially two sources: loss in the time-domain and/or a time-domain elastic response that must be convolved with the displacement rather than a constant that is simply multiplied by the displacement. A general model for loss in the time-domain is the convolution of the strain-rate with a causal "loss relaxation" function. Measurements of the frequency response of the shear modulus provide a method to compare different elastic response functions and loss relaxation functions.

In this presentation, frequency response measurements from different agar and B-gel phantoms are compared from 50-800 Hz against several simple but general time-domain models of the elastic response function and the loss relaxation function. It is found that the elastic response function can be well modeled as an impulse (delta) function with height given by the (static) shear modulus, while the loss-relaxation function can be modeled with a causal generalized Gaussian or a generalized Cauchy with height, width, and power parameter dependent on the material in question. The potential of using these parameters for improved tissue characterization is described.

51 **A REVIEW OF ELASTICITY IMAGING IN SKELETAL MUSCLE. PART 1 – BIOMECHANICAL MODELS.**

*Stephen F. Levinson[1], Sheryl M. Gracewski[2]*

[1]Department of Physical Medicine and Rehabilitation, Department of Electrical and Computer Engineering, and Department of Biomedical Engineering, University of Rochester School of Medicine and Dentistry, 601 Elmwood Avenue, Box 664, Rochester, NY, USA; [2]Department of Mechanical Engineering and Department of Biomedical Engineering, University of Rochester School of Engineering and Applied Sciences, Rochester, NY, USA.

Although tissue elasticity imaging is generally thought of in terms of its ability to detect hard, malignant lesions, some of the earliest work in the field was done in skeletal muscle. Skeletal muscle is of unique interest in that its physiology is inherently mechanical and elasticity imaging provides the promise of a true functional imaging modality for the study of human performance, sports medicine and rehabilitation. Methods developed for use in skeletal muscle might also find application in cardiovascular imaging. Unfortunately, muscle is an inherently complex tissue, being dynamic, anisotropic and nonlinear. To date virtually all measurements of muscle elasticity using methods of elastography (sonoelastography and MRE) have been static and relied on assumptions of isotropy, linearity and homogeneity. In Part One of this presentation, we will review the history of ultrasonic elasticity measurement in muscle, starting with the field of muscle mechanics and some of the earliest work in acoustic microscopy. We will delve into the first attempt to apply anisotropic linear equations to ultrasonic data. We will then explore the 3 static methods of sonoelastography that have found application in the study of muscle and look at the results obtained by our group and by others. In each case, we will examine the biomechanical models employed from a theoretical standpoint and using finite element simulations. The advantages and disadvantages of each method will be explored and the potential for dynamic application will be evaluated.

The authors acknowledge the support of the NIH (#1R01HD35638) and of the Rochester Center for Biomedical Ultrasound.

52 **A REVIEW OF ELASTICITY IMAGING IN SKELETAL MUSCLE. PART 2 – DYNAMICS AND PHYSICAL ACOUSTICS.**

*Stephen F. Levinson[1], Sheryl M. Gracewski[2]*

[1]Department of Physical Medicine and Rehabilitation, Department of Electrical and Computer Engineering, and Department of Biomedical Engineering, University of Rochester School of Medicine and Dentistry, 601 Elmwood Avenue, Box 664, Rochester, NY, USA; [2]Department of Mechanical Engineering and Department of Biomedical Engineering, University of Rochester School of Engineering and Applied Sciences, Rochester, NY, USA.

Although most models of tissue elasticity that have been applied to muscle imaging are static models, muscle is an inherently dynamic tissue with physical properties that can change in a period of milliseconds. It is the dynamic nature of muscle that is of particular importance in functional imaging, and methods of elasticity imaging in muscle will ultimately have to involve dynamic models of elasticity. In Part Two of the presentation, we will explore existing, largely 1-dimensional models of muscle viscoelasticity and evaluate their applicability to existing methods of elastography. We will also delve into the previously unexplored realm of the physical acoustics of muscle, which could have a substantial impact on the elasticity-imaging field as methods become more refined.

We will explore the phenomenon of muscle fiber resonance that gives rise to audible sounds during muscle contraction, and the field of acoustic myography that has arisen from this. We will also explore the response of the muscle stretch reflex to vibration as measured using electromyography and consider the effect that this could have on dynamic elastic modulus measurements. Finally, we will discuss the approaches that are currently under investigation for dynamic tissue elasticity imaging and consider how these might deal with the reality of the physical acoustics of muscle *in situ*.

The authors acknowledge the support of the NIH (#1R01HD35638) and of the Rochester Center for Biomedical Ultrasound.

54 **PHANTOMS FOR ELASTICITY IMAGING.**

*Timothy Hall.*
University of Kansas Medical Center, Department of Radiology, Kansas City, KS, 66160-7234, USA.

We have been investigating materials for use in elasticity phantoms. Among the primary criteria for these phantoms are that they must have bulk mechanical and acoustical properties that mimic tissue, and these properties must be predictable based on constituent materials and verifiable with independent measurements.

We previously reported the use of agar gels and gelatin gels cross linked with formaldehyde and paraformaldehyde. Initial studies employing 1Hz cyclic loading of 10% strain demonstrated that agar samples have nonlinear stress-strain relationships. And exhibit small hysteresis, whereas gelatin samples exhibit linear stress-strain relationships with little hysteresis. Extended studies of the gelatin materials demonstrated that their compression modulus continued to increase 1 yr post manufacturing. Although that stiffness was predictable, the large increase in modulus with time was undesirable.

More recently we have been using glutaraldehyde as a cross linking agent in gelatin phantoms. With this agent, gelation occurs very fast (sometimes too fast), and the gel reaches its ultimate modulus in a few days post-manufacture. However, the rapid cross lining induced with glutaraldehyde can create problems in trying to create a bond between a target and its background. We will discuss these observations and make recommendations for manufacturing techniques and gelatin and glutaraldehyde concentrations required to obtain a desired compression modulus.

We have also tested the use of mixtures of gel types (e.g., type-A and type-B gelatin, gelatin and agar). Although these combinations have been reported in the literature, their stress-strain relationships are not well documented and the results will be surprising to many. That relationship provides evidence for the nature of the gel matrix that is formed as a result of gel mixtures.

29 **STABLE HETEROGENEOUS PHANTOMS FOR TESTING PERFORMANCE OF US AND MR ELASTOGRAPHY SYSTEMS.**

*EL Madsen,[1] GR Frank,[1] TA Krouskop,[2] T Varghese,[1] F Kallel,[3] TA Stiles[1], J Ophir[3].*
[1]Medical Physics Department, University of Wisconsin, Madison, WI, USA; [2]Department of Physical Medicine, Baylor University, Houston, TX, USA; [3]Department of Radiology, Ultrasonics Laboratory, University of Texas Medical School, Houston, TX, USA.

A need exists for temporally stable tissue-mimicking phantoms that contain inclusions for testing performance of elastography systems. The elastic contrast ratio (C) between inclusion and surroundings should remain unchanged so that it would not be necessary to keep producing replacement phantoms. (C = Young's modulus (E) for the inclusion divided by that for its surroundings.) If possible, phantoms should be tissue-mimicking for both US (ultrasound) and MR; i.e., in addition to Young's moduli, ultrasound propagation speed and attenuation slope and the NMR relaxation times, $T_1$ and $T_2$, should be representative of those in soft tissues.

Two types of materials have been developed. One type consists of safflower-oil-in-gelatin emulsions that allow control of E via oil concentration. The addition of formaldehyde raises the melting point to over 100°C, and 1% thimerosal acts as a preservative. These materials are most suitable for US since the $T_2/T_1$ ratios are too large (typically 0.5). Values of E range from 15 to 120 kPa, as measured on an Instron® testing machine. Eight monthly measurements showed that E rises about 20% over the first 4 months and decreases by about 20% over the second 4 months. However, the value of C for materials in heterogeneous phantoms remained essentially invariant.

These heterogeneous phantoms consist of cubes of background material, 10 cm on a side, with a 1 or 2 cm diameter cylindrical inclusion with a higher E value than the background. While the value of C remained invariant over many months, the size and shape of the inclusions were also stable; thus, no long-term diffusion effects occur.

Five replicas of the first version of such phantoms were produced. The background material is 32% safflower oil and the inclusion is pure gelatin (0% oil). Over a 9-month period, the C values were 1.64, 1.71, 1.63, 1.73, 1.79 and 1.80 (±0.10). Another monitored phantom has a background of 50% oil and an inclusion of 0% oil and C of 2.8.

The second type of material is an aqueous agar/gelatin in which the dry weight gelatin is constant throughout any phantom. Addition of $Cu^{++}$-EDTA provides controlled lowering of $T_1$, and the $T_2/T_1$ ratios mimic tissues. Thus, the phantoms are suitable for US and MR. Long-term stability results have been similar to those for the oil-in-gelatin phantoms. Four phantoms have been made with C values ranging from 1.3 to 7.

Recently, a prototype spherical lesion detectability phantom was made from the oil-in-gelatin type materials for testing the performance of US elastography. Nine unique versions of spherical inclusions are represented with diameters of 3, 4, or 6 mm and C values estimated at 2.8, 2.3 or 1.7. (Young's moduli have not yet been measured at this writing.) There are 3 of each version of spherical inclusion, all at different depths (2.5, 5.0 and 7.5 cm) in the 10x10x10 $cm^3$ cube. Initial elastograms were made using an Aloka SSD 2000 (Aloka Inc., Tokyo, Japan) scanner with a 7.5 MHz linear array. None of the spheres with C estimated at 1.7 were detected, although all spheres with C estimated at 2.8 or 2.3 were detected.

Acknowledgement: The work performed at the University of Texas site was supported in part by National Cancer Institute Program Project P01-CA64597.

62 **USING THE ATL HDI-1000 ULTRASOUND SCANNER FOR TISSUE ELASTICITY IMAGING.**

*Ajay Anand[1], Peter Kaczkowski[1], Ron Daigle[2], Lawrence Crum[1].*
[1]Center for Industrial and Medical Ultrasound/Dept. of Electrical Engineering, University of Washington, Seattle, WA, USA; [2]Intersonics, 22126 NE 62nd Place, Redmond, WA, 98053, USA.

Introduction: The ability to acquire and process RF data at high frame rates while the tissue is subject to external compression is important for generating strain elastograms with a high SNR and to reduce artifacts resulting from temporal decorrelation. We have developed a software system to perform RF data acquisition using a commercially available clinical ultrasound scanner (ATL HDI-1000, Philips Medical Systems, Bothell, WA). The scanner functions on a new software dominant architecture, thus permitting straightforward external control of its operation as well as relatively easy access to RF data. The features of the system and the results obtained in an experiment to generate strain elastograms are discussed below.

Methods: In our setup, a PC running the software program developed in Labview™ is the master controller. It sends control signals to the HDI-1000 via Telnet to initiate acquisition of RF data frames at periodic intervals based on the frame rate programmed by the user. Since the entire acquisition is controlled externally by the PC, control of other devices (e.g. external compressor typically used to induce motion under controlled conditions in elastography) can be easily incorporated.

Experiments to generate strain elastograms were conducted. A tissue-mimicking phantom with an inclusion (polyacrylamide gel with 7% acrylamide concentration for the background and 15% for the inclusion making it stiffer) loaded with scatterers was subject to external compression in small steps using a mechanical fixture holding the scanhead (L11-5, Philips Medical Systems) attached to a 3-D motion stage. The acquisition sequence begins with a telnet command sent by the program to the HDI-1000 to acquire a RF data frame. After the frame has been acquired (50-100 ms), it sends a command to the motion stage to move the transducer towards the phantom, compressing it by a specified amount. The above sequence is repeated until the phantom has been subject to the desired total displacement with RF data frames collected in between displacement steps. The RF data collected was processed offline in MATLAB™ and strain elastograms were generated.

Results: The PC-based software system completely synchronizes the RF data acquisition with the motion controller. Frame rates of 10 fps were obtained for a lateral image width of 3.5 cm and imaging depth of 5.5 cm using the L11-5 scanhead. The frame rate increases to 30 fps on using a reduced lateral image width thus showing promise for freehand elastography applications. The working of the system will be presented in detail. Strain elastograms computed by processing the RF data obtained with this system will also be presented.

Conclusion: A software based RF data acquisition system for the ATL HDI-1000 platform has been successfully developed. A number of research groups currently own the ATL HDI-1000 to meet RF data acquisition needs. Our software helps make the ATL HDI-1000 a versatile data acquisition platform and demonstrates the potential for its use in elastography applications.

Acknowledgements: This work is partially supported by the U.S. Army MRMC/TATRC (DAMD 17-002-0063, DAMD 17-02-2-0014) and Office of Naval Research (N00014-01-G-0460).

06 **CARDIAC ELASTOGRAPHY: 2D IMAGING OF MYOCARDIAL STRAIN.**

*T. Varghese[1] , J.A. Zagzebski[1], P. Rahko[2], C.S. Breburda[2].*
[1] Dept. of Medical Physics, [2] Dept. of Cardiology, The University of Wisconsin-Madison, Madison, WI, 53706, USA.

Evaluation of cardiac function by imaging the mechanical properties of heart muscle over the cardiac cycle may provide significant new information for diagnosis of coronary artery disease. Cardiac elastography is a promising new method for obtaining strain information that can be used for diastolic staging and quantitative stress echocardiography. Our objectives are to evaluate elastography for imaging the displacement and strain in cardiac muscle in 2-D for diagnosis of cardiac disease. The hypothesis is that cardiac elastography can provide quantitative and translation-independent measures of myocardial strain during the cardiac cycle, thereby providing a 2-D method for characterizing regional myocardial function and clearly depicting areas of hypokinesia and akinesia associated with ischemia and infarction.

A GE Vingmed Vivid 5 ultrasound system was used to obtain 2-D gray scale and RF frames, the latter used for strain estimation. A cross correlation algorithm was used to estimate tissue displacements, whose axial gradient yielded the strain. The RF frame rate was 50/second, which enables tracking of small compressions of the heart muscle and limits motion artifacts. Two patients (P, 1 m, 1 f, mean age 71.5 ± 4.9 yrs) diagnosed with coronary artery disease and dilated cardiomyopathy, and three healthy male volunteers (V, mean age 20.3 ± 1.57 yrs) were imaged. Two observers performed qualitative visual assessments (QVA) of 1-second strain image loops. Spatial and temporal “A-line” interrogation of strain images allowed the quantitative assessment of anatomical and dynamic strain throughout the cardiac cycle. In the parasternal long axis view tissue strain of the anteriospetal (AS) wall, the posteriormedial papillary muscle (PM), and the posterior wall (PW) were measured at end systole (ES) and end diastole (ED). QVA revealed peak strain in normals occurred at the papillary muscle and posterior wall in end systole and was more evenly distributed in end diastole. Both patients, however, exhibited peak strain at the PM in end systole.

Cardiac-elastography may avoid the disadvantage of observer-dependant judgment of myocardial contraction and relaxation by providing quantitative indices of regional myocardial function. In this talk, we will present cardiac-elastograms obtained in all the imaging views of clinical interest. This 2-D strain imaging technique could be incorporated into future clinical scanners.

*This work is supported by start-up funds provided to Dr. Varghese by the Department of Medical Physics, Medical School and Graduate School at the University of Wisconsin-Madison.

10 **ELASTOGRAPHY IN ANIMAL MODELS: LESION DETECTION AND COMPARISON WITH SONOGRAPHY.**

*C. R. B. Merritt[1], C. Dascenzo[1], F. Forsberg[1], J. Ophir[2].*
[1]Thomas Jefferson University, Philadelphia, PA, USA; [2]University of Texas Medical School, Houston, TX, 77030, USA.

Purpose: Studies have shown the feasibility of obtaining high quality elastograms of prostate and renal tissue *in vitro* and from normal and abnormal breast tissue *in vivo*. In order to further extend experience with elastography, and to define its clinical potential, *in vivo* and *in vitro* evaluation of elastography in animal models is required. Our studies seek to establish and optimize techniques for acquiring elastograms from living animals to image normal and abnormal tissues.

Materials and Methods: Elastograms were generated using an automated device by direct scanning on the liver in ten rabbits and six swine. All studies were conducted using an ATL HDI 1000 scanner and an L7-11 linear array transducer. In swine scanning was performed under general anesthesia directly on the exposed surface of the liver in suspended respiration. Lesions in rabbits were evaluated *in vivo* and after sacrifice of the animal. In rabbits,VX-2 tumors produced by injection of tumor cells directly into the liver were evaluated *in vivo* and *in vitro*. In swine, lesions ranging from 5mm to 15mm in diameter created by ethanol injection or radiofrequency ablation were evaluated. When possible, lesions were identified with sonography and elastograms of areas of interest were then obtained. In some cases lesions were essentially invisible on sonograms and elastograms were obtained from known injection sites marked on the surface of the liver. A variety of precompression and displacements were evaluated and the resulting elastograms were compared with sonograms and measurements of gross pathology at autopsy.

Results: In rabbits, VX-2 tumors appeared as extremely subtle focal lesions on conventional sonograms. Elastograms of these tumors showed high contrast focal lesions with increased stiffness. Correlation of lesion size measured on elastograms with direct measurements of the tumors was good. In both rabbits and swine, lesions created by radiofrequency ablation or ethanol injection were not identifiable by conventional ultrasound imaging. All lesions were readily identifiable in the elastograms, appearing as well-defined high contrast lesions of increased stiffness. Lesions created by RF ablation were visible with sonography, although findings were subtle. Elastograms of these lesions also showed high contrast with distinct borders. Correlation of elastographic measurements and gross tissue pathology of all lesions was excellent.

Conclusions: Our results indicate the feasibility of obtaining high contrast elastograms of focal hepatic lesions *in vivo*. Lesions imaged by elastography were seen with greatly enhanced contrast compared to conventional sonograms. Elastographic findings also showed excellent correlation with direct measurement of lesion size. Major problems encountered in obtaining quality elastograms *in vivo* include artifacts due to respiratory motion and difficulty in localizing small lesions with ultrasound.

Acknowledgments: This work was supported by National Cancer Institute Program Project Grant P01-CA64597.

13 ***IN VIVO* ELASTOGRAPHY OF THE BREAST: PRELIMINARY FINDINGS.**

*Christopher B. Merritt[1], Colleen Dascenzo[1], Flemming Forsberg[1], Jonathan Ophir[2].*
[1]Thomas Jefferson University, Philadelphia, PA, USA; [2]University of Texas Medical School, Houston, TX, USA.

Purpose: Studies have shown the feasibility of obtaining high quality elastograms of prostate and renal tissue *in vitro* and from normal and abnormal breast tissue *in vivo*. In order to further extend experience with elastography to define its clinical potential, *in vivo* evaluation of elastography in patients is required. Our studies seek to establish and optimize techniques for acquiring elastograms from patients with breast masses.

Materials and Methods: Elastograms were generated using an automated device to control transducer positioning and displacement during the acquisition of ultrasound radiofrequency data for construction of elastograms using methods previously reported by Ophir et. al. (Proc. Inst. Mech. Eng. [H], 1999;213:203-33). Ultrasound data were collected using an ATL HDI 1000 scanner and an L7-11 linear array transducer. Patients with breast masses identified by palpation or mammography were selected for evaluation. All patient studies were conducted under an IRB approved protocol and written consent was obtained. Experiments were designed to evaluate the feasibility of obtaining images of breast lesions with automated control of the transducer for a variety of combinations of tissue displacement (0.25 to 1.25%) and precompression (0.0 to 10.0%). A total of 6 patients have been evaluated to date with tissue diagnoses of cyst, fibroadenoma, and invasive carcinoma.

Results: Lesions seen with ultrasound were visualized in the elastograms in all six patients, with variable quality. In three of the six patients (one cancer, one fibroadenoma, and an intraductal papilloma) images were judged to be of good to excellent quality. In the remaining three (two with fibroadenomas and one with fibrocystic change), image quality was compromised by artifact. Image quality appeared to be more affected by motion artifact, that by variation of data acquisition parameters.

Conclusions: Our results, though preliminary, indicate the feasibility of obtaining high contrast elastograms of focal breast lesions *in vivo*. Lesions imaged by elastography were seen with enhanced contrast compared to conventional sonograms. Elastographic findings also showed good correlation with direct measurement of lesion size. Major problems encountered in obtaining quality elastograms *in vivo* include artifacts due to motion and difficulty in localizing small lesions with ultrasound.

Acknowledgments: This work was supported by National Cancer Institute Program Project Grant P01-CA64597.

14 **REAL-TIME ULTRASOUND ELASTICITY IMAGING IN THE BREAST CLINIC – WORK IN PROGRESS.**

*WE Svensson[1], A Connors[1], S Comitis[1], D Chopra[1], D Sinnett[2], P Forouhi[2], G Layer[2], C Lowery[3], P Von Behren[3].*

[1]Departments of Radiology and [2]Surgery, Charing Cross Hospital (Hammersmith Hospitals Trust), Imperial College School of Medicine, London, UNITED KINGDOM; [3] Siemens Medical Systems Ultrasound Group, USA.

Aim: To evaluate real time elasticity imaging on a clinical ultrasound system used in routine breast ultrasound imaging in a dedicated symptomatic and breast screening unit.

Method: Real Time Strain Imaging (Software from Hall & Zhu of KUMC) was implemented on a Siemens Elegra ultrasound scanner. Breast imaging performed with VFX 13-5 and 7.5L40 linear array b transducers. Patients attending for routine breast ultrasound in the work up of mammographic or palpable focal breast abnormalities are invited to have breast strain imaging at the end of their ultrasound examination if there is a focal abnormality. The strain images are assessed during the clinic and correlated with subsequent histology and follow up.

Results: To date 78 lesions in 75 patients have been assessed and correlated with the subsequent diagnosis - 16 cancers, 32 fibroadenomas, 11 cysts, 8 ANDI, 5 inflammatory masses, 2 intramammary lymph nodes, 2 normal breasts, 1 radial scar and 1 gynaecomastia.

15 cancers were larger than the grey scale image while one (mucinous cancer) was the same size. 27 fibroadenomas had a smaller area of stiffness, 2 were the same size and 3 were larger than the equivalent grey scale image (three were in fatty breasts while two were larger than the area assessed for stiffness). Some fibroadenomas had focal areas (poles) of stiffness at their margins. Compared with the grey scale image strain images of cysts were smaller and tended to have a halo or banana of increased stiffness.

Inflammatory masses and non-specific change such as ANDI and microcystic change were mainly smaller (9) with 3 equal and 1 larger area of stiffness compared with the grey scale image. The two intramammary lymph nodes had a larger region of stiffness than their grey scale image while the gynaecomastia, normal breast tissue and radial scar all had no discernable focal area of stiffness to equate with the grey scale or palpable abnormality.

Visibility of benign lesions in the strain image ranged from indistinct to very obvious, while the 16 cancers ranged from fairly obvious to obvious. The image quality varied with the number of lesions tested by the operator, showing that these initial results have been obtained on a varied learning curve.

The results suggest greater accuracy than may have been expected. This could be explained by observer bias due to knowledge of grey scale findings and clinical details except that there was some divergence of strain results from grey scale and colour Doppler results. The other more likely explanation is that the real time results allowed immediate repetition of the elasticity examination if areas of stiffness were equivocal – this allowed greater certainty of the absence of stiffness or the presence of focal stiffness.

Conclusion: These initial results support earlier work by members of this group with this system and a similar system developed at the Royal Marsden, London. The elasticity images would have changed the diagnosis of an echogenic cyst from solid to cystic, would have excluded the presence of cancer in the gynaecomastia which had a worrying grey scale and colour flow appearance, and would have increased diagnostic confidence in most of the fibroadenomas and all the cancers.

30 **ULTRASOUND ELASTICITY IMAGING OF DEEP VENOUS THROMBOSIS.**

*J.M. Rubin[1], S. Aglyamov[2], A.R. Skovoroda[2], D.D. Myers, Jr.[3], S.K.Wrobleski[3], T.W. Wakefield[3], M. O'Donnell[2], S.Y. Emelianov[2].*

Departments of [1]Radiology, [2]Biomedical Engineering and [3]Surgery, University of Michigan, Ann Arbor, MI, 48109, USA.

Introduction: Each year, hundreds of thousands of patients suffer from blood clots originating in the deep veins of the legs, and "compression" ultrasound has become the primary diagnostic screening test for deep venous thrombosis (DVT). Compression ultrasound is performed by marching down a subject's leg imaging the femoral vein in transverse orientation while simultaneously deforming the vein with the ultrasound imaging scanhead. If the walls collapse there is no thrombus, if they don't collapse, there is. However, once detected, acute, subacute and chronic DVT should be differentiated to identify the most appropriate treatment. Up until now, there has been no reliable method for making this distinction. Since thrombi always harden over time, it may be possible to age DVT using ultrasound elasticity imaging, thus providing an important clinical tool to both assist DVT diagnosis and manage therapy.

Materials and Methods: We have performed elasticity imaging on a series of Sprague-Dawley rats with experimentally generated 2-day (acute), 6-day (subacute), and 9-day (chronic) old inferior vena caval (IVC) thrombi. In addition, two patients with DVTs of known ages were imaged: one subject had a clinically chronic, at least, 3-year old thrombus, while the second subject's thrombus was considered subacute at 25 days old. A Siemens Elegra scanner was used to first confirm the presence of thrombus, and then to image and collect phase sensitive B-Scan frames in real-time during compression ultrasound. In rats, continuous deformations of the abdominal wall and underlying tissue were applied using a 7 MHz linear transducer attached to mechanical screw-driven translating device. In human studies, the imaging studies were performed freehand, i.e., the deformations were applied manually with a linear 5 MHz transducer. The frame-to-frame motion was estimated using a two-dimensional complex correlation based speckle tracking technique. The age of venous thrombi was first estimated by quantitative analysis of strain and decorrelation images as well as corresponding B-Scans. Finally, the results were verified based on reconstructed elastic properties of thrombi.

Results: Older thrombi in rats were regularly harder than younger thrombi. Typical results showed that six-day old thrombi were about twice as hard as two-day old thrombi, while nine-day old thrombi were at least an order of magnitude harder than two-day old thrombi. Reconstructive elasticity imaging confirmed these findings.

In humans, the chronic thrombus was quite homogeneous and 4-5 times harder than the vessel wall. The subacute thrombus was much more heterogeneous and was 3-9 times softer than the vessel wall. These results gave hardness ratios between the chronic and subacute thrombi of factors of 12-45. A highly conservative error analysis showed that the chronic thrombus was at least 6 times harder than the subacute thrombus.

Discussion: The results strongly suggest that ultrasound elasticity imaging can detect, diagnose and age deep venous thrombosis. The results, although preliminary, are consistent between the rat model and human subjects showing that thrombi measurably harden over time, making elasticity imaging a very attractive method of determining the age of venous thrombi.

Support in part from the National Institutes of Health under grants DK47324, HL47401, HL68658, and HL63148, Department of Defense (USAMRMC CDMRP) under grant DAMD17-01-1-0562, and the Ultrasound group of Siemens Medical Systems, Inc. (Issaquah, WA) is gratefully acknowledged.

39 **A FAST ACQUISITION SYSTEM FOR RADIAL COMPRESSION ELASTOGRAPHY OF THE PROSTATE *IN-VIVO*.**

*Rémi Souchon, Valérie Detti, Jean-Yves Chapelon.*
INSERM, Lyon, FRANCE.

For elastographic imaging *in vivo*, high acquisition speed is essential to reduce decorrelation effects due to undesired motion. A fast acquisition system for prostate elastography is presented.

A uniform radial compression is applied using a balloon that covers a 5.5 MHz transrectal imaging probe. An ultrasound scanner provides sector scans of the prostate. It was slightly modified to output the analog radio-frequency (RF) signal. A computer equipped with an analogue to digital converter (ADC) board ensures real-time digitization of the RF data. Compression and digitization are simultaneously triggered by the computer. Acquisition speed is only limited by the 8-frames/sec frame rate provided by the ultrasound scanner. At this frame rate, a 1.5 seconds-long multi-compression sequence can be digitized using the maximum sampling rate available. A 1.5% average compression of the prostate is achieved during this time.

Displacements are cumulated over the multi-compression sequence. They are calculated from overlapping segments of the pre- and post-compression RF signals using the cross-correlation technique with parabolic interpolation. Every pre-compression segment is compared to the corresponding segments of neighboring RF lines to estimate lateral motion. Global stretching of post-compression segments is applied. Strain is estimated from the gradient of the displacements. The strain estimation process may by repeated using the initial strain estimation for local stretching to improve the quality of the elastogram. High resolution of the ADC board (14 bits) and high sampling rate (100 MHz) are used to minimize respectively the effect of quantization noise on sonographic SNR and the bias error on time delay estimates due to interpolation. To allow comparison between different elastograms and between patients, the elastograms are normalized relative to the average strain measured inside the prostate.

Examples of transverse elastograms acquired on a patient undergoing high intensity focused ultrasound (HIFU) therapy of prostate cancer are presented. The presence and the position of the adenocarcinoma were detected on the elastogram and confirmed using MRI. It was also possible to see the HIFU lesion during and after the therapy session. The feasibility of using elastography *in vivo* to visualize malignant tumor and HIFU lesion in the prostate was demonstrated.

This work was supported in part by the National Cancer Institute (USA) Program Project Grant 2P01-CA64597 to the University of Texas Medical School.

42 **CARDIAC ELASTOGRAPHY: DETECTING PATHOLOGICAL CHANGES OF THE MYOCARDIUM.**

*Elisa E. Konofagou[1], Timothy Harrigan[2], Scott Solomon[3].*
[1]Focused Ultrasound Laboratory, Department of Radiology – MRI research, Brigham and Women's Hospital, Harvard Medical School, Boston, MA, USA; [2]Exponent, Inc, Failure Analysis Associates, Houston, Texas, USA; [3]Cardiovascular Division, Brigham and Women's Hospital, Harvard Medical School, Boston, MA, USA.

Estimation of the mechanical properties of the cardiac muscle has been shown to play a crucial role in the detection of cardiovascular disease. Current echocardiography-based cardiac motion estimation techniques, such as Doppler Myocardial Imaging (DMI), have been shown to suffer from various artifacts. Elastography was recently shown feasible on RF data from a normal human heart *in vivo* providing reliable and reproducible displacement and strain estimates from multiple sonographic views [1]. In this paper, the role of elastography in the detection of ischemia is explored in simulations and *in vivo* experiments.

Finite-element simulations of a portion of the cardiac muscle containing an ischemic region were considered. The ischemic region was three times stiffer than the normal cardiac muscle, whose elastic modulus was set equal to 30 kPa following previously reported results [2]. The cardiac cycle was simulated with alternating compressive and tensile strains applied on the target ranging between –30% and 20%. Given the deformations measured within the target, the incremental elastic modulus could be estimated and mapped using adaptive finite-element methods. We then demonstrated this technique utilizing 2D B-scan data in a patient with a known myocardial infarction. Envelope-detected sonographic data from a Hewlett-Packard Sonos-5500 system using a harmonic imaging probe operating at 1.8/3.6 MHz was used to estimate regional wall motion and deformation. Displacement and strain estimates were obtained in both the non-infarcted, normally contracting interventricular septum and the infracted apical region in an apical four-chamber view.

By obtaining ciné-loop and M-Mode elastograms from both normal and ischemic regions in both simulations and experiments, the ischemic region could be identified by a lower incremental axial strain range (-1 to 2%) than the normal region (-20 to 10%) and by a lower incremental axial displacement range (-0.1 to 1 mm) than the normal region (-3 to 3 mm). Given the low variation of the motion estimates at the ischemic region, the modulus calculated was shown to be up to ten times higher than that of the normal region.

As predicted by simulations, elastography was shown feasible in a typical clinical setting and useful in the detection of cardiac disease. The deformation and modulus data were shown to vary by up to an order of magnitude between the normal and pathological regions, underlying thus the role of elastography in the detection of cardiovascular disease. The combination of information on motion, deformation and mechanical property estimation is expected to constitute a unique and easily accessible tool in noninvasive cardiac diagnosis.

[1] Konofagou E.E., D'hooge J. and Ophir J., Cardiac Elastography – An *In Vivo* Feasibility Study, Ultrasound in Medicine and Biology 28(4), 475-482, 2002.
[2] Bertrand M.E., Rousseau M.F., Lefebvre J.M., Lablanche J.M., Asseman P.H., Carre A.G. and Lekieffre J.P., Left-ventricular compliance in acute transmural myocardial infarction in man, Eur. J. Cardiol. 7 Suppl: 179-193, 1978.

43 **REAL-TIME STRAIN IMAGING FOR PROSTATE CANCER DIAGNOSTICS – NEW CLINICAL RESULTS.**

*U. Scheipers[1], H. Ermert[1], A. Lorenz[1,2], A. Pesavento[1,2], H.-J. Sommerfeld[3], M. Garcia-Schuermann[3], K. Kuehne[3], T. Senge[3], S. Philippou[4].*[1]Institut fuer Hochfrequenztechnik, Ruhr-Universitaet, Bochum, GERMANY; [2]Ingenieurbuero Lorenz & Pesavento GmbH, Bochum, GERMANY; [3]Urologische Universitaetsklinik, Marienhospital Herne, GERMANY; [4]Institut für Pathologie, Augustakrankenanstalten, Bochum, GERMANY; [1,2,3,4]Kompetenzzentrum Medizintechnik Ruhr, Bochum, GERMANY.

As the incidence of the prostate carcinoma is one of the highest cancer risks in men in the western world and its position in cancer mortality statistics is also among the highest, prostate diagnostics is of high importance in today's health system. The prostate carcinoma is only curable at an early stage. Therefore, early detection is extremely important. The different types of diagnostics that are used today (digital rectal examination, transrectal B-mode ultrasound and PSA value analysis) lack reliability and thus are not sufficient. Results of diagnostics using conventional B-mode ultrasound are still highly dependent on the physician's skills.

Strain imaging allows displaying the local stiffness of tissue. As tumors of the prostate are not always visible in conventional B-mode ultrasound but often are harder than normal tissue, strain imaging has the capability to image tumors that are not visible in conventional ultrasound systems.

Formerly, strain imaging was far away from being real-time and thus was clinically and commercially not important. The system developed at Ruhr-University Bochum is based on a novel fast signal processing approach using the phase-root-seeking algorithm and standard, low cost PC hardware. The system acquires RF-data from a conventional ultrasound machine, performs the strain imaging process and displays both, the B-mode image and the strain image simultaneously on a PC screen in real time. All calculations are done by the standard processor of a PC reaching a frame rate of 30 fps, calculating roughly 500,000 image pixels per second. Next to the PC based add-on system, a fully digital in-system application, which is running on the ultrasound machine's own system, has been developed and tested as well.

Currently the diagnostic impact of real-time strain imaging is investigated in a clinical trial at our University Hospital. Both, a Combison 330 (analog system) and a Voluson 730 (fully digital) ultrasound system (Kretztechnik AG, Austria) are used in the trial. By now 260 patients underwent the strain imaging procedure. We are going to present new results of our current clinical trial including real-time strain imaging movies and histologies (obtained after prostatectomy). Patient compliance is high, because diagnostics using real-time strain imaging do not extend the normal examination time. Using strain imaging as the only diagnostic tool a specificity of 84 % and a sensitivity of 78 % for cancer detection was found which is high above the figures that can be obtained using conventional diagnostic modalities, i.e. PSA value analysis, digital rectal examination and transrectal B-mode ultrasound.

Upcoming clinical studies will include an extended patient group and using real-time strain imaging as a guiding modality for prostate biopsies.

A project of the Ruhr Center of Competence for Medical Engineering (KMR), funded by the German Federal Ministry of Education and Research (bmb+f grant No. 13N8079).

53 **REAL-TIME FREEHAND ELASTICITY IMAGING.**

*Timothy Hall, Yanning Zhu.*
University of Kansas Medical Center, Department of Radiology, Kansas City, KS, 66160-7234, USA.

We are continuing the development and clinical testing of a software application that runs on an unmodified commercial clinical ultrasound system and displays B-mode and mechanical strain images side-by-side in real-time. Currently the strain image frame rate is about 7 frames/sec for 3cm x 3cm field of view. That frame rate has proven sufficiently fast to provide feedback information allowing control of the boundary conditions of compression/release to consistently obtain high-quality strain image sequences.

Laboratory tests of this system have focused on phantoms where basic image quality measures of contrast, resolution, and noise have been investigated. Clinical testing has focused on breast tumor discrimination, although a collaborating site is also investigating its use in thyroid imaging.

Results of clinical tests are consistent with observations published by Garra et al., though our results provide insight into some difficulties discussed in that report. Specifically, freehand scanning and real-time feedback allow scanning any area of the breast with relative ease. Invasive ductal carcinomas are considerably larger in strain images than in B-mode. Most interestingly, fibroadenomas, which are the most common benign solid lesions, demonstrate strain image contrast that depends on the magnitude of the applied deformation.

Given that relative lesion size (B-mode versus strain image) and deformation-dependent lesion contrast appear to by useful lesion discrimination criteria, we will describe our work toward improving the observer's ability to define consistent lesion boundaries and judge relative lesion contrast. For example, one problem is frame-to-frame variability in the apparent lesion border due to small variations in displacement estimates. One approach is to use image persistence, but this adds a spatial blur to a moving object. Alternatives to persistence will be discussed and their performance reported.

58 **ULTRASOUND FREEHAND ELASTOGRAPHY: EVALUATION OF DIAGNOSTIC POTENTIAL IN CLINICAL BREAST IMAGING.**

*JC Bamber[1], NL Bush[1], DO Cosgrove[2], MM Doyley[1], FG Fuechsel[2], NR Miller[1], F Tranquart[3].*
[1]Institute of Cancer Research and Royal Marsden NHS Trust, Sutton, Surrey, UNITED KINGDOM; [2]Hammersmith Hospitals Trust, London, UNITED KINGDOM; [3]University Hospital, Tours, FRANCE.

We have previously described the concept of freehand elastography using hand-induced motion of the ultrasound probe to palpate the breast and a system that, by rapid acquisition of a large number radio frequency echo frames, overcomes many of the disadvantages associated freehand probe motion. In this paper we present further details of this method, show example images that illustrate the appearances of different types of breast masses, describe imaging artefacts that we have observed (some of which are useful) and present the results from an extensive multivariate feature analysis of images from 70 lesions in 63 patients. The study was conducted with the intention of improving our understanding of both the relationship of freehand elasticity imaging (FEI) to sonography and the clinical impact that FEI is likely to have as an adjunct to breast sonography. A particular feature of this comparison was that the sonographic features we evaluated included those from relative motion assessment (RMA), a term that we have used to describe the technique of visually assessing tissue mechanical properties by observing the relative motion of tissue structures on real-time sonography during palpation.

FEI produced images with sufficient spatial and contrast resolution to visualise normal and abnormal breast anatomy. Good strain contrast can be observed between glandular tissue and fatty tissue, and also from fibrous anatomical structures such as coopers ligaments and small very stiff inclusions such as calcifications. The echoes from these structures and shear effects observed at tissue boundary interfaces, strongly determine appearances in normal tissue.

Results from an overall subjective judgement of diagnostic grade (likelihood of being malignant) revealed that strain imaging improves differential diagnosis of benign from malignant lesions of the breast and adds diagnostic confidence when viewed alongside ultrasound data. These findings were confirmed and extended using multivariate discriminant analysis and logistic regression to develop discriminant models. The best performing feature set for an ultrasound-only discriminant model produced a cross-validated diagnostic sensitivity of 88% and specificity of 81%. This compared with 96.7% sensitivity and 81% specificity for the best combination of the ultrasound and EI features.

We conclude, like others who have carried out related studies, that strain imaging appears to offer additional diagnostic information not obtained from sonography alone. Our results also suggest however, that some of the visually apparent information in elastograms is either not available from, or is not so easily appreciated by, RMA using real-time sonography. Nevertheless, it is interesting that for some strain image features, once they have been identified in the elastogram one can learn to see them using RMA. The nature of the additional information available from FEI suggests that with expected future improvements in image quality and fully real-time implementation, it would be worth evaluating the contribution that FEI could make to the earlier detection of breast cancer. Finally, the list of strain image effects and artefacts that we have documented from this study may contribute to teaching and improved interpretation of strain images of the breast.

07 **COMPLETE PROCESSING FOR QUANTITATIVE INTRAVASCULAR ULTRASOUND ELASTOGRAPHY.**

*Elisabeth Brusseau[1], Jérémie Fromageau[1], Chris de Korte[2,3], Philippe Delachartre[1], Didier Vray[1], Anton F.W. van der Steen[2,3].*

[1]CREATIS UMR CNRS 5515, affiliated to INSERM, Lyon, FRANCE; [2]Experimental Echocardiography, Thoraxcenter, Erasmus University Rotterdam, Rotterdam, THE NETHERLANDS; [3]Interuniversity Cardiology Institute of the Netherlands (ICIN), THE NETHERLANDS.

Background: A major complication of atherosclerosis remains plaque rupture, which consequences might be sudden ischaemic death or myocardial infarction. Plaque rupture is caused by complex mechanisms correlated with plaque composition, morphology, mechanical properties and blood pressure solicitation. Knowledge of the local elastic properties of a plaque and of the surrounding tissues could thus be of fundamental interest to assess the plaque vulnerability, and to predict the disease evolution. These properties can be investigated by intravascular ultrasound elastography. In this study, we present the complete processing we dedicate to the investigation of atherosclerosis.

Method: This processing is composed of 3 main steps: endoluminal border detection, local strain estimation and Young's modulus reconstruction. Because the transducer is positioned in the lumen and not in direct contact with tissues, a registration of the signals relative to the arterial wall, and acquired at different pressure levels is necessary. This needs the segmentation of the endoluminal contour. The adopted approach uses the technique of snakes and exploits the property that has ultrasound texture brightness to be represented by Rayleigh distributions. The contour is thus statistically estimated as the border that separates optimally two Rayleigh distributions. However, contrary to classical snake algorithms that require a ROI manual selection prior to border detection, our method is fully automatic. This characteristic has been achieved by the introduction of an automatic adaptive and iterative reduction of the region of interest.

Beginning of the pre- and post-compression signals being registered, the strain distribution is then estimated with a method we developed, based on the principle that tissue deformation induces, within RF signals, variations comparable to local scaling factors. This method has been proved to be accurate for strains up to 7% and adapted to investigate highly heterogeneous tissues like atherosclerotic vessels.

The final step is the estimation of the compression modulus, using strain and displacement estimates. For a cylindrical symmetry, the radial and tangential strains are both expressed as the radial displacement-to-radius ratio, but with different signs. A linear combination of these two parameters thus permits the derivation of a coefficient linked to the mechanical parameters. Since strain had been estimated in step 2, the displacement needs only to be computed. This is performed by using a time-delay estimation technique. The tangential strain is then deduced from the displacement, and the elastic modulus is evaluated from the two strain fields.

Results: The method was tested with both simulations and 2-layers intravascular cryogel phantoms. Simulations combine a finite element modeling with the ultrasound field calculation. Phantom RF data were acquired with a CVIS ultrasound scanner working with a 40 MHz single rotating element, and were digitized at 500MHz with a Lecroy 9374L oscilloscope. Resulting elastograms show a good agreement with phantoms mechanical parameters, and demonstrate the ability of the method to produce quantitative images of elasticity.

17 **RESOLUTION IN ELASTOGRAPHY[†].**

*R. Righetti, S. Srinivasan, J. Ophir.*
The University of Texas Medical School, Department of Radiology, Ultrasonics Laboratory, Houston, TX, USA; University of Houston, Electrical and Computer Engineering Department, Houston, TX, USA.

A theoretical and simulation study of the limits of the spatial resolution in elastography was performed. The resolution was defined as the minimum distance between two equally stiff lesions embedded in a softer homogeneous background, as measured from the strain images. The effects of the ultrasonic and processing parameters on the obtainable spatial resolution were investigated. For the simulation study, a finite-element (FE) simulation was performed to simulate a 2D (plane strain) square phantom containing two hard lesions, symmetrically placed along or across the axis of symmetry of the phantom. In order to determine the interactions between the elastographic resolution and the ultrasonic system parameters, various transducer field models (different frequency, bandwidth, and beamwidth) were created. The corresponding elastograms were processed using the gradient strain estimator with adaptive stretching.

Theory and simulations indicate that the lower bounds on the axial and lateral resolution in elastography are governed respectively by the bandwidth and the beamwidth of the ultrasound system. The results also show that, for a given ultrasound system, the resolution is determined by the processing parameters (cross-correlation window length and overlap between windows).

[†]This work was supported by a Program Project Grant (PPG) P01-CA64597 from the National Cancer Institute (USA).

16 **TRADEOFFS BETWEEN THE AXIAL RESOLUTION AND THE SIGNAL-TO-NOISE RATIO IN ELASTOGRAPHY.**

*S. Srinivasan, R. Righetti, J. Ophir.*
The University of Texas Medical School, Department of Radiology, Ultrasonics Laboratory, 6431 Fannin St., Houston, TX 77030, USA; University of Houston, Electrical and Computer Engineering Department, 4800 Calhoun Rd., Houston, TX 77204, USA.

Strain estimation in ultrasound-elastography is typically performed through a gradient operation on the displacement estimates that are obtained through cross-correlation of the pre- and post-compression RF A-lines. Some factors that quantify the quality of the resulting strain estimates are the elastographic SNR ($SNR_e$), the contrast-to-noise ratio ($CNR_e$), and the spatial resolution. These quality factors depend on the mechanical parameters (such as the applied strain and the boundary conditions), the acoustic parameters (such as the sonographic SNR, the center frequency, and the bandwidth), and the signal processing parameters (such as the window length and the window separation). Theoretical developments in elastography have established functional relationships between the $SNR_e$ and $CNR_e$ and these parameters. Similarly, simulations have established empirical relationships between the axial resolution and the acoustic and signal processing parameters.

We find that a trade-off exists between the achievable $SNR_e$ ($CNR_e$) and the axial resolution in elastography and that the trade-off occurs only with respect to the signal processing parameters. Theoretical work on the spatial resolution accompanied with simulations and experiments were used to confirm such an observation. The trade-off between the $SNR_e$ ($CNR_e$) and the resolution was found to be non-linear, with large improvements in the $SNR_e$ being possible at the expense of small reductions in the axial resolution. All the quality factors improve with the acoustic parameters, which suggests the preferred use of transducers with high absolute bandwidths and center frequencies.

Supported by National Cancer Institute (USA) Program Project Grant P01-CA64597.

19 **AXIAL AND CONTRAST RESOLUTION OF ELASTOGRAPHY BASED ON TIME DELAY ESTIMATION.**

*K. M. Hiltawsky, H. Ermert.*
Institute of High Frequency Engineering, Ruhr University, Bochum, GERMANY.

Ultrasonic strain imaging (elastography) has been investigated by many researchers, including theoretical analysis, *in vitro* studies and clinical experiments (*in vivo*). However, the clinical benefit of the method concerning an improvement of diagnostic sensitivity and specificity of cancerous lesions has not been shown yet. There is an explanatory gap between the excellent performance of the method in theoretical experiments and in *in vitro* studies, respectively, and the decay of strain image quality in case of clinical examinations.

Elastograms show the internal mechanical strain distribution of an object due to the application of an external force. Although the internal strain distribution of an object due to external forces is governed by a three-dimensional and non-linear set of equations, hard inclusions turn out to have strain values close to zero, whereas an underlying softer tissue would be imaged as a region with higher strain values. As ultrasound signals are sampled from ultrasound waves, which propagate in axial direction, displacement images and strain images, respectively, are usually calculated from time delay estimates.

We developed a model that accounts for elastographic noise due to lateral displacements of the object under compression. The model includes the focus-dependent lateral beam width of the ultrasound pulse, ultrasound system parameters (bandwidth, center frequency, window length, electronic signal-to-noise ratio, correlation coefficient) and elastic parameters (strain distribution). The resulting “uncertainty relation in elastography” could be verified using a two-dimensional ultrasound simulator for simulating the ultrasound system and using FEM-experiments for simulating two-dimensional displacement fields due to external compression. Furthermore, time delay estimates from consecutive and overlapping windows turned out to be highly correlated. We could find a linear relationship between the covariance of time delay estimates and the window length of the underlying time delay estimation method, as has already been described by Varghese and Bilgen. Using this relation and the resulting covariance matrix C of time delay estimates, we simulated displacement data and calculated the derivate locally using a least-square estimator. In case of overlapping time delay estimation windows, we also considered the covariance matrix C.

The result of our work can be summarized as follows. The Cramér-Rao-Lower-Bound (CRLB) as a minimum variance for an unbiased time delay estimator restricts the quality of strain images (SNR, contrast resolution) to a certain level, if the local derivative is calculated from a least-square fit. Furthermore, the axial resolution of a strain imaging system, described by the ability of a system to detect a 6 dB increase/decrease in elastic modulus, is limited by the window length of the time delay estimation method, i.e., on the order of several wavelengths of the ultrasound pulse.

08 **THE ESTIMATION OF MOTION GRADIENTS BY MEANS OF TWO-DIMENSIONAL CUBIC B-SPLINES.**

*Jan D'hooge[1,2,3], Piet Claus[2], B.Bijnens[2], J.Thoen[3], F.Van de Werf[2], G.R.Sutherland[2], P.Suetens[1].*
[1]Medical Image Computing, Dept. of Electrical Engineering, Katholieke Universiteit Leuven, Leuven, Belgium; [2]Dept. of Cardiology, Katholiek Universiteit Leuven, Leuven, Belgium; [3]Dept. of Physics, Katholiek Universiteit Leuven, Leuven, BELGIUM.

In elastography, tissue strain is calculated as the spatial gradient in tissue motion caused by the deformation. Normalization of the motion and strain estimates to the time period over which the deformation occurred, results in velocity and strain rate estimates respectively. The latter deformation characteristic has been shown to be particularly interesting in cardiac deformation analysis.

A major practical difficulty to this methodology is that calculating a gradient numerically is sensitive to noise as during this process the noise is typically amplified. For this reason, motion or velocity estimates are usually regularized, e.g. filtered, in space and/or time prior to applying the gradient operator (e.g. linear regression). The purpose of this study was to overcome this practicality by calculating the spatial gradient analytically rather than numerically. Hereto, a cubic B-spline, i.e. a piecewise polynomial, was fitted through the velocity estimates.

Methods: Digital radio-frequency (RF) data of cyclically compressed gelatine phantoms were acquired using M-mode imaging. A Toshiba Powervision 6000 equipped with an RF interface for research purposes was used. The average compression strain rate was varied between 0.5-1.0s- 1 as realistic values for myocardial systolic strain rate. The pulse repetition- and transmission frequencies were set to 5kHz and 3.7MHz respectively. Both homogeneous and non-homogeneous phantoms were used. Velocity estimates were made using a cross-correlation method of temporally successive RF segments. A weighted 2D _t was made through the velocity estimates at all image depths and at all time instances using a cubic B-spline surface. Weights were chosen to be inversely proportional to the maximal cross-correlation. Strain rate was then obtained as the analytical partial derivative of the B-spline surface in the depth direction. Cumulative strain was subsequently calculated as the analytical integral of the (B-spline) strain rate curve over time.

Results: The phantom work showed that strain rate and cumulative strain estimates correlated well with the theoretical values. Moreover, it showed discontinuities to be preserved.

Conclusions: B-spline fitting of velocity estimates provides an accurate method towards strain rate and cumulative strain estimation. It not only makes the estimation process more robust but could also improve the spatial resolution of the estimates.

Acknowledgement: This work was supported by the Fund for Scientific Research- Flanders (FWO).

09 **A SIMULATION STUDY ON THE PERFORMANCE OF DIFFERENT ESTIMATORS FOR TWO-DIMENSIONAL VELOCITY ESTIMATION.**

*Stian Langeland[1], Jan D'hooge[1,2.3], Hans Torp[4], Bart Bijnens[1], P.Suetens[2].*

[1]Dept. of Cardiology, Catholic University of Leuven, Leuven, BELGIUM; [2]Medical Image Computing, Dept. of Electrical Engineering, Catholic University of Leuven, Leuven, BELGIUM; [3]Dept. of Physics, Catholic University of Leuven, Leuven, BELGIUM; [4]Dept. of Physiology and Biomedical Engineering, The Norwegian University of Science and Technology, Trondheim, NORWAY.

Regional strain and strain rate imaging have been introduced as new tools to quantify regional myocardial function. Since strain rate is the spatial velocity gradient, the calculation reduces to velocity estimation and a gradient operation. Current velocity estimation techniques are 1- dimensional (1D) and thus angle dependent. Techniques have been described that allow 2D velocity estimation by tracking of radio frequency (RF) patterns within a 2D RF image. The purpose of this study was to find the optimal estimator for tracking of the RF patterns both axially and laterally.

Methods: RF data sets were obtained using a simulation environment based on the impulse response method. Simulations were performed at high temporal resolution (500 Hz). This can be achieved in practice using 12 transmit beams for depths < 120 mm. The angle of the scan sector was set to 15 degrees and parallel beam forming resulted in 24 image lines. The simulated transducer was a 64 element phased array transmitting at 2.5 MHz and 60% bandwidth. Estimators investigated for 2D RF tracking were: crosscorrelation (XC), normalized cross-correlation (NXC), sum of absolute differences (SAD) and sum of squared differences (SSD). Robustness of these estimators, in both axial and lateral direction was tested for: amplitude in axial velocity, amplitude in lateral velocity, interaction of one on the other and amplitude in axial strain rate. 2D tracking of the RF patterns with a 1D kernel was performed, after lateral interpolation of the RF images. In order to enable subsample velocity estimation, cosine interpolation was performed for XC, NXC, and SSD, while the intrinsic character of SAD doesn't allow this. Performance was measured as the mean, squared estimation error, over the whole image.

Results: Different estimators showed large differences in robustness of velocity estimation, both in axial and lateral direction. While NXC, SAD and SSD showed good performance for all tests, XC was outperformed. For all test, SSD performed slightly better than NXC and SAD, but the differences between SSD and NXC were small. Conclusion: 2D velocity estimation showed not to be feasible using XC. However, NXC, SAD and SSD showed accurate axial and lateral results. As calculation times for these are similar, SSD was found to be the preferred estimator.

59 **FAST AND ROBUST STRAIN ESTIMATION IN ELASTOGRAPHY[†].**

*S. Kaisar Alam.*
Riverside Research Institute, 156 William Street, New York, NY, 10038, USA.

In elastography, tissue under examination is externally compressed and a map of the resultant deformation is estimated by analyzing the pre- and post-compression echo signals. In addition to the change in signal shape from tissue deformation, non-axial tissue motion also reduces correlation between the pre- and post-compression echo signals. Global temporal stretching of post-compression signals by a factor that compensates for the applied strain significantly improves the "quality" of strain estimates. In a natural extension of this approach, a search is performed at each data window for the stretch factor that maximizes the correlation between the pre- and post-compression echo signal segments (adaptive stretching). Adaptive stretching performs well under harsh signal environments (because the correlation is maximum at each location), however is computation intensive because many iterations may be required at each location. In contrast, global stretching is a fast algorithm, but performs well only in areas where local strains are close to the applied strain.

We propose a method that strikes a balance between the speed of global stretching and the performance of adaptive stretching. In this method, several strain maps are computed by performing global stretching with a range of different stretch factors. The correlation between the pre- and post-compression echo segments is the maximum when the stretch factor corresponds to the local strain. Thus, the area in each computed strain image with strain values closely corresponding to the uniform stretch factor will contain "good quality" strain estimates. To produce a single elastogram at the end, these strain maps are combined as follows. Correlation values quantify the "quality" of strain estimates; thus, at each location we identify the strain map with the maximum correlation, and the strain value in that strain map at that location is chosen for the combined map.

Initial simulation and experimental results demonstrate that the described strain estimator is significantly less susceptible to signal degradation than conventional strain estimators. Results from data generated by finite-element simulation and phantom experiments show that the variable stretching strain estimator is fast and can produce excellent strain estimates in the presence of large strains (used applied strains as high as 16%) and undesirable motion (deliberately caused moderate non-axial motion and rotation).

[†] Supported in part by NIH grant CA84274.

64 **CONVERGENCE AND REGULARIZATION IN TISSUE MOTION ESTIMATION USING THE LAGRANGIAN SPECKLE MODEL.**

*Guy Charron, Roch Maurice, Michel Bertrand.*
Institut de génie biomedical, École Polytechnique, C.P. 6079, succ. Centre-ville, Montréal, (Québec), H3C 3A7, CANADA.

The description of ultrasound speckle dynamics in Lagrangian coordinates sets the theoretical foundation of a tissue motion estimator we proposed. Essentially the method consists of determining the parameters of a warping operator which at all times t brings back the RF or B-Mode signal samples to the position they originally "occupied" at a given reference time $t = t_0$. Such operation continuously achieves tissue motion compensation and the result thus obtained is a spatio-temporal function we named the Lagrangian Speckle Image $I_{LAG}$. Under the conditions for artefact-free speckle motion, in absence of out-of-plane motion and for a small in-plane motion, $I_{LAG}$ would be a stable, stationary speckle pattern. Hence motion estimation could be seen as seeking the $I_{LAG}$ parameters that would minimize the sum of squares of $(I_0 - I_{LAG})$ where $I_0$ is for example a pre-compression image. To do that, we used a method that implements a regularized, gradient-based algorithm for non-linear constrained minimization. For small regions, the 2-D tissue motion model we used was that of an affine transform thus requiring six parameters to be found. Four of these parameters directly lead to the partial derivatives of the displacement field, and thus lead to the strain tensor. Hence the method can be classified as a 2-D adaptive strain estimator.

The estimator proceeds iteratively by adjusting the motion parameters so that at every iteration the error norm gets smaller, subject to some constraints. Starting from an initial guess of the solution (which in the simplest case would be the parameter for zero translation and no deformation), the adjustment is determined by solving a set of linear equations, which represents the changes in pixel intensity that occurs for a small perturbation of the motion parameters. It can be shown that the set of linear equations are identical to the optical flow equations evaluated at each pixel position for a linear velocity field. Factors determining the rate of convergence are examined using Matlab's Optimization Toolbox with simulated and experimental image sequence data. Those factors include the initial parameter values, the 2D measurement-window size, the prescribed values for the parameters upper and lower bounds, the signal noise and the noise due to tissue strain and rotation. This study will be useful for designing robust and efficient tissue strain estimator.

Acknowledgments: Supported by the National Research Council of Canada, FCAR (Quebec Ministry of Education). A part of the project upon which this publication is based was performed pursuant to the University of Texas Grant CA64597-01 with the NIH, USA.

24 **HAPTIZATION OF ELASTIC OBJECT USING MAGNETIC RESONANCE ELASTOGRAPHY.**

*Masataka Imura, Mikio Suga, Osamu Oshiro, Kotaro Minato, Kunihiro Chihara.*
Nara Institute of Science and Technology, Nara, JAPAN.

Tissue elasticity is one of the fundamental and important pieces of information for physician's diagnoses and surgeon's operation. Elasticity is indispensable parameter on the virtual reality (VR) system, for instance tele-palpation and surgical simulator. To reproduce elasticity of diseased tissues of patients, the following techniques must be established: (1) obtaining elasticity and viscosity of tissues by noninvasive measurement, (2) constructing haptic model including the measured modulus properly, and (3) providing interactive force feedback based on solution of the haptic model. The paper describes the development of the haptization system utilizing both medical imaging and virtual reality technologies.

To estimate the shear modulus and the viscosity of an elastic material, we adopted MRE (magnetic resonance elastography). MRE is an MRI (magnetic resonance imaging) sequence that can visualize propagating strain waves in materials. Applying vibration to the measurement object, elastic information of a measurement object can be calculated non-destructively from the acquired images. We have been studying the estimation of the elastic information using MRE, where the shear modulus could be calculated from the phase change of the obtained MRE signal and the viscosity could also be calculated from the amplitude attenuation. Using a clinical MR imager (Siemens Magnetom Vision), we obtained MRE signals of phantoms, which consist of agarose gel and PVA (polyvinyl alcohol) with the concentration of 5, 6, 7.5 and 9 phantoms. Simultaneously, the elastic values were measured destructively using the dynamic test equipment (UBM Rheogel - E4000). The dynamic test is the typical measurement method for elastic information. The shear modulus and the viscosity obtained from both methods show the good correlation, which indicates that MRE has the useful methodology to obtain the elastic information non-destructively.

To calculate the dynamics of elastic objects, we constructed the haptic model based on mass-spring model. The model reflects the measured elasticity and viscosity onto the coefficient of spring and damper of the model and provides the dynamic change of object. Then the system presents force feedback according with an external force with a haptic device. The developed system is evaluated by comparing force feedback of the four obtained elastic models.

The experimental result indicated that the system enabled the discrimination of the elastic models with the different elasticity and viscosity.

This work is supported by the Special Coordination Funds of the Science and Technology Agency of Japanese Government.

31 **PROCESSING ALGORITHMS FOR TRACKING LASER SPECKLE SHIFTS IN ACOUSTO-OPTICAL ELASTOGRAPHY OF SKIN.**

*Sean J. Kirkpatrick[1], Donald D. Duncan[2].*

[1]Oregon Medical Laser Center, Providence St. Vincent Medical Center, 9205 SW Barnes Rd., Portland, OR, 97225 USA; [2]The Johns Hopkins University, Applied Physics Laboratory, Laurel, MD, 20910, USA.

Various methods for determining the strain-induced shift in laser speckle patterns have been investigated and compared for optical elastography applications. The different methods included cross-correlation, minimum mean square error, maximum likelihood and maximum entropy approaches. These different approaches have been applied to experimental and simulated situations in which the speckle shift between subsequent records was small (less than 0.5 camera pixels per record) and situations in which the shift was large (greater than 0.5 pixels per record). The maximum likelihood and maximum entropy approaches were found to be particularly useful when the speckle shifts were small, whereas the more conventional cross-correlation approach performed well, and was computationally less expensive, when the shifts were large. Furthermore, the performance of the maximum likelihood approach was analyzed in the presence of increasing amounts of Gaussian noise. The analysis characterized the performance (bias and RMS deviation) of the estimator as a function of signal-to-noise ratio. This SNR parameter is a convenient surrogate for decorrelation of sequential speckle patterns such as are seen in biological tissues. Bias as a function of SNR displayed sigmoidal behavior. For high SNR's, the bias approached a small, generally non-zero, error and at low SNR's it approached an error of 100%. RMS variation displayed a sigmoidal behavior as well with varying SNR. For high SNR's, it approached a very small non-zero value and gradually approached a higher-level asymptote for low SNR's. Based on these simulations, the maximum likelihood estimator was shown to produce accurate predictions for instantaneous speckle motions of approximately ± 0.1 pixel/record up to ± 0.8 pixel/record. Finally, the maximum likelihood approach for tracking small speckle shifts was applied to the investigation of the viscoelastic behavior of skin using an acousto-optical elastography approach. Using this approach, local mechanical variations in porcine skin due to chemically induced artificial lesions were identified and viscoelastic parameters were quantified in the healthy and 'diseased' skin.

This work was funded in part by NSF Grants #0196172 and #0201841.

45 **STEADY-STATE MAGNETIC RESONANCE HARMONIC ELASTOGRAPHY: CONTRAST DETAILED ANALYSIS AND PRELIMINARY CLINICAL EVALUATION.**

*Marvin M. Doyley[1,2], John B. Weaver[1,2], Elijah E. W. Houten[2], Francis E. Kennedy[2], Keith D. Paulsen[2,3].*

[1]Department of Radiology, Dartmouth-Hitchcock Medical Center, Lebanon, NH, 03756 USA; [2]Thayer School of Engineering, Dartmouth College, Hanover, NH, 03755, USA; [3]Norris Cotton Cancer Center, Lebanon, NH, 03756, USA.

Elastography is a new medical imaging modality, which has the potential for detecting breast cancer earlier and reducing the benign biopsy rates by exploiting large differences in the shear modulus between normal and diseased breast tissues. Consequently, we have developed a prototype magnetic resonance (MR) based elastographic system for clinical breast imaging with the patient lying prone. The system consists of a synchronous data acquisition system that can acquire sequences of relative phase images from a 1.5 Tesla whole body imager (GE Medical Imaging Systems, Milwaukee) whilst the breast is palpated dynamically using a custom made piezoelectric actuator (100-200 Hz, 80 μm). The phase and amplitude of the induced 3-D time-harmonic, steady-state displacement distribution is measured by applying a point-wise least squares fitting procedure to the MR phase images. Modulus elastograms are subsequently computed by applying a subzone inversion technique, which utilizes the finite element method and a modified Newton-Raphson iterative scheme to the measured displacements. Performance was assessed by conducting elastographic imaging on gelatin phantoms embedding inclusions of varying sizes and modulus contrasts. Accuracy was assessed by comparing the mean shear modulus recovered at the location of the inclusions relative to independent estimates of shear modulus measured using a dynamic mechanical analyzer; whereas lesion detectability was objectively assessed by measuring the contrast-to-noise ratio (CNR) of the reconstructed objects. An object was considered to be accurately characterized if the mean shear modulus at the location of the lesion was within 25 % of the true value; whereas it was perceived as being detected when the inclusion CNR was greater or equal to 2. The results demonstrates that focal lesions as small as 5 mm in diameter can be detected with our prototype system providing there is a threshold modulus contrast of 14 dB, but it was unable to accurately recover the shear modulus of such small lesions. Nevertheless, given sufficient modulus contrast the prototype system could accurately recover the shear modulus of focal lesions that were at least 10 mm in diameter (within 25 % of the true value). The results of preliminary clinical evaluation of the prototype system performed with the informed consent on healthy volunteers (n=5) and breast cancer patients (n=2) recruited from Dartmouth-Hitchcock medical center, revealed that the quality of modulus elastograms was sufficiently high for visualizing normal and abnormal breast anatomy.

05 **ELASTOGRAPHIC IMAGING OF THERMAL LESION FORMATION *IN-VIVO* ALONG WITH 3-D VISUALIZATION DURING RF ABLATION.**

*T. Varghese[1], J.A. Zagzebski[1], Q. Chen[1], U. Techavipoo[2], Wu Liu[1], F.T. Lee[3] Jr.*
[1]Dept. of Medical Physics, [2]Dept. of Electrical Engineering, [3]Dept. of Radiology, The University of Wisconsin-Madison, Madison, WI, 53706, USA.

Elastography is a promising tool for visualizing the zone of necrosis resulting from Radio-frequency ablation (RFA). Since heat-ablated tissues have increased stiffness compared to normal tissue, this modality may prove useful for following the results of RFA. *In-vivo* elastography of the liver and other abdominal organs have not been previously attempted, primarily due to the difficulty in providing controlled compressions. In this presentation two strategies for generating thermal lesion elastograms *in vivo* will be discussed. In addition, we present quantitative volume estimates obtained from 3-D imaging of the thermal lesion.

RFA was performed *in-vivo* on a female pig under general anesthesia using a RITA 1500 electrosurgical device. An Acuson 128XP real-time scanner was used to monitor the treatment. Two techniques were used to generate the *in-vivo* elastograms. In the first technique we applied controlled compressions near the site of the thermal lesion using the RFA probe as the displacement device. The second technique utilized the compression of the liver due to motion of the diaphragm during respiration. Pathology images for comparison were also obtained in the same image plane used for elastography by slicing through the fixed excised liver tissue. The thermal lesion boundaries are barely perceptible with conventional ultrasound. However, thermal lesions appear as distinct, dark regions in elastograms derived using both techniques.

Thermal lesions generated in liver lobes *in-vitro* at different temperatures and heating durations were imaged using an Aloka SSD2000 real-time scanner. Prior to imaging the samples were encased in gel blocks. 3-D visualization of the thermal lesions was obtained by reconstructing the lesion from multiple slice elastograms, obtained by scanning the entire lesion in a linear manner. Pathology images for comparison were obtained in the same planes used for elastography by slicing through the gelatin and tissue phantom using external markers as guides. Digitized gross pathology images were used to compute the lesion volumes, which were compared with volumes obtained by elastography. For a sample of 40 thermal lesions we obtain a correlation $r = 0.937$ for area estimates and $r = 0.979$ for volume estimates between *in-vitro* elastography and pathology. The areas obtained using elastography slightly underestimate the lesion areas. This result demonstrates that elastographic estimates of thermal lesion size may be conservative, i.e., they likely would not lead to catastrophic errors in estimation of thermal lesion size for use in human-patient studies.

*This work is supported by start-up funds provided to Dr. Varghese by the Department of Medical Physics, Medical School and Graduate School at the University of Wisconsin-Madison and by NIH grant R01 CA39224.

65 **THREE-DIMENSIONAL FUSION OF PROSTATE HISTOLOGY WITH SONOELASTOGRAPHY IMAGES.**

*Lawrence S. Taylor, Kevin J. Parker, Brian C. Porter, Clark Zhe Wu[1], Deborah J Rubens[2], Gyongyi M Nadasdy[3], P. Anthony di'Santagnese[3], David Pasternack[3], Raymond B Baggs[3], Edward M Messing[4].*
[1]Department of Electrical and Computer Engineering, University of Rochester, Rochester, NY, USA; [2]Department of Radiology, [3]Department of Pathology, [4]Department of Urology, Strong Memorial Hospital, University of Rochester, Rochester, NY, USA.

A whole mount pathology/histology protocol for 3D tissue reconstruction has been developed to compare the geometry, size and spatial location of tumors (or other lesions) identified in the histology data with that from the 3D sonoelastography images. A method of soft tissue fusion and image registration using the correlation of two surfaces is described then used to validate the accuracy of a three-dimensional ultrasound sonoelastography imaging system. Digital photographs of whole mount histology of each cancerous prostate are reconstructed to create a 3D surface of the gland's capsule. A 3D sequence of B-scan ultrasound images was also acquired and the gland surface was outlined then reconstructed to create a 3D surface. These two surfaces were then aligned using a 3D correlation algorithm with six degrees of freedom. After alignment, the tumor delineation determined by the pathologist is compared and fused with the tumor imaged using sonoelastography. Sonoelastography images of a case of prostate cancer validated by this technique are presented.

23 **UNIQUE ELASTIC MODULUS RECONSTRUCTION WITH LITTLE OR NO BOUNDARY DATA.**

*Paul E. Barbone[1], Jeffrey C. Bamber[2].*
[1]Center for Biodynamics and Dept. of Aerospace & Mechanical Engineering, Boston University, Boston, MA 02215, USA; [2]Joint Dept. of Physics, Institute of Cancer Research and Royal Marsden Hospital, Sutton, Surrey, UNITED KINGDOM.

We have shown recently that the standard formulation of the (2D) inverse problem associated with Elastic Modulus Imaging (EMI) has no unique solution. The practical implication of this that though a reconstruction might converge, there is no guarantee that it bears any resemblance to the actual stiffness distribution measured. A modification of the standard procedure, however, can be proven mathematically to provide a unique solution. The method requires additional data over and above standard elastography. We show how the additional data may be obtained in a straightforward manner. As a result, the method lends itself well to clinical application and measurements *in vivo* when boundary conditions are poorly characterized. In this paper we describe the method, prove its uniqueness, discuss aspects of its numerical implementation, and show example applications.

34 **A FAST ITERATIVE SCHEME FOR QUANTITATIVE ELASTICITY IMAGING BASED ON AN ADJOINT FORMULATION.**

*Assad A. Oberai, Nachiket Gokhale[1], Marvin M Doyley[2,3].*
[1]Department of Aerospace and Mechanical Engineering, Boston University, 110 Cummington Street, Boston, MA, 02215, USA; [2]Thayer School of Engineering, Dartmouth College, Hanover, NH, 03755, USA; [3]Department of Radiology, Dartmouth-Hitchcock Medical Center, Lebanon, NH, 03755, USA.

The ability to image quantitatively the elastic properties of tissues has several applications, including detection and differential diagnosis of certain cancer. At its core lies the solution of an inverse problem: Given the displacement in a incompressible, elastic media, determine the distribution of shear modulus. This problem is solved by: a) The direct approach: Equations for the static equilibrium yield a partial differential equation for the shear modulus, which is solved numerically; b) Iterative or the indirect approach: Computing the optimal shear modulus distribution minimizes a functional that measures the difference between the measured and a predicted displacement field. To find the minima, iterative algorithms are used. The optimization parameters are the nodal interpolant of the spatial distribution of shear modulus.

The main advantages of the iterative approach over the direct approach are its robustness to noise, and the ease with which it can accommodate variations in problem parameters. Its main drawback is speed. While the direct approach requires a single forward solution, the iterative approach requires around M*N solves, where M is the number of iterations of the optimization algorithm and N is the number of unknown shear modulus parameters. Typical values of M and N are 30 and 1000 respectively. For larger problems, and in three dimensions N is around 20,000 and the iterative approach is prohibitive.

In this paper, we describe a new iterative methodology based on the adjoint elasticity equations. This approach requires only 2*M forward solves regardless of N, thus greatly speeding the reconstruction. It has the potential of making the reconstructions real-time and increasing their accuracy. The basic features of the approach are:

1) To solve the minimization problem, algorithms that require the derivative (also called the gradient vector) of the functional with respect to the optimization parameters are used (e.g. BFGS).
2) To calculate the gradient, adjoint elasticity equations are utilized. This requires the solution of one primal and one dual problem. This cost is independent of N, the number of shear modulus parameters. The straightforward approach currently in use requires N such solves.

   Using the proposed method we present results for:

   a) Synthetic data: We consider problems with varying levels of noise, multiple inclusions, and large number of parameters (20,000). For smaller problems (about 1000 parameters), accurate reconstructions are obtained in about 25 iterations in less than 30 seconds on a desktop. For problems with 20,000 unknowns this takes about 20 minutes.
   b) Tissue phantoms: Two samples, one with a single inclusion and another with three inclusions are considered. Ultrasound measurements are made using an Acuson 128XP ultrasound scanner. Axial displacement is estimated by processing consecutive pairs of RF images. The shear modulus distribution is calculated on a 30*30 grid. The reconstruction takes about half a minute and converges in 30 iterations. Results devoid of serious artifacts are obtained.

We conclude by performing a theoretical cost analysis of our scheme in relation to other commonly used techniques and describe several interesting extensions of this methodology.

48 **MAXIMUM-LIKELIHOOD ESTIMATOR FOR QUANTITATIVE VIBRATION ELASTOGRAPHY IN ISOTROPIC SOFT-TISSUES.**

*Travis Oliphant.*
Department of Electrical and Computer Engineering, Brigham Young University, Provo, UT, 84602, USA.

Quantitative vibration elastography describes a method where mechanical vibrations are used to excite shear waves in soft-tissues at 10-1000 Hz. Measurements of the resulting displacements are then made (typically using ultrasound or magnetic resonance (MR) techniques), and these displacements are subsequently used to construct estimates of mechanical stiffness.

This method differs from static methods in that quantitative estimates of modulus can be made in source-free regions without knowledge of boundary conditions. It has been most often applied using magnetic resonance techniques (MR Elastography), but the same measurements have also been made using ultrasound.

Reconstruction of the modulus estimate from local displacement measurements has been the subject of several studies and several algorithms exist. Using Green's function analysis, this presentation will describe the maximum-likelihood estimator (MLE) for shear-modulus reconstruction of isotropic soft-tissues from vibration elastography data. The MLE estimates both the true displacement and the shear modulus at the same time while minimizing a function of only one variable because the estimate of true displacement can be related through the shear modulus to the displacement measurements with a linear function. Because the true displacement is estimated along with the shear modulus, it is especially suited for processing noisy ultrasound-measured displacements.

The performance of this estimator will be compared against the Cramér-Rao (CR) bound and a previously published fast estimator implemented as the ratio of two filters (direct Helmholtz inversion). It will be demonstrated that the fast algorithm achieves the performance of the MLE and the CR bound when the window size is on the order of 0.7 of a wavelength or less.

56 **PARAMETER SENSITIVITY IN RECONSTRUCTIVE ELASTIC PROPERTY IMAGING.**

*Elijah E. W. Houten[1], Keith D. Paulsen[1,3], Marvin M. Doyley[1,2], Francis E. Kennedy[1], John B. Weaver[1,2].*

[1]Thayer School of Engineering, Dartmouth College, Hanover, NH, 03755, USA; [2]Department of Radiology, Dartmouth-Hitchcock Medical Center, Lebanon, NH, 03756, USA; [3]Norris Cotton Cancer Center, Lebanon, NH, 03756, USA.

A non-linear optimization approach to reconstructive elastic property imaging allows the generation of property distribution images for each of the parameters of the elasticity equations. For imaging based on a linear elastic model, distributions of Lamé's moduli, μ and λ, as well as material density, ρ, may be recovered. The accuracy of these reconstructed property descriptions will be a function of the sensitivities of the equation system and the conditioning of the matrices for the iterative inversion process. Thus the choice of parameters for image reconstruction must strike a balance between the accuracy with which the elastic system being imaged is described, and the inherent parameter sensitivities in the image reconstruction process. To investigate the dynamics of this trade off a simulation study was undertaken with a MR Elastography method already in use for phantom and clinical studies. The model for this study consisted of a simple box geometry with a spherical inclusion whose properties were varied independently by differing amounts. Using this model, displacement solutions were generated for various perturbations of the mechanical properties of the inclusion. From these displacement fields, property distributions were reconstructed for a range of combinations of imaging parameters. For example, the displacement solution may have been calculated for a 25% increase in density within the inclusion, all other properties being homogeneous for the entire volume. From this displacement field, reconstructions of shear modulus, λ modulus, density and the meaningful combinations of the three, were made. Results were then compared with the known distributions used for the displacement calculation. Overall, it was seen that shear modulus was the most robust of the elasticity parameters for reconstruction. In reconstructing other parameters in addition to shear modulus it was found that density distributions were more effectively generated than λ modulus distributions. Additionally, it was seen that errors in density estimates had a more significant effect on the resulting shear modulus images than errors in lambda modulus estimates. Reconstruction of all three elastic parameters proved ineffective without a high degree of regularization. These results indicate that a reconstruction method which images shear modulus and density, assuming a fixed λ modulus distribution, would most effectively take into account mechanical property variations within the medium while maintaining appropriate conditioning of the inversion matrices for accurate parameter estimation.

55 **MEASUREMENTS OF TENDON ELASTIC PROPERTIES.**

*Pai-Chi Li, Po-Ling Kuo.*
Department of Electrical Engineering, National Taiwan University, No. 1, Sec. 4, Roosevelt Road, Taipai, TAIWAN, ROC.

The primary rehabilitation focus on tendon injury is to restore its mechanical function. To monitor the recovery process, sonoelastography has been proposed as an objective, non-invasive measure to evaluate mechanical properties of injured tendons. In an *in-vitro* study, we had reconstructed the one-dimensional transverse strain distribution inside tendon using speckle tracking. Four pairs of Achilles tendons from four rabbits were obtained. Each pair contained one abnormal tendon resulting from ischemia and a normal one as control. Tendons were embedded into phantoms and an ultrasound transducer was used. By incremental compressions, the transverse strain distributions of tendons were computed. Histology specimens and B-mode sonograms were also collected for each tendon. Correlated with histology, strain distribution significantly showed a better tissue differentiation than B-mode sonograms. In another study, we investigated the applicability of a transverse isotropic model on tendon mechanics. Six bovine tendons were used for sound velocity estimation and compressive Young's modulus measurement at different strains and directions along transverse plane. The estimated Young's modulus was computed from the linear elastic tensor constants derived from the measured sound velocities. The measured Young's modulus was obtained by direct compression of tendon using a 3-axis stepper motor and electronic balance at different strain rates. Young's moduli acquired form both methods were correlated. Results showed that the tendon is transverse isotropic but it becomes more isotropic at a higher strain. Also, the elastic properties of tendon can be approximated by a linear elastic model at a high strain rate.

Acknowledgement: Support from National Science Council of ROC under grant #NSC-90-2213-E-002-127 is greatly appreciated.

33 **DEVELOPMENT OF FREEHAND ULTRASOUND ELASTICITY IMAGING SYSTEM AND *IN-VIVO* RESULTS.**

*Takeshi Matsumura[1], Satoshi Tamano[1], Tsuyoshi Mitake[1], Tsuyoshi Shiina[2], Makoto Yamakawa[2], Naotaka Nitta[2], Ei Ueno[3].*

[1]Research & Development Center, Hitachi Medical Corporation, JAPAN; [2]Institute of Information Sciences & Electronics, University of Tsukuba, JAPAN; [3]Institute of Clinical Medicine, University of Tsukuba, JAPAN.

Elasticity imaging is one of new imaging methods that offer promising prospects. Because it constructs the image based on the information that is different from conventional 2D imaging, there is hope that it will produce information that could be used in the clinic. But, it was necessary to make many calculations to construct elasticity image compared with conventional 2D imaging. Since some issues, like having to wait a few minutes to see the elasticity image and so on, were involved, there were difficulties during *in vivo* evaluation at the bedside. To solve this problem, we developed high-speed free hand ultrasound elasticity imaging system by applying the Extended Combined Autocorrelation Method (extended CAM). The system is configured by modified commercial ultrasound scanner with 7.5MHz linear ultrasound probe and a PC with dual pentium4 processors which work at a 2.2 GHz clock rate. Upon pressing the body by the probe in free hand, the echo signals that correspond to multi-frame images are captured by the PC. On the PC, the log compression, the envelope detection, the edge enhancement and some other parameters apply to the echo signal for 2D image. And autocorrelation applies to the envelope component and carrier component of echo signals at pre-compression and post-compression to detect strain. Our elasticity image is based on this strain information. After processing, geometric conversion is made to both images for scan conversion. For viewing, the elasticity images are constructed as translucent color images and combined with 2D conventional images that are the black and white image. The images that were completed are stored on hard disk as AVI format which is suitable for motion picture viewing. We realized high-speed system by adopting extended CAM algorithm and making program task division for dual processor to be efficient in processing. As that result, it takes approximately 0.2 second to generate an elasticity image and a 2D image. The spatial filter for smoother image, scan conversion for the polar to Cartesian coordinates, the log compression for the echo signal and some other signal processing are included in the above time.

Our system was evaluated in a clinical trial at the Institute of Clinical Medicine, University of Tsukuba. As *in vivo* results in breast for 21 volunteer patients, high quality elasticity images were easily obtained. We observed invasive ductal carcinoma and non-invasive ductal carcinoma as hard tissue. It is difficult to define the size of carcinoma by using ultrasound 2D image compared with MRI image. But, it was confirmed that it is easier to define by using elasticity image. We will increase the number of cases and further analyze the correspondence between elasticity images and pathology.

61 **ELASTOGRAPHIC IMAGING OF SMALL ANIMAL ONCOLOGY MODELS.**

*Mehmet Bilgen[1], Seshadri Srinivasan[1,2], Lawrence B. Lachman[3], Jonathan Ophir[1,2].*
[1]Department of Radiology, University of Texas Medical School, Houston, Texas, 77030, USA; [2]University of Houston, Electrical and Computer Engineering Department, 4800 Calhoun Rd., Houston, TX, 77204, USA; [3]Department of Bioimmunotherapy, University of Texas M.D. Anderson Cancer Center, Houston, Texas, 77030, USA.

Small animal oncology models have become essential tools for studying the etiology of human tumor diseases, developing effective therapies as well as assessing the efficacy of treatment [1]. Lesions in these models are generally induced by chemical or viral agents, radiation, transplantation of tumor cell lines or genetic engineering. Such lesions are easily palpable by hand because the host tissue is relatively softer, and are interestingly known to exhibit gross bioelastic behavior that is comparable with their counterparts in humans. Evaluation of the bioelastic properties of these lesions in small animal oncology models and characterization of the spatio-temporal evolution of their bioelasticity during their growth are believed to provide unique signatures in cancer research, but yet to be investigated *in vivo*. In this research, such quantitative studies were initiated, for the first time, by performing ultrasonic elastographic experiments on a mouse tumor cell line designated as 66.3. The 66.3 cells were implanted into the mammary fat pad to grow the tumor on the left side of female BALB/c mice below the fore-limb [2]. In the first set of measurements, the tumors measuring approximately 1 cm in diameter were removed from the host and embedded in gel blocks. In the second set, whole animals with tumors with diameters of about 2 cm were embedded in gel blocks for *in situ* measurements. In either case, 60×75×75 $mm^3$ gelatin blocks were manufactured to have Young's modulus values comparable to fat tissue (~5 kPa). After proper placement, the blocks were scanned using an elastography imaging system [3]. The pre- and post-compression RF data were acquired from multiple orientations and transducer locations under 1 % axial compression using both 5 and 7.5 MHz ultrasonic array probes of 38 mm aperture, and processed to obtain axial stain images under various parameter settings. Typical sets of elastograms and the corresponding sonograms obtained in these experiments are illustrated in Figs. 1 and 2, clearly demonstrating the feasibility of applying the elastography technique to small animals. For *in vitro* studies, the tumors were delineated in the sonograms with the regions of hyperintense speckle, and in the elastograms with dark intensity, but with excellent contrast with respect to the background. In *in situ* studies, the speckle patterns in tumors and host tissues were very similar in general, but, in some cases, the tumors were visualized easily in sonograms from the reflections at their borders. This paper will also compare the axial strain values measured in *in vitro* and *in situ* tumors, demonstrate the effects of lateral shift between the transducer and the tumor on the elastograms and also present a detailed analysis of the data processing strategies for obtaining optimal elastographic imaging performance in the studies of small animal oncology models [4].

[1] Houdebine LM. The methods to generate transgenic animals and to control transgene expression. Journal of Biotechnology 98 (2002) 145–160.
[2] Lachman LB, et al. DNA vaccination against neu reduces breast cancer incidence and metastasis in mice. Cancer Gene Therapy 8 (2001) 259-268.
[3] Srinivasan S, Kallel F, Ophir J. Estimating the elastographic signal-to-noise ratio using correlation coefficients. Ultrasound in Medicine and Biology 28(3) (2002), 359-368.
[4] Bilgen M. Dynamics of errors in 3D motion estimation and implications for strain-tensor imaging in acoustic elastography. Physics in Med. Biol. 45 (2000) 1565-1579.

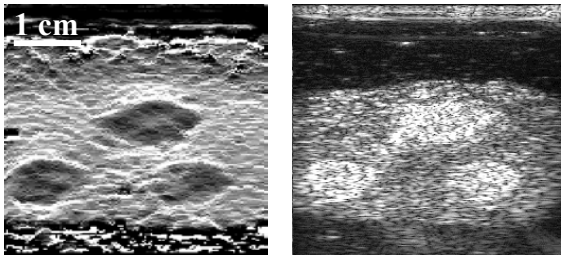


**Figure 1.** *In vitro* elastogram (left) and the corresponding sonogram (right) of three tumors embedded in a gel block. Dark regions in the elastogram indicate stiff tissue as compared to the soft background.

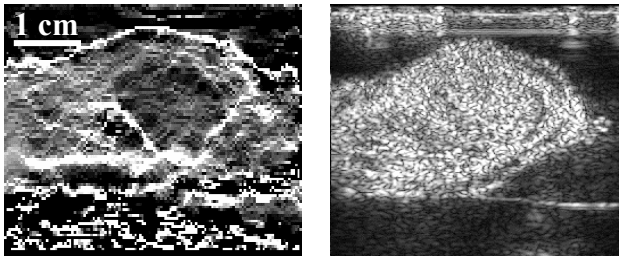


**Figure 2.** *In situ* elastogram (left) and the corresponding sonogram (right) of mouse oncology model embedded in a gel block. Note the good tumor contrast in the elastogram.

63 **STRAIN INDUCED DAMAGE TO BREAST TUMOR TISSUE.**

*Thomas A. Krouskop[1], Pamela S. Younes[2], Tom Wheeler[2].*
[1]Dept. of Physical Medicine and Rehabilitation, [2]Dept. Of Pathology, Baylor College of Medicine, Houston, TX, 77030, USA.

During a previous study of the compressive behavior of breast tissues, it was observed that when some malignant tumors were strained more than 5%, there was a decrease in their stiffness that did not reverse when the loads were removed. This behavior was observed when the tissues were subjected to cyclic loadings. Under the test conditions, when the strain range was greater than 5%, the first cycle of the loading always produced a modulus measurement 25% - 50% greater than the modulus calculated using data from subsequent loading cycles. However, this behavior did not occur with all malignant breast tumors. Based on the results of the first study, a follow-up study has been conducted to gain more insight into this non-reversible behavior and to determine the characteristics of the tumors that exhibit the behavior.

Tissue samples were procured from the pathology department of a teaching hospital associated with Baylor College of Medicine. The samples were obtained when tissue specimens were sent to the frozen section laboratory from the operating room. When the tissue was processed in the laboratory, sections of the desired tissue were prepared for histological analysis and representative sections were collected for the mechanical testing. The test specimens refrigerated in saline at 3 °C until they were tested. Once the mechanical testing was completed, the tissue samples were returned to the pathology department for histological evaluation and classification by a board certified pathologist.

Mechanical testing was done using a hydraulic servo Instron testing machine fitted with a 10 Newton load cell. The Instron testing machine that was used for the testing was interfaced with a computer controller that was programmed to provide the desired displacement-loading pattern. In these experiments, the Instron was programmed to load the tumor tissue samples with a single ramp displacement from 0% strain to 10% strain at a rate of 1% per second. The testing of each sample was completed within two hours of the time that the tissue was delivered to the frozen section laboratory at the hospital so that deterioration is minimized. The temperature of the laboratory where the testing was conducted was maintained at 25° C ± 2° C during the testing.

The test data show that when infiltrating carcinomas were strained more than 5%, irreversible damage occurred that reduced the modulus of the tissue. This phenomenon did not occur when the malignant tumors displayed lobular features.

03 **2-D TRANSIENT ELASTOGRAPHY WITH AN ULTRA-FAST ULTRASONIC SCANNER.**

*Mathias Fink, Laurent Sandrin, Mickael Tanter, Stefan Catheline, Sana Chaffai, Jeremy Bercoff, Jean-Luc Gennisson.*
Laboratoire Ondes et Acoustique, E.S.P.C.I., 10 rue Vauquelin 75231 Paris cedex 05, FRANCE.

An ultrafast scanner is used for quantitatively mapping the shear elasticity of soft tissues. The Ultrafast Scanner provides images of the echogenicity of tissues similar to standard echographic device, but with a frame rate that is 200 times faster. It allows one to detect tissue motion induced by low frequency shear waves. From these displacements, a shear elasticity map is constructed using local inverse problem algorithms. In order to obtain unbiased shear elasticity, different generators of shear waves will be discussed. Preliminary *in vivo* results in breast will be also presented that demonstrate the interest of this technique.

44 **MONITORING OF MODULUS CHANGES WITH TEMPERATURE USING A FREQUENCY SHIFT METHOD.**

*Elisa Konofagou, Kullervo Hynynen.*
Focused Ultrasound Laboratory, Department of Radiology - MRI research, Brigham and Women's Hospital – Harvard Medical School, Boston, MA, USA.

In mechanics, the resonance frequency of a material with a particular geometry is typically linked to its mechanical properties and more precisely, to its stiffness. A frequency shift therefore typically denotes a change in stiffness. It has been previously shown that a variation in tissue temperature results in a subsequent change of the tissue stiffness. It has also been demonstrated that the amplitude of Ultrasound-Stimulated Acoustic Emission (USAE) signal is sensitive to tissue temperature and, therefore, can help detect it. Its amplitude, however, is sensitive both to acoustical and mechanical parameters, that at most frequencies have opposite effects due to temperature. In this paper, we explore the feasibility of a frequency shift of the resonant peaks of the USAE signal for monitoring the tissue stiffness variation with temperature. In a numerical simulation, the variation of the frequency shift at different temperatures is shown. Then, in a series of experiments involving a gel phantom and porcine muscle tissue, the frequency shift variation is shown to follow the known stiffness changes due to temperature. It is also shown to indicate reversible changes as well as the onset of thermal coagulative necrosis that is marked by a monotonically increasing positive frequency shift. The experimental frequency shifted around a peak at 22.1-22.5 kHz within a range of -250 to 80 Hz and -200 Hz to 250 Hz for the gel and muscle tissue for the temperatures of 25-70°C and 30-70°C, respectively. Simulation and *ex vivo* experimental results indicate that the USAE frequency shift method can help dissociate the mechanical from the acoustical parameter dependence as well as detect thermal coagulative necrosis.

49 **DIRECTIONAL FILTERING AND SIMPLE FREQUENCY ESTIMATION: A FAST, SIMPLE METHOD FOR QUANTITATIVE VIBRATION ELASTOGRAPHY RECONSTRUCTION.**

*David A. Thayer, Travis E. Oliphant.*
Department of Electrical and Computer Engineering, Brigham Young University, Provo, UT, 84602, USA.

Quantitative Vibration Elastography uses (low-frequency) mechanical vibration to excite soft-tissues and then reconstruct mechanical stiffness from the resulting displacement measurements. Both ultrasound and magnetic resonance (MR) techniques can be used to measure displacement. Ultrasound typically has better temporal sampling but is subject to more noise than MR measurements.

In isotropic soft-tissues, the dominant motion at low frequencies can be reasonably described using the Helmholtz equation in regions of constant shear modulus. This presentation analyzes and demonstrates a fast method for reconstructing shear modulus that exploits this Helmholtz model of motion when "plane-wave excitation" is used. The method consists of a series of directional filters on the displacement data to isolate traveling plane waves. To each directional filter output, traditional frequency estimation (Kay's method) is applied and the final reconstructed image is obtained using a weighted average of the results from each directional filter. This technique shows promise as a fast, simple processing method that produces results similar to more computationally intensive methods.

Advantages of the new technique include high signal-to-noise ratio, low computational cost, simplicity of implementation, and compensation for null-spots in the data. Using Kay's estimator for frequency estimation after the directional filter does not allow for complex-valued shear modulus estimation. However, using the directional filters with other fast reconstruction techniques is possible and improves results due to the automatic compensation for null-spots where these reconstructions are especially sensitive.

This approach is validated on simulated data, which is also used to demonstrate the familiar noise vs. resolution tradeoff for the new technique. Comparisons in processing speed, susceptibility to noise, and resolution are then made to the maximum likelihood estimator, direct Helmholtz inversion, and an adaptive "matched filter" technique.

38 **PROSTATE ELASTOGRAPHY: CAUSES OF DECORRELATION *IN-VIVO*.**

*Rémi Souchon[1], Jonathan Ophir[2,3], Seshadri Srinivasan[2,3], Jean-Yves Chapelon[1].*
[1]INSERM, Lyon, FRANCE; [2]Ultrasonics Laboratory, Dept. of Radiology, University of Texas Medical School, Houston, TX, 77030, USA; [3]University of Houston, Electrical and Computer Engineering Department, 4800 Calhoun Rd., Houston, TX, 77204, USA.

Decorrelation between pre- and post-compression RF signals is to be minimized in elastography, since it prevents reliable strain estimation and visualization. To gain a better understanding of sources of decorrelation *in vivo*, transverse elastograms were acquired *in vivo* on patients diagnosed with prostate cancer, and areas of decorrelation were studied.

Compression was applied by inflation of a balloon that covers a transrectal ultrasonic imaging probe. The probe was held stable, attached to a motorized holder. Elastograms and cross-correlation maps were calculated using overlapping RF segments. To minimize decorrelation due to lateral motion, the algorithm calculates lateral displacements by searching for the maximum of the cross-correlation function on neighboring RF lines. An iterative adaptive stretching of the post-compression RF signal was performed to minimize decorrelation related to local strain. Two iterations were used.

It was found that decorrelation in the elastogram was directly related to the acquisition frame rate. The average correlation inside the prostate was shown to decrease with decreasing frame rate, thus suggesting the existence of out-of-plane motion. The presence of this out-of-plane motion was confirmed by longitudinal scans in real-time sonography of the prostate, showing that respiration induces an elevational displacement. The amplitude of the displacement could easily reach five millimeters.

At high frame rate, induced strains are small and therefore do not contribute significantly to decorrelation. Decorrelation was mainly associated with low sonographic signal to noise ratio (SNRs) in hypoechoic areas. The maximum, minimum, average and standard deviation of the correlation value were calculated as a function of SNRs, showing that the highest correlation value achievable depends on SNRs, as expected from theory.

Decorrelation was observed following the prostate boundaries. Because the prostate is not tightly attached to surrounding fatty tissues, it was hypothesized that slip conditions between loosely connected tissues were responsible for the presence of decorrelation in this area. Decorrelation areas not related to the above-mentioned phenomena may be explained by non-stationary RF signals in the presence of pulsatile blood flow.

These results suggest the use of a high acquisition frame rate system to minimize decorrelation associated with out-of-plane motion, and of a high transmit gain to increase SNRs. High SNRs is important to minimize decorrelation noise in hypoechoic areas, often associated with adenocarcinoma. It is expected that a better understanding of the sources of decorrelation in elastograms acquired *in vivo* might help improve future elastographic imaging systems, and might be used to identify clinically significant information.

This work was supported in part by the National Cancer Institute (USA) Program Project Grant 2P01-CA64597 to the University of Texas Medical School.

60 **MAPPING OF TEMPERATURE ELEVATION USING ULTRASOUND PHASED ARRAYS.**

*E.E. Konofagou[1], S. Sokka[1,2], J. Thierman[1,2], K. Hynynen[1].*

[1]Focused Ultrasound Laboratory, Department of Radiology – MR Research, Brigham and Women's Hospital – Harvard Medical School, Boston, MA, USA; [2]Health Science and Technology Program, Harvard-MIT Division, Cambridge, MA, USA.

Temperature monitoring is most important during the application of thermal treatment, such as in the case of Focused Ultrasound Surgery (FUS). Currently, Magnetic Resonance Imaging (MRI) is the predominant method for temperature mapping of FUS. However, its high cost, low temporal resolution and limited availability and applicability often result in its restricted use. In this paper, a new device for mapping temperature-related tissue changes is introduced that only uses focused ultrasound to both apply and monitor the treatment temporally and spatially. By utilizing the principle of the recently introduced Ultrasound-Stimulated Acoustic Emission (USAE) [1] and its temperature dependence [2] as well as the phased array capability of steering the beam, the temperature distribution during the application of the treatment could be assessed. The array had 62 elements out of which 52 were utilized and its axial and steering focusing ranges were 30 to 60 mm and -10 to 10 mm, respectively. Furthermore, the array had a linear geometry and was divided into two sub arrays in such a fashion that half of the elements were at 1.08 MHz and half were chirped at frequencies ranging from 1.08 to 1.12 MHz; the difference frequency ranging, thus, between 0 and 40 kHz. A total of 11 locations focused at 50 mm axial depth and spanning in a lateral range from -5 to 5 mm across the focal spot of the transducer were used. Heating at 20 W (electrical power) was applied for 10 s at the central location (i.e., at 0 mm) and then the USAE measurement “sweeping” was applied in a repeated sequence across the focus. The target used here was a silicone gel (GE RTV 6166) with tissue-mimicking properties. The temperature spot could be detected during the application of the treatment and the temperature elevation could be both mapped spatially and monitored temporally. Our plan is to use the same array for the therapy sonication and monitoring of the treatment. This technique holds great promise for realizing the ultimate clinical goal: an economic, fully integrated closed loop feedback system for therapy control.

[1] Fatemi,M.; Greenleaf, J.F., Ultrasound-stimulated Vibro-Acoustic Spectrography, Science, vol. 280, pp. 82-85, 1998.

[2] Konofagou E.E., Thierman J. Karjalainen T. and Hynynen K., The Temperature Dependence of Ultrasound-Stimulated Acoustic Emission, Ultras. Med. Biol. 28(3), 331-338, 2002.

70 **CONSTRAINED BREAST ELASTOGRAPHY: PHANTOM STUDY AND APPLICATION IN *IN-VITRO* BREAST TISSUE MEASUREMENT.**

*A. Samani, D.B. Plewes.*
Department of Medical Biophysics, Sunnybrook and Women's College Health Sciences Centre, University of Toronto, Toronto, CANADA.

The fact that pathological processes yield variations in tissue elasticity has been known for thousands of years. This led to the widely used method of manual palpation of soft tissues, which is a simple qualitative way of determining the stiffness of suspicious areas, compared to the surrounding tissues. Recent studies on breast tissues both *in-vivo* and *in-vitro* have confirmed that quantitative knowledge of tissue elasticity can be used effectively for breast cancer diagnosis. This idea has led to the development of various elastography techniques. These techniques consist of mechanical stimulation of the tissue, measuring the resulting deformation, and finally reconstructing the elasticity distribution from the measured data using an inversion technique. In this study, we use quasi-static actuation and measure the resulting displacement using a NMR phase-contrast technique. For elasticity reconstruction, other investigators make no assumptions on elasticity distribution. This leads to ill-conditioned problems that can be solved using data filtering and regularization techniques. In our technique, however, it is assumed that conventional MRI imaging, which provides the geometry of normal tissues and tumors, precedes the elastography test. Furthermore, it is assumed that the elastic modulus variation throughout the volume of each tissue type is negligible. The latter assumption provides constraints that decrease the number of unknowns to the number of the breast tissue types seen on the MRI image. As a result the elastography inverse problem becomes well conditioned, SNR requirements become very modest, and data filtering and regularization, which often lead to artifacts, are not required. Moreover, this technique requires only one displacement component measurement for isotropic elastic modulus reconstruction. This model can be extended easily for anisotropic moduli reconstruction provided all three displacement components are available. This technique has been validated with a phantom study with very good results. Furthermore, it was implemented into an *in-vitro* breast tissue elasticity measurement method. Results of the phantom study and elasticity measurement will be presented.

47 **DEVELOPMENT AND APPLICATIONS OF A TISSUE ULTRASOUND PALPATION SENSOR (TUPS).**

*Yongping Zheng, Guohua Pan, Jane Ho, Arthur F.T. Mak.*
Rehabilitation Engineering Center, The Hong Kong Polytechnic University, Kowloon, HONG KONG.

Manual palpation on the skin using fingers is widely used to assess the stiffness of various soft tissues. Palpation produces a subjective assessment and, therefore, requires substantial clinical experience. In addition, the qualitative nature of such assessments makes the accumulation of knowledge difficult and teaching/learning imprecise. In this abstract, we introduced a portable tissue ultrasound palpation sensor (TUPS), which was used to measure the thickness and stiffness of different tissue layers. We also introduced the foot plantar tissue assessment for the patients with rheumatoid arthritis using TUPS.
The portable TUPS comprised of an indentation probe and a control box. The hand-held probe included an ultrasound transducer at the tip and an in-series compressive load cell. The control box had a microprocessor module, electronic circuits and LCD display. During a test, the hand-held probe was placed on the tissue surface with a bony substratum. As the operator manually loaded and unloaded the probe on the tissue surface, a program embedded in the microprocessor module continuously caused an ultrasound emitter to emit ultrasound pulses into the soft tissue. The ultrasound echo signal reflected from the bony interface was received and its flight times were used by the program to calculate the original thickness and the deformation of the soft tissue. The corresponding load applied to the tissue was continuously measured by the load cell. After collecting the data for a preset number of loading-unloading cycles, the program computed the Young's modulus of the soft tissue from the load-indentation response using an analytical solution of indentation on a layer. Repeatability tests for intra-operator (twice), inter-operator (three), inter-machine (four), and inter-probe (two different diameters, 6 and 9 mm) were conducted on a silicon phantom for the TUPS.

This portable TUPS was used for the assessment of foot plantar tissues of the patients with rheumatoid arthritis (RA). The assessment was conducted at the heel, 1$^{st}$ metatarsal head and 5$^{th}$ metatarsal head of 31 normal patients and 30 RA patients. The average ages of the normal subjects and patients were 37 and 53, respectively. The intra- and inter-operator repeatability for the measurement on the plantar tissues was performed by two operators. The tissue thickness and stiffness of normal and patient subjects were compared.

Results showed the repeatability of the intra-operator, inter-operator, inter-machine, and inter-probe of the TUPS measurement for the silicon layer was better than 5% for a confidence level of 95%. The intra-operator repeatability for the three testing sites on the foot plantar was 9% and 13% for the measurement of thickness and Young's modulus, respectively. Similarly, the inter-operator repeatability was 10% and 18% for the measurement of thickness and Young's modulus, respectively. It was demonstrated that the plantar tissue thickness of the RA patients was significantly ($p<0.05$) larger than that of the normal subjects for all the three testing sites. This device can also be used for the assessment of other soft tissues, where the manual palpation is used.

Acknowledgement: This work is partially supported by The Hong Kong Polytechnic University and Research Grant Council of Hong Kong (PolyU5199/02E).

71 **THE DEPENDENCE OF ULTRASOUND STIMULATED ACOUSTIC EMISSIONS ON STIFFNESS, FREQUENCY, AND DEPTH IN A PHANTOM GEL.**

*J Thierman[1,2], EE Konofagou[1], K Hynynen[1].*
[1]Brigham and Women's Hospital – Harvard Medical School, Boston, MA, USA; [2]Health Science and Technology Program, Harvard-MIT Division, Cambridge, MA, USA.

Ultrasound Stimulated Acoustic Emissions (USAE) has shown promise as a new method for non-invasive testing and imaging based on a modeling study, results in the temperature response of the USAE signal , and results from theoretical work and experiments with calcified aortic sections . However, the precise relationship of the magnitude of the USAE response to the target stiffness has yet to be studied. In addition, other important factors including the relationship of the response to the applied difference frequency and the tissue penetration depth have not been examined in a controlled manner. This paper presents the results of a study of the USAE response to changes in target stiffness and depth in a silicone phantom gel material. Five silicone gels were prepared ranging in shear modulus from 1 to 10 kPa. The measured speed of sound, attenuation, and densities of the gels were the same for all five gels. In the dual frequency experiments, the gels were sonicated with a pulse from two focused ultrasound transducer elements. One element sonicated at 1.624 MHz the other at 1.654 MHz. Their focal length was 10 cm. The two elements were mounted at an angle to one another so that their foci intersected. This intersecting region of the two pressure fields was applied both to the phantom gel surfaces and the gel centers. The results demonstrate a decreasing response at the difference frequency with increasing gel stiffness in both locations in the phantom material. The high frequency (1.6 MHz) signal was also recorded and remains relatively constant with gel stiffness. These results together with the nearly identical measure acoustical properties of the five gel samples support a simple mechanical model explanation for the decreased difference frequency response with increasing material shear modulus.

72 **IN-VIVO RESULTS USING A ZERO-CROSSING STRAIN ESTIMATOR FOR ELASTOGRAPHY**†

*S Srinivasan[1,2], R Souchon[3], J Ophir[1,2].*
[1]Ultrasonics Laboratory, Dept. of Radiology, University of Texas Medical School, Houston, TX, 77030, USA; [2]University of Houston, Electrical and Computer Engineering Department, 4800 Calhoun Rd., Houston, TX, 77204, USA; [3]INSERM, Lyon, FRANCE.

A novel zero-crossing tracking strain estimation technique (ZCT) has been developed for elastography [1]. This technique is based on tracking the zero-crossings between the pre-and post-compression A-lines, and does not require global or adaptive A-line stretching. For multi-compression elastography, ZCT can be implemented as a temporal tracking scheme, where a temporal track of the zero-crossings between successive RF A-lines is obtained, or as a cumulative averaging scheme, where accumulation of the inter-frame strains is performed to yield high elastographic SNR. Other advantages of the technique include fast processing and potential for simple hardware implementation. The limitations of the technique are the need for small compression steps due to lack of robustness when large compression steps (>3%) are used. Simulations and experiments were performed to illustrate its utility as an alternative strain estimation technique.

The feasibility of using ZCT as an on-line guidance for in vivo experiments was demonstrated using real-time data acquired from prostates at 8 frames per second using a 5 MHz transducer sampled at 100 MHz. The results obtained using ZCT was compared with cross-correlation based algorithms and no significant differences were found (Figs. 1 and 2). The algorithm was capable of handling up to 20 frames per second without any overheads. With the acquisition of only the zero-crossings from the A-line, the frame-rates could be improved further to provide a simultaneous real-time sonogram-elastogram display.

[1] Srinivasan S, Ophir J. A zero crossing strain estimator for elastography. Ultrasound in Medicine and Biology 2002, In press.

a) ZCT b) Cross-correlation

Fig. 1: In vivo elastograms of a prostate during HIFU treatment showing a lesion on the left side. a) ZCT and b) Cross-correlation

a) ZCT b) Cross-correlation

Fig. 2: In vivo elastograms of a prostate with an elongated cancerous tumor and a circular urethral probe. a) ZCT and b) Cross-correlation

†Supported by National Cancer Institute Program Project Grant P01-CA64597

# CONTINUING MEDICAL EDUCATION

## Goals of the Conference

The goal of this Conference is to advance the field of measurement and imaging of the elastic attributes of soft tissues by ultrasound through tutorial and scientific presentations of the state of the art in the field. The early efforts in this field were reported some 20 years ago, but in the last decade there has been a steady increase in interest in this topic with new methods and results (some from cases *in-vivo*) now being routinely published. New applications for this methodology include breast and prostate cancer detection and classification, monitoring of transplant kidney rejection, cancer therapy monitoring using high-intensity focused ultrasound (HIFU), characterization of intra-arterial plaque in cardiovascular disease, skin and tissue engineering, and muscle dynamics including the myocardium. We expect that the conference will provide a unique and unified forum that will bring together researchers from several countries, and that it will ultimately contribute to the rapid development and clinical introduction of this new medical imaging technology.

## Conference Description and Needs Assessment

The target audience for this conference is physicians and scientists interested in the advancement of imaging techniques for early detection of disease. This conference will provide an educational experience for all clinical specialties dealing with cancer diagnosis, specifically, for radiologists specializing in ultrasound or MRI imaging techniques.

Standard medical practice of soft tissue palpation is based on the qualitative assessment of the low-frequency stiffness of tissue. In many cases, despite the difference in stiffness, the small size of a pathological lesion and/or its location deep in the body preclude its detection and evaluation by palpation. In general, the lesion may or may not possess echogenic properties that would make it ultrasonically detectable. For example, tumors of the prostate or the breast could be invisible or barely visible in standard ultrasound examinations, yet be much harder than the surrounding tissue. Diffuse diseases such as cirrhosis of the liver are known to significantly increase the stiffness of the liver tissue as a whole, yet they may appear normal in conventional ultrasound examinations. Since the echogenicity and the stiffness of tissue are generally uncorrelated, it is expected that imaging tissue stiffness parameters will provide new information that is related to tissue structure and/or pathology.

This conference will present a diverse set of topics related to the imaging of tissue elasticity The topics are important to clinical professionals who want a strong understanding of the engineering principles behind this imaging modality and who want to use this knowledge, combined with their medical experience and education, to contribute to the advancement of a technology that could lead to improved early diagnosis and treatment of cancer as well as other clinical applications such as atherosclerosis, diffuse liver disease, venous thrombosis, heart disease, and skeletal muscle rehabilitation.

Attendees should leave this conference with a greater understanding of the work being done on the imaging of the properties of tissues and the potential clinical applications of this research. The knowledge gained could be used in future clinical procedures or as a basis for investigations into the use of tissue elasticity imaging in their specific clinical area.

## Conference Objectives

As a result of attending this conference, participants should be able to understand the following topics:

- Tissue mechanical measurement techniques;
- The latest methods for biomechanical tissue modeling;
- The mechanical properties of tissues;
- Comparison of methods for imaging elastic tissue properties;
- Signal processing and new measurement and imaging algorithms;
- Application of forward and inverse problems in elasticity imaging;
- The review of clinical applications and current results;
- The use of latest phantoms and instrumentation;
- The advantages of three-dimensional and multi-modality applications;
- Complementary elasticity imaging techniques (MRI and optical).

SONOGRAPHERS: The American Registry of Diagnostic Medical Sonographers (ARDMS) will accept Category 1 credits earned at this conference and approved by ACCME. Sonographers will receive a certificate at the end of this conference to send to ARDMS.

### Continuing Medical Education Certification

The University of Rochester School of Medicine and Dentistry is accredited by the Accreditation Council for Continuing Medical Education (ACCME) to provide continuing medical education for physicians.

The University of Rochester School of Medicine and Dentistry designates this educational activity for a maximum of 20.0 hours in Category 1 credit toward the AMA Physician's Recognition Award. Each physician should claim only those hours of credit that he/she actually spent in the educational activity.

*CME Certification*

*Sponsored by:*

UNIVERSITY OF
ROCHESTER
SCHOOL OF MEDICINE & DENTISTRY
*Office of Continuing Professional Education*

## Notes

## Notes

## Notes